Supplement of Hydrol. Earth Syst. Sci., 25, 1671–1687, 2021
https://doi.org/10.5194/hess-25-1671-2021-supplement

Hydrology and Earth System Sciences
Open Access
EGU

Supplement of

Groundwater level forecasting with artificial neural networks: a comparison of long short-term memory (LSTM), convolutional neural networks (CNNs), and non-linear autoregressive networks with exogenous input (NARX)

Andreas Wunsch et al.

Correspondence to: Andreas Wunsch (andreas.wunsch@kit.edu)

Supplementary Material

Content Overview:

- Table S1 lists all hydrographs including information such as identifiers and coordinates
- Tables S2 to S4 summarize the results of the hyperparameter optimization for all models
- Tables S5 and S6 give information on the forecast accuracy of all models
- Fig. S1 to S34: Seq2Val Results
- Fig. S35 to S68: Seq2Seq Results
- Figure S69 explores the robustness of the models in terms of ensemble error variance
- Figures S70 to S72 give further details on how the length of the training data set influences the seq2val model performance. Figure S73 examines the same effect when training ends even 5 years earlier and Fig. S74 examines the development of several statistic measures in a comparable set up
- Figures S72 to S141 show the training and early stopping loss (MSE) convergence for each of the ten random initializations of the models.

.

List of Tables

List of Figures

Table S1: List of all wells included in the dataset. ID refers to the respective data web service.

Dataset_ID	ID	Name	X	Y	Coord.Sys.	Country
BW_1-115-8	1/115-8	1115 SCHUTTERWALD	416098	5369591	ETRS_1989_UTM_Zone_32N	Germany
BW_103-261-4	103/261-4	MALSCH	452062	5415349	ETRS_1989_UTM_Zone_32N	Germany
BW_104-114-5	104/114-5	1807 RENCHEN 1	425124	5383055	ETRS_1989_UTM_Zone_32N	Germany
BW_104-307-0	104/307-0	GWM SK 22 - 3021A, Reilingen	468049	5458156	ETRS_1989_UTM_Zone_32N	Germany
BW_138-019-0	138/019-0	FLB 5 Breisach-Hochstetten	396354	5319363	ETRS_1989_UTM_Zone_32N	Germany
BW_157-260-8	157/260-8	1555 BRUCHHAUSEN	453043	5418954	ETRS_1989_UTM_Zone_32N	Germany
BW_1851-305-1	1851/305-1	GWM 1 TIEF, DOSSENHEIM	473896	5477008	ETRS_1989_UTM_Zone_32N	Germany
BW_710-256-3	710/256-3	ALTLUSSHEIM M	463216	5461626	ETRS_1989_UTM_Zone_32N	Germany
BW_765-306-3	765/306-3	KETSCH SCHLEIWIESE T	463711	5467331	ETRS_1989_UTM_Zone_32N	Germany
BW_781-304-2	781/304-2	GWM Tief, Heddesheim	473915	5486080	ETRS_1989_UTM_Zone_32N	Germany
HE_11874	11874	RUESSELSHEIM	462420	5537724	ETRS_1989_UTM_Zone_32N	Germany
HE_12905	12905	GROSS-ROHRHEIM	461300	5508386	ETRS_1989_UTM_Zone_32N	Germany
HE_12946	12946	FEHLHEIM	468827	5505887	ETRS_1989_UTM_Zone_32N	Germany
HE_13490	13490	HOFHEIM	458537	5500283	ETRS_1989_UTM_Zone_32N	Germany
HE_13518	13518	LAMPERTHEIM	468337	5494261	ETRS_1989_UTM_Zone_32N	Germany
RP_2375118200	2375118200	1174 II Neupotz	451064	5439203	ETRS_1989_UTM_Zone_32N	Germany
RP_2375283300	2375283300	1273 III Leimersheim	452633	5439833	ETRS_1989_UTM_Zone_32N	Germany

Table S2: Results of bayesian hyperparameter optimization (NARX models).

NARX		Inputs			Model Parameters						
		rH	T	Tsin	Hidden size	ID P	ID rH	ID T	ID Tsin	ID GWL_{t-1}	FD
seq2val	BW_1-115-8	0	1	1	1	52	-	3	29	-	47
	BW_103-261-4	1	1	0	18	12	3	52	-	-	39
	BW_104-114-5	0	1	1	14	8	-	50	4	-	36
	BW_104-307-0	0	1	1	20	50	-	52	51	-	11
	BW_138-019-0	0	0	1	19	24	-	-	50	-	50
	BW_157-260-8	1	1	0	14	21	52	52	-	-	23
	BW_1851-305-1	1	1	1	10	40	12	34	13	-	34
	BW_710-256-3	0	0	1	18	12	-	-	46	-	9
	BW_765-306-3	1	0	1	17	18	51	-	46	-	33
	BW_781-304-2	1	1	0	10	41	40	52	-	-	38
	HE_11874	0	0	1	18	37	-	-	49	-	47
	HE_12905	1	0	1	9	5	2	-	17	-	4
	HE_12946	1	0	0	7	44	47	-	-	-	45
	HE_13490	1	0	0	17	48	48	-	-	-	21
	HE_13518	1	0	0	20	52	32	-	-	-	10
	RP_2375118200	1	1	1	12	42	47	35	1	-	26
	RP_2375283300	1	1	1	8	11	21	47	25	-	4
seq2val GWL_{t-1}	BW_1-115-8	0	1	0	1	13	-	19	-	44	8
	BW_103-261-4	1	0	0	1	17	19	-	-	50	8
	BW_104-114-5	1	0	1	1	3	44	-	30	13	2
	BW_104-307-0	0	0	1	3	28	-	-	11	14	10
	BW_138-019-0	0	1	1	4	2	-	5	48	8	3
	BW_157-260-8	0	1	1	1	19	-	18	7	3	1
	BW_1851-305-1	0	1	0	1	12	-	26	-	5	14
	BW_710-256-3	0	0	1	2	3	-	-	35	5	3
	BW_765-306-3	0	0	0	3	2	-	-	-	45	2
	BW_781-304-2	1	1	0	3	6	8	10	-	28	4
	HE_11874	0	1	1	4	4	-	13	32	51	11
	HE_12905	1	1	0	1	18	7	21	-	30	1
	HE_12946	1	0	0	1	2	16	-	-	3	12
	HE_13490	0	1	1	8	3	-	6	44	28	1
	HE_13518	1	1	1	1	4	22	10	14	1	9
	RP_2375118200	0	1	1	7	7	-	28	38	7	8
	RP_2375283300	0	0	1	2	3	-	-	35	5	3
seq2seq	BW_1-115-8	0	1	0	1	2	-	9	-	-	8
	BW_103-261-4	0	1	1	17	1	-	1	4	-	3
	BW_104-114-5	0	1	1	1	4	-	8	8	-	4
	BW_104-307-0	1	0	0	17	11	11	-	-	-	5
	BW_138-019-0	0	0	0	1	8	-	-	-	-	2
	BW_157-260-8	1	1	0	20	10	2	1	-	-	3
	BW_1851-305-1	0	0	0	10	11	-	-	-	-	7
	BW_710-256-3	1	0	0	20	12	4	-	-	-	1
	BW_765-306-3	0	0	1	20	4	-	-	7	-	3
	BW_781-304-2	1	0	0	17	11	11	-	-	-	5
	HE_11874	1	1	1	8	10	8	12	5	-	12
	HE_12905	1	1	0	12	6	6	1	-	-	8
	HE_12946	1	0	0	20	12	7	-	-	-	5
	HE_13490	1	1	0	3	4	4	1	-	-	3
	HE_13518	1	1	0	18	10	7	12	-	-	12
	RP_2375118200	1	1	1	2	10	11	4	12	-	12
	RP_2375283300	1	0	0	4	8	4	-	-	-	3
seq2seq GWL_{t-1}	BW_1-115-8	0	1	1	1	3	-	12	1	11	8
	BW_103-261-4	1	0	1	7	6	11	-	3	8	2
	BW_104-114-5	1	1	1	2	6	2	12	3	11	6
	BW_104-307-0	0	1	0	19	12	-	1	-	12	2
	BW_138-019-0	1	0	0	8	9	2	-	-	2	6
	BW_157-260-8	1	1	1	2	2	3	11	4	1	1
	BW_1851-305-1	1	1	0	17	10	10	5	-	2	6
	BW_710-256-3	0	1	1	1	3	-	6	12	3	11
	BW_765-306-3	0	1	1	5	3	-	3	7	5	9
	BW_781-304-2	1	0	0	20	9	3	-	-	1	7
	HE_11874	1	1	1	20	3	10	11	8	10	8
	HE_12905	0	1	1	4	8	-	9	7	8	9
	HE_12946	0	0	0	17	1	-	-	-	11	12
	HE_13490	1	0	1	6	2	2	-	12	6	9
	HE_13518	0	1	1	1	12	-	1	7	10	12
	RP_2375118200	0	1	0	2	7	-	11	-	10	2
	RP_2375283300	1	0	0	1	12	6	-	-	2	1

Table S3: Results of bayesian hyperparameter optimization (LSTM models).

LSTM		Inputs			Model Parameters		
		rH	T	Tsin	Hidden size	Seq. Length	Batch size
seq2val	BW_1-115-8	1	0	1	65	40	21
	BW_103-261-4	1	0	1	164	23	84
	BW_104-114-5	0	1	0	144	35	135
	BW_104-307-0	1	0	1	65	40	21
	BW_138-019-0	1	0	0	228	19	191
	BW_157-260-8	1	0	1	65	40	21
	BW_1851-305-1	1	1	1	218	32	189
	BW_710-256-3	1	0	0	82	20	16
	BW_765-306-3	1	0	1	95	10	25
	BW_781-304-2	1	1	0	60	1	180
	HE_11874	1	1	1	201	45	48
	HE_12905	0	0	1	113	38	40
	HE_12946	1	0	1	65	40	21
	HE_13490	1	0	0	79	51	36
	HE_13518	1	1	0	229	49	43
	RP_2375118200	1	0	1	65	40	21
	RP_2375283300	1	0	1	117	12	41
seq2val GWL_{t-1}	BW_1-115-8	0	0	1	78	10	16
	BW_103-261-4	1	1	1	240	2	32
	BW_104-114-5	1	1	1	79	14	17
	BW_104-307-0	1	1	0	116	35	18
	BW_138-019-0	0	1	1	76	2	19
	BW_157-260-8	1	1	1	136	1	16
	BW_1851-305-1	0	1	1	124	49	17
	BW_710-256-3	0	0	1	78	10	16
	BW_765-306-3	0	0	1	81	23	16
	BW_781-304-2	0	0	0	175	1	18
	HE_11874	1	0	1	183	1	16
	HE_12905	0	0	1	7	2	17
	HE_12946	0	1	1	196	1	33
	HE_13490	1	0	0	171	1	27
	HE_13518	1	1	0	39	50	16
	RP_2375118200	1	0	1	24	50	16
	RP_2375283300	0	1	0	255	2	16
seq2seq	BW_1-115-8	0	0	1	78	10	16
	BW_103-261-4	0	0	1	115	15	40
	BW_104-114-5	1	0	1	65	40	21
	BW_104-307-0	1	1	0	229	49	43
	BW_138-019-0	0	1	1	108	1	16
	BW_157-260-8	0	1	0	206	48	49
	BW_1851-305-1	0	1	1	121	51	19
	BW_710-256-3	1	1	0	111	19	29
	BW_765-306-3	1	0	1	108	36	39
	BW_781-304-2	0	0	0	148	1	178
	HE_11874	1	1	0	229	49	43
	HE_12905	0	0	1	78	10	16
	HE_12946	0	0	1	244	2	51
	HE_13490	1	0	1	62	39	18
	HE_13518	1	0	1	65	40	21
	RP_2375118200	0	0	1	106	31	40
	RP_2375283300	1	0	1	65	1	31
seq2seq GWL_{t-1}	BW_1-115-8	0	0	0	108	51	25
	BW_103-261-4	0	1	1	175	38	16
	BW_104-114-5	1	1	0	224	50	16
	BW_104-307-0	1	0	1	245	2	30
	BW_138-019-0	0	0	1	209	5	17
	BW_157-260-8	0	0	1	255	49	20
	BW_1851-305-1	0	0	1	78	10	16
	BW_710-256-3	0	1	1	246	26	57
	BW_765-306-3	0	0	1	229	50	45
	BW_781-304-2	0	0	0	112	5	22
	HE_11874	1	1	1	198	1	16
	HE_12905	1	0	1	223	2	16
	HE_12946	1	1	0	233	8	28
	HE_13490	0	0	0	158	47	16
	HE_13518	0	0	1	81	23	16
	RP_2375118200	1	1	0	72	2	16
	RP_2375283300	1	1	1	221	5	173

Table S4: Results of bayesian hyperparameter optimization (CNN models).

CNN		Inputs			Model Parameters			
		rH	T	Tsin	No. of filters	Dense size	Seq. Length	Batch size
seq2val	BW_1-115-8	0	0	1	107	109	36	39
	BW_103-261-4	1	1	0	48	205	30	71
	BW_104-114-5	0	0	1	53	175	35	116
	BW_104-307-0	1	0	0	55	184	46	75
	BW_138-019-0	0	0	1	200	55	36	51
	BW_157-260-8	1	0	1	212	62	31	19
	BW_1851-305-1	0	0	1	80	156	44	26
	BW_710-256-3	0	0	1	46	82	21	17
	BW_765-306-3	1	0	1	200	250	19	20
	BW_781-304-2	1	0	0	220	63	43	22
	HE_11874	1	0	0	159	107	48	58
	HE_12905	0	0	1	205	51	36	49
	HE_12946	1	0	0	226	41	49	108
	HE_13490	1	1	0	27	5	50	21
	HE_13518	1	0	0	183	69	43	22
	RP_2375118200	0	0	1	205	51	36	49
	RP_2375283300	1	0	1	30	79	14	17
seq2val GWL_{t-1}	BW_1-115-8	0	0	1	95	3	1	42
	BW_103-261-4	1	0	1	227	232	1	33
	BW_104-114-5	0	1	1	115	243	13	43
	BW_104-307-0	0	0	1	155	152	11	25
	BW_138-019-0	0	0	0	74	173	1	21
	BW_157-260-8	0	1	0	248	125	4	16
	BW_1851-305-1	0	0	1	243	177	1	19
	BW_710-256-3	0	0	1	123	197	26	16
	BW_765-306-3	0	0	1	38	78	18	16
	BW_781-304-2	0	1	0	88	111	1	17
	HE_11874	1	1	0	172	201	7	16
	HE_12905	0	1	0	198	94	2	20
	HE_12946	0	0	0	165	206	2	26
	HE_13490	0	0	1	237	170	2	18
	HE_13518	1	1	1	72	31	1	37
	RP_2375118200	0	0	1	100	150	5	30
	RP_2375283300	1	1	0	172	242	2	20
seq2seq	BW_1-115-8	1	1	0	248	127	29	178
	BW_103-261-4	0	0	1	205	51	36	49
	BW_104-114-5	0	1	1	194	153	30	154
	BW_104-307-0	1	1	1	78	123	34	23
	BW_138-019-0	0	0	0	34	161	1	29
	BW_157-260-8	0	0	1	205	51	36	49
	BW_1851-305-1	0	1	0	212	51	34	61
	BW_710-256-3	1	1	1	78	123	34	23
	BW_765-306-3	0	1	0	80	192	38	90
	BW_781-304-2	1	0	0	52	2	50	94
	HE_11874	1	1	1	78	123	34	23
	HE_12905	0	0	1	38	78	18	16
	HE_12946	1	1	1	78	123	34	23
	HE_13490	1	1	1	78	123	34	23
	HE_13518	1	0	0	159	107	48	58
	RP_2375118200	1	0	1	238	105	19	34
	RP_2375283300	1	1	1	246	139	2	170
seq2seq GWL_{t-1}	BW_1-115-8	1	0	1	242	133	10	155
	BW_103-261-4	0	1	1	118	255	30	49
	BW_104-114-5	0	0	1	112	245	19	44
	BW_104-307-0	0	1	1	236	100	18	20
	BW_138-019-0	0	0	0	45	142	9	20
	BW_157-260-8	0	1	0	212	62	34	77
	BW_1851-305-1	0	0	0	54	174	3	20
	BW_710-256-3	1	1	1	244	106	17	31
	BW_765-306-3	0	0	1	114	242	18	47
	BW_781-304-2	0	0	1	254	87	47	20
	HE_11874	1	1	0	255	181	6	19
	HE_12905	1	1	0	56	86	21	28
	HE_12946	0	0	1	62	213	21	18
	HE_13490	0	1	1	243	118	21	33
	HE_13518	1	0	1	243	103	9	25
	RP_2375118200	1	1	0	137	227	2	34
	RP_2375283300	1	1	1	51	149	2	26

Table S5: Forecasting results of all sequence-to-value models.

		Seq2Val							Seq2Val (GWL_{t-1})						
	ID	NSE	R2	RMSE	rRMSE	Bias	rBias	PI	NSE	R2	RMSE	rRMSE	Bias	rBias	PI
NARX	BW_1-115-8	0.68	0.83	0.17	11.85	-0.13	-8.86	-8.55	0.86	0.85	0.11	7.89	-0.04	-2.82	-3.23
	BW_103-261-4	0.67	0.77	0.21	8.45	-0.13	-5.24	-5.42	0.93	0.91	0.10	3.89	0.00	-0.15	-0.36
	BW_104-114-5	0.84	0.87	0.17	5.80	-0.08	-2.58	-0.33	0.89	0.89	0.14	4.87	-0.01	-0.19	0.06
	BW_104-307-0	-0.68	0.71	0.25	13.88	-0.23	-12.55	-85.04	0.96	0.96	0.04	2.08	0.00	-0.17	-0.92
	BW_138-019-0	0.06	0.13	0.11	5.46	-0.05	-2.58	-0.81	0.41	0.31	0.08	4.33	-0.01	-0.45	-0.14
	BW_157-260-8	0.78	0.90	0.13	8.11	0.11	6.45	-5.86	0.96	0.95	0.06	3.43	0.00	-0.08	-0.23
	BW_1851-305-1	0.75	0.71	0.15	8.40	0.05	2.61	-3.34	0.90	0.84	0.09	5.29	0.02	1.03	-0.72
	BW_710-256-3	0.42	0.62	0.31	9.41	-0.17	-5.36	-4.65	0.84	0.84	0.16	4.91	-0.01	-0.34	-0.54
	BW_765-306-3	0.30	0.40	0.53	13.58	-0.24	-6.12	-2.27	0.67	0.66	0.37	9.32	-0.06	-1.60	-0.54
	BW_781-304-2	0.90	0.60	0.18	7.12	-0.10	-4.21	-26.70	0.99	0.96	0.04	1.81	0.00	-0.06	-0.80
	HE_11874	0.35	0.75	0.24	13.42	-0.17	-9.38	-55.95	0.99	0.99	0.03	1.45	-0.01	-0.40	0.33
	HE_12905	0.26	0.67	0.40	11.86	-0.31	-9.28	-14.92	0.92	0.90	0.14	4.01	-0.03	-0.87	-0.82
	HE_12946	0.86	0.18	0.25	8.67	0.08	2.88	-42.39	1.00	0.93	0.04	1.52	0.00	-0.08	-0.33
	HE_13490	0.56	0.75	0.24	11.89	-0.22	-10.47	-28.53	0.98	0.96	0.05	2.43	-0.01	-0.26	-0.23
	HE_13518	0.76	0.87	0.20	9.05	-0.19	-8.38	-53.81	0.99	0.98	0.03	1.47	0.00	0.09	-0.46
	RP_2375118200	0.55	0.78	0.17	14.45	-0.15	-12.17	-14.48	0.95	0.93	0.06	4.64	-0.02	-1.57	-0.59
	RP_2375283300	0.68	0.66	0.20	9.33	-0.11	-5.12	-1.77	0.81	0.74	0.16	7.27	-0.06	-2.56	-0.68
LSTM	ID	NSE	R2	RMSE	rRMSE	Bias	rBias	PI	NSE	R2	RMSE	rRMSE	Bias	rBias	PI
	BW_1-115-8	0.76	0.83	0.15	10.36	-0.10	-6.63	-6.24	0.87	0.86	0.11	7.63	-0.04	-2.48	-2.93
	BW_103-261-4	0.61	0.72	0.23	9.21	-0.15	-6.07	-6.66	0.91	0.89	0.11	4.32	-0.01	-0.44	-0.69
	BW_104-114-5	0.61	0.71	0.26	9.02	-0.14	-4.90	-2.24	0.88	0.88	0.15	4.96	-0.01	-0.35	0.02
	BW_104-307-0	0.49	0.50	0.14	7.58	-0.03	-1.39	-24.89	0.95	0.95	0.04	2.34	-0.01	-0.61	-1.48
	BW_138-019-0	-0.01	0.00	0.11	5.65	-0.04	-2.24	-0.95	0.37	0.29	0.09	4.47	-0.02	-0.78	-0.22
	BW_157-260-8	0.81	0.84	0.12	7.39	0.04	2.36	-4.68	0.96	0.95	0.06	3.54	0.00	0.08	-0.30
	BW_1851-305-1	-0.13	0.15	0.32	17.93	0.24	13.56	-18.79	0.90	0.83	0.09	5.29	0.01	0.61	-0.72
	BW_710-256-3	0.48	0.57	0.29	8.94	-0.12	-3.67	-4.00	0.78	0.79	0.19	5.75	-0.04	-1.28	-1.07
	BW_765-306-3	0.41	0.42	0.49	12.56	-0.15	-3.74	-1.78	0.67	0.66	0.37	9.44	-0.08	-2.16	-0.57
	BW_781-304-2	0.11	0.00	0.53	21.24	-0.48	-19.48	-245.79	0.99	0.95	0.05	1.89	0.00	-0.06	-0.95
	HE_11874	0.45	0.49	0.22	12.31	0.05	2.62	-47.10	0.98	0.98	0.04	2.09	0.00	-0.16	-0.39
	HE_12905	0.20	0.62	0.41	12.27	-0.32	-9.54	-15.66	0.88	0.86	0.16	4.76	-0.03	-0.75	-1.51
	HE_12946	0.46	0.52	0.49	17.02	-0.44	-15.06	-166.68	0.99	0.91	0.05	1.67	0.00	0.05	-0.62
	HE_13490	-0.33	0.62	0.42	20.58	-0.40	-19.35	-87.98	0.98	0.94	0.06	2.68	0.01	0.27	-0.51
	HE_13518	0.33	0.36	0.34	14.99	-0.29	-12.74	-144.04	0.99	0.96	0.04	1.83	0.00	-0.11	-1.16
	RP_2375118200	0.63	0.75	0.16	13.11	-0.12	-10.11	-11.33	0.94	0.91	0.07	5.47	-0.03	-2.40	-1.14
	RP_2375283300	0.41	0.56	0.28	12.82	-0.20	-9.27	-4.15	0.77	0.68	0.17	8.00	-0.05	-2.49	-1.00
CNN	ID	NSE	R2	RMSE	rRMSE	Bias	rBias	PI	NSE	R2	RMSE	rRMSE	Bias	rBias	PI
	BW_1-115-8	0.61	0.75	0.19	13.05	-0.13	-8.83	-10.48	0.89	0.89	0.10	7.00	-0.03	-2.35	-2.30
	BW_103-261-4	0.65	0.72	0.22	8.72	-0.12	-4.73	-5.88	0.92	0.89	0.11	4.25	0.00	-0.19	-0.63
	BW_104-114-5	0.72	0.75	0.22	7.62	-0.07	-2.43	-1.32	0.89	0.89	0.14	4.75	-0.01	-0.34	0.10
	BW_104-307-0	0.61	0.69	0.12	6.67	0.06	3.14	-19.07	0.95	0.95	0.04	2.28	-0.01	-0.28	-1.34
	BW_138-019-0	-0.10	0.03	0.11	5.88	-0.06	-2.96	-1.11	0.36	0.27	0.09	4.51	0.01	0.38	-0.24
	BW_157-260-8	0.83	0.84	0.11	7.00	0.02	1.40	-4.10	0.96	0.95	0.05	3.36	0.00	-0.04	-0.18
	BW_1851-305-1	0.17	0.27	0.28	15.38	0.19	10.87	-13.55	0.90	0.84	0.09	5.30	0.02	1.33	-0.73
	BW_710-256-3	0.51	0.65	0.28	8.61	-0.11	-3.23	-3.64	0.79	0.79	0.18	5.67	-0.03	-0.90	-1.01
	BW_765-306-3	0.47	0.46	0.46	11.85	-0.10	-2.44	-1.47	0.70	0.69	0.35	8.98	-0.07	-1.72	-0.42
	BW_781-304-2	0.30	0.62	0.47	18.84	-0.44	-17.92	-193.19	0.99	0.95	0.05	1.99	0.01	0.22	-1.17
	HE_11874	0.59	0.63	0.19	10.66	0.06	3.29	-35.09	0.99	0.99	0.03	1.75	-0.01	-0.31	0.03
	HE_12905	0.06	0.49	0.45	13.33	-0.33	-9.78	-18.65	0.92	0.90	0.13	3.96	-0.03	-0.78	-0.73
	HE_12946	0.26	0.43	0.58	19.97	-0.56	-19.18	-229.89	0.99	0.90	0.05	1.76	0.00	-0.04	-0.79
	HE_13490	0.82	0.71	0.16	7.55	-0.09	-4.59	-10.99	0.98	0.95	0.05	2.58	0.00	-0.01	-0.40
	HE_13518	0.75	0.62	0.20	9.05	-0.16	-6.89	-51.88	0.99	0.96	0.04	1.97	0.01	0.39	-1.49
	RP_2375118200	0.12	0.79	0.24	20.23	-0.22	-18.58	-28.33	0.95	0.93	0.06	4.75	-0.02	-1.92	-0.62
	RP_2375283300	0.49	0.59	0.26	11.92	-0.18	-8.24	-3.46	0.80	0.74	0.16	7.37	-0.06	-2.63	-0.70

Table S6: Forecasting results of all sequence-to-sequence models.

		Seq2Seq							Seq2Seq (GWLt-1)						
	ID	NSE	R2	RMSE	rRMSE	Bias	rBias	PI	NSE	R2	RMSE	rRMSE	Bias	rBias	PI
NARX	BW_1-115-8	0.68	0.43	0.18	12.38	-0.09	-5.98	0.09	0.59	0.42	0.20	13.74	-0.13	-9.17	-0.26
	BW_103-261-4	0.75	0.51	0.14	5.41	-0.08	-3.38	0.38	0.84	0.63	0.09	3.64	-0.03	-1.00	0.63
	BW_104-114-5	0.59	0.28	0.24	8.03	-0.05	-1.56	0.38	0.60	0.36	0.24	8.14	-0.03	-1.11	0.27
	BW_104-307-0	0.74	0.31	0.07	4.13	0.00	0.00	0.02	0.90	0.55	0.05	2.75	0.01	0.31	0.61
	BW_138-019-0	-0.06	0.08	0.09	4.79	-0.05	-2.40	0.10	0.31	0.10	0.08	4.06	-0.03	-1.48	0.28
	BW_157-260-8	0.88	0.55	0.08	4.63	-0.01	-0.46	0.52	0.72	0.48	0.12	7.07	0.01	0.64	0.20
	BW_1851-305-1	0.73	0.30	0.10	5.51	0.06	3.12	0.06	0.77	0.33	0.09	5.16	0.07	3.75	-0.09
	BW_710-256-3	0.76	0.62	0.12	3.76	-0.03	-0.89	0.81	-0.15	0.16	0.31	9.36	-0.06	-1.82	0.13
	BW_765-306-3	-0.07	0.16	0.52	13.17	-0.21	-5.47	0.05	-0.31	0.21	0.55	14.12	-0.16	-4.17	-0.03
	BW_781-304-2	0.89	0.13	0.14	5.62	-0.10	-4.12	-1.15	0.96	0.34	0.10	3.86	0.01	0.28	0.04
	HE_11874	0.90	0.72	0.07	3.89	-0.02	-0.97	0.78	0.93	0.86	0.06	3.61	0.00	-0.22	0.83
	HE_12905	0.32	0.32	0.25	7.40	-0.01	-0.28	0.11	0.05	0.50	0.33	9.75	-0.04	-1.15	-0.33
	HE_12946	0.89	0.20	0.17	5.92	-0.14	-4.75	-5.97	0.98	0.22	0.08	2.71	0.04	1.24	-0.92
	HE_13490	0.84	0.37	0.08	3.90	-0.03	-1.67	0.48	0.87	0.38	0.10	4.87	0.00	0.06	0.33
	HE_13518	0.88	0.42	0.08	3.60	-0.04	-1.85	0.19	0.77	0.41	0.14	6.02	-0.01	-0.23	-1.14
	RP_2375118200	0.46	0.35	0.14	11.35	-0.07	-5.37	0.02	0.81	0.46	0.08	6.90	-0.03	-2.68	0.60
	RP_2375283300	0.30	0.19	0.23	10.47	-0.17	-7.68	-0.36	0.18	0.19	0.25	11.48	-0.18	-8.28	-0.38
LSTM	ID	NSE	R2	RMSE	rRMSE	Bias	rBias	PI	NSE	R2	RMSE	rRMSE	Bias	rBias	PI
	BW_1-115-8	0.24	0.70	0.22	15.28	-0.17	-11.65	-0.49	0.57	0.66	0.18	12.34	-0.08	-5.30	0.05
	BW_103-261-4	0.46	0.62	0.22	8.73	-0.15	-5.92	-0.69	0.74	0.65	0.14	5.46	-0.04	-1.57	0.26
	BW_104-114-5	0.51	0.46	0.25	8.60	-0.01	-0.48	0.34	0.56	0.37	0.27	9.26	0.02	0.82	0.32
	BW_104-307-0	0.78	0.68	0.09	4.79	0.05	2.51	-0.58	0.86	0.75	0.07	3.69	0.01	0.38	0.35
	BW_138-019-0	0.00	0.37	0.09	4.66	-0.04	-2.05	0.10	0.00	0.40	0.09	4.55	-0.02	-0.95	0.07
	BW_157-260-8	0.38	0.60	0.18	10.82	-0.13	-8.04	-1.19	0.72	0.67	0.10	6.44	0.00	0.28	0.28
	BW_1851-305-1	-0.06	0.41	0.28	15.57	0.25	13.79	-4.12	0.61	0.47	0.13	7.13	0.07	3.67	-0.42
	BW_710-256-3	-0.12	0.51	0.28	8.64	0.01	0.27	-0.01	-0.27	0.47	0.30	9.31	-0.05	-1.62	0.12
	BW_765-306-3	-0.12	0.34	0.56	14.33	-0.15	-3.84	0.04	-0.03	0.30	0.58	14.84	-0.17	-4.37	0.01
	BW_781-304-2	0.29	0.01	0.44	17.70	-0.43	-17.37	-15.22	0.95	0.61	0.09	3.66	0.01	0.32	-0.27
	HE_11874	0.80	0.92	0.14	7.54	-0.01	-0.41	0.36	0.85	0.92	0.09	4.94	-0.01	-0.57	0.73
	HE_12905	-0.01	0.49	0.34	10.14	-0.25	-7.35	-0.43	0.15	0.55	0.26	7.73	-0.19	-5.77	-0.17
	HE_12946	-0.47	0.32	0.81	27.99	-0.81	-27.89	-113.32	0.99	0.37	0.05	1.80	0.01	0.41	0.09
	HE_13490	-0.08	0.43	0.30	14.72	-0.30	-14.47	-4.39	0.75	0.37	0.17	8.03	-0.01	-0.35	-0.28
	HE_13518	0.40	0.63	0.32	14.20	-0.32	-13.96	-5.50	0.96	0.74	0.06	2.87	-0.02	-0.71	0.49
	RP_2375118200	0.12	0.62	0.21	17.73	-0.20	-16.81	-1.49	0.60	0.68	0.13	10.94	-0.05	-4.54	0.05
	RP_2375283300	0.07	0.38	0.29	13.37	-0.24	-11.02	-0.92	0.22	0.22	0.25	11.52	-0.21	-9.65	-0.64
CNN	ID	NSE	R2	RMSE	rRMSE	Bias	rBias	PI	NSE	R2	RMSE	rRMSE	Bias	rBias	PI
	BW_1-115-8	0.49	0.60	0.22	15.25	-0.16	-10.96	-0.41	0.45	0.54	0.18	12.67	-0.11	-7.36	-0.31
	BW_103-261-4	0.54	0.65	0.21	8.29	-0.13	-5.26	-0.69	0.71	0.63	0.13	5.20	-0.02	-0.80	0.18
	BW_104-114-5	0.57	0.43	0.30	10.34	-0.04	-1.24	0.09	0.55	0.47	0.24	8.36	0.01	0.47	0.30
	BW_104-307-0	0.49	0.59	0.12	6.67	0.09	4.93	-0.91	0.83	0.66	0.07	3.64	-0.02	-0.89	0.16
	BW_138-019-0	0.00	0.26	0.09	4.65	-0.04	-2.17	0.13	0.04	0.23	0.09	4.62	-0.03	-1.56	0.08
	BW_157-260-8	0.45	0.65	0.17	10.42	-0.08	-4.83	-0.91	0.62	0.66	0.13	8.03	0.00	0.01	-0.09
	BW_1851-305-1	-0.18	0.48	0.28	15.74	0.25	14.15	-3.98	0.57	0.52	0.13	7.03	0.09	4.77	-0.67
	BW_710-256-3	0.07	0.41	0.30	9.09	0.01	0.17	0.16	0.00	0.45	0.29	9.01	0.01	0.30	0.22
	BW_765-306-3	-0.28	0.32	0.56	14.41	-0.26	-6.64	-0.03	-0.16	0.35	0.55	13.99	-0.17	-4.28	0.05
	BW_781-304-2	0.23	0.06	0.45	18.33	-0.44	-17.94	-17.34	0.96	0.36	0.10	3.95	-0.02	-0.87	-0.70
	HE_11874	0.66	0.90	0.16	9.07	0.01	0.50	0.18	0.87	0.95	0.08	4.40	0.00	0.03	0.79
	HE_12905	-0.42	0.46	0.34	9.99	-0.28	-8.45	-0.68	0.36	0.49	0.27	7.97	-0.03	-0.83	-0.02
	HE_12946	0.46	0.09	0.50	17.33	-0.50	-17.26	-66.68	0.98	0.30	0.09	2.94	-0.02	-0.75	-0.85
	HE_13490	0.62	0.37	0.19	9.22	-0.16	-7.58	-1.64	0.83	0.57	0.14	6.63	0.00	-0.11	0.20
	HE_13518	0.43	0.54	0.28	12.17	-0.27	-11.96	-3.08	0.93	0.75	0.07	3.30	0.03	1.16	0.38
	RP_2375118200	0.22	0.50	0.19	15.55	-0.18	-14.46	-0.67	0.61	0.63	0.14	11.18	-0.05	-3.86	0.18
	RP_2375283300	0.14	0.27	0.30	13.60	-0.24	-11.03	-0.88	0.42	0.18	0.22	10.19	-0.13	-5.93	-0.24

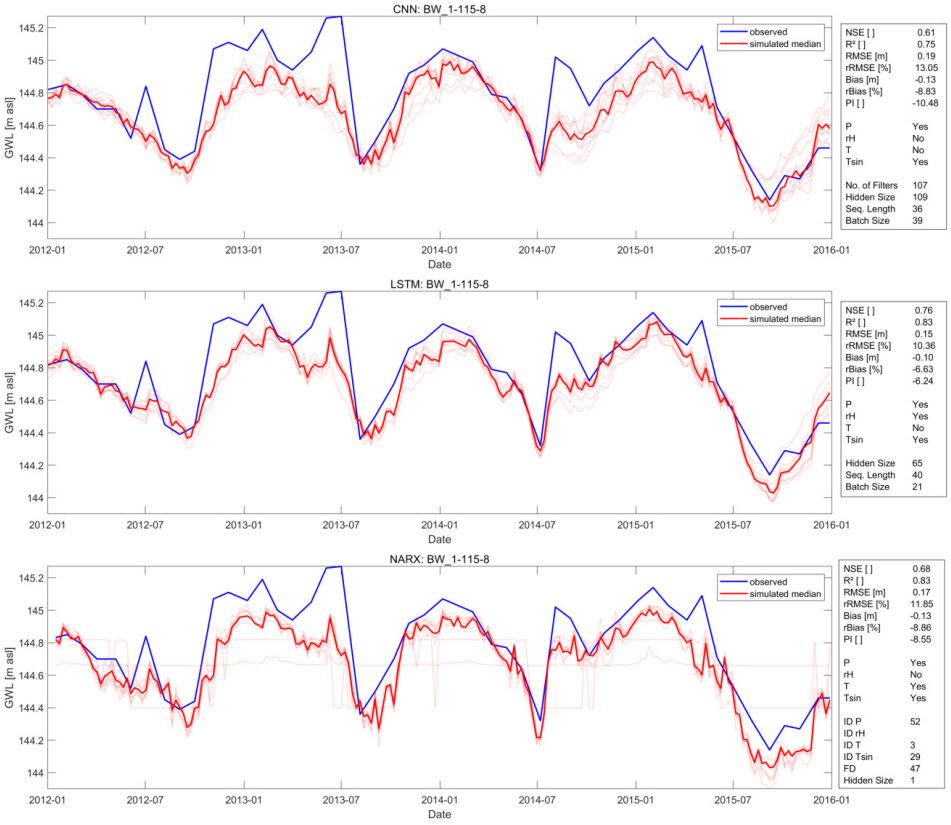

Figure S1: Seq2Val test results for well BW_1-115-8

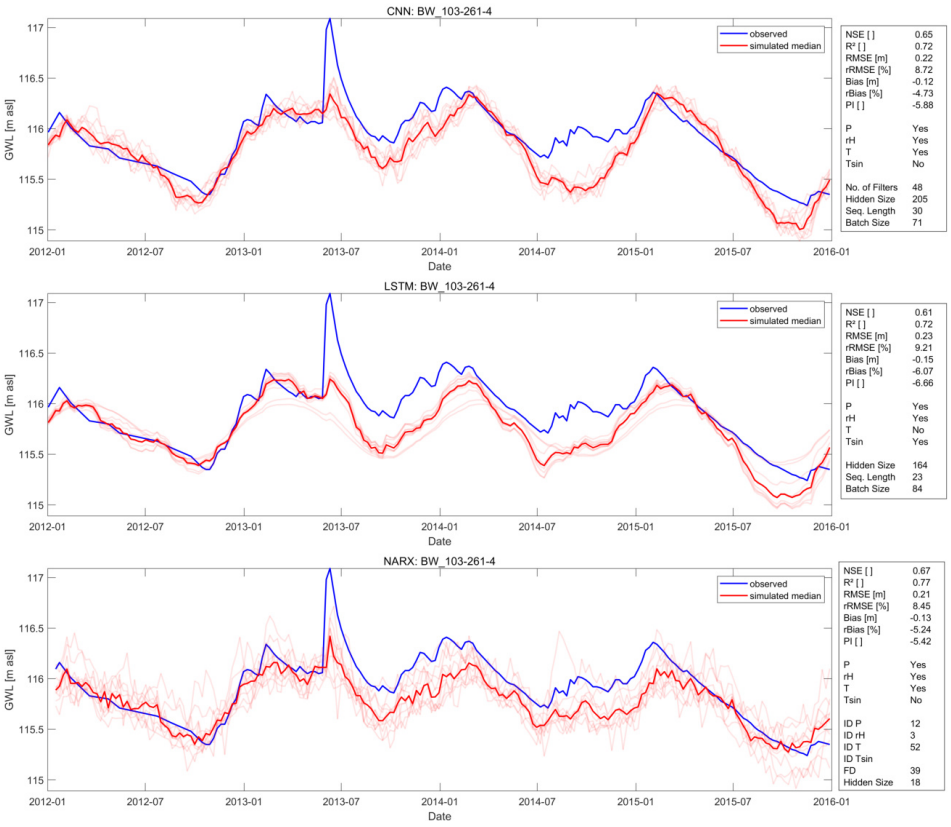

Figure S2: Seq2Val test results for well BW_103-261-4

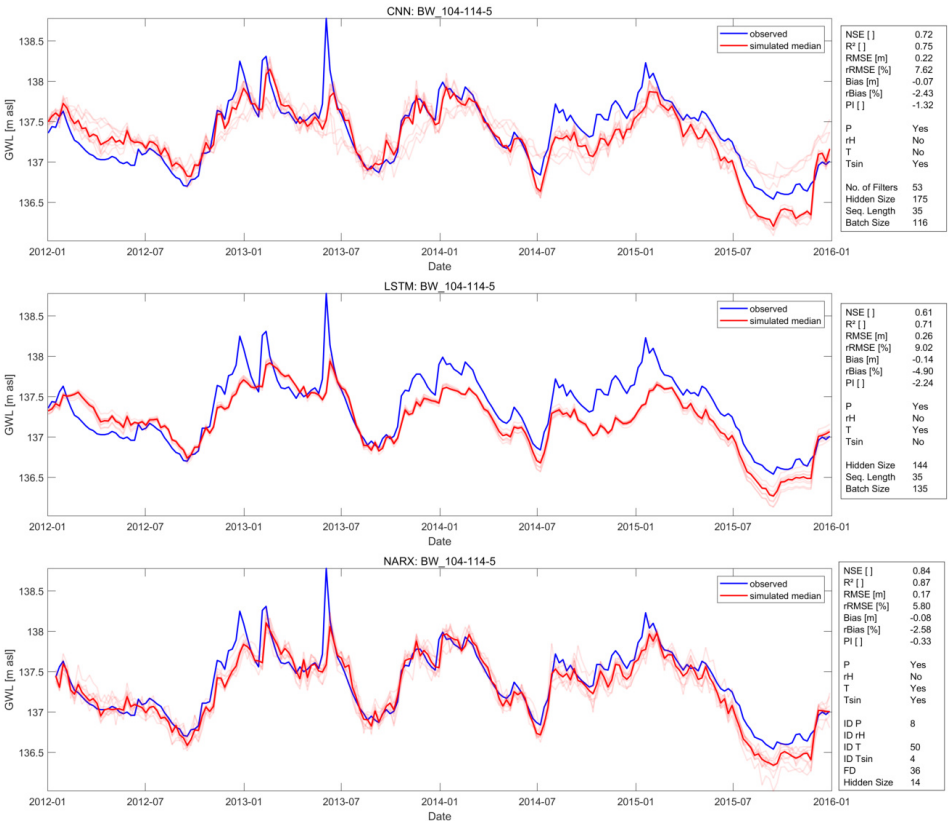

Figure S3: Seq2Val test results for well BW_104-114-5

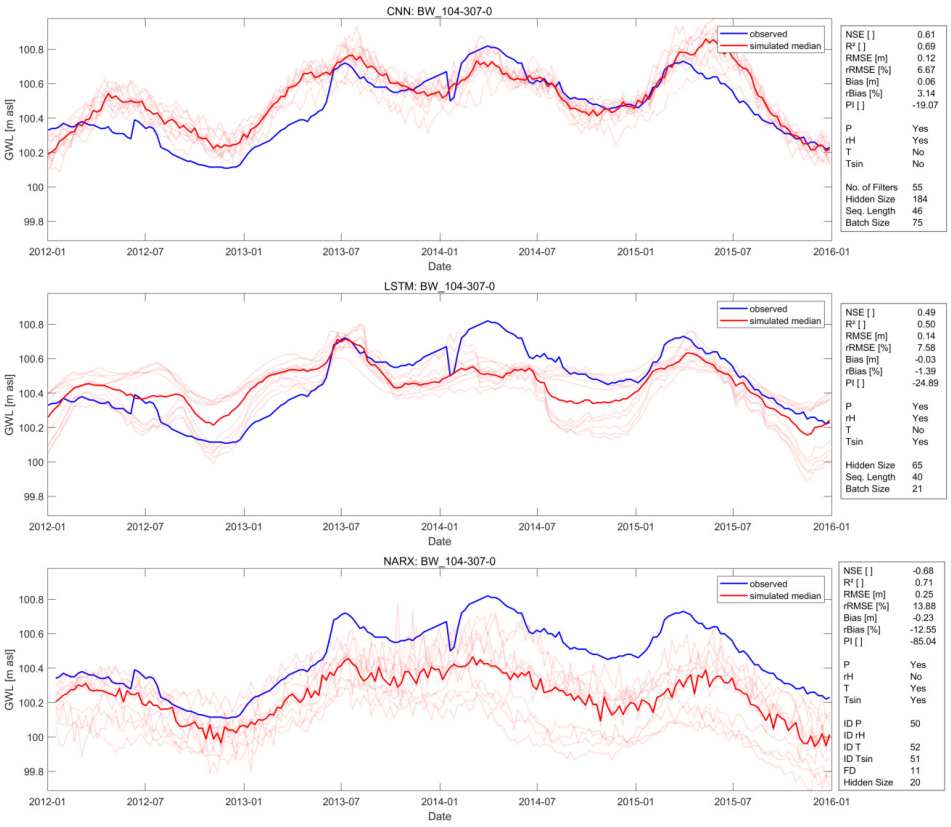

Figure S4: Seq2Val test results for well BW_104-307-0

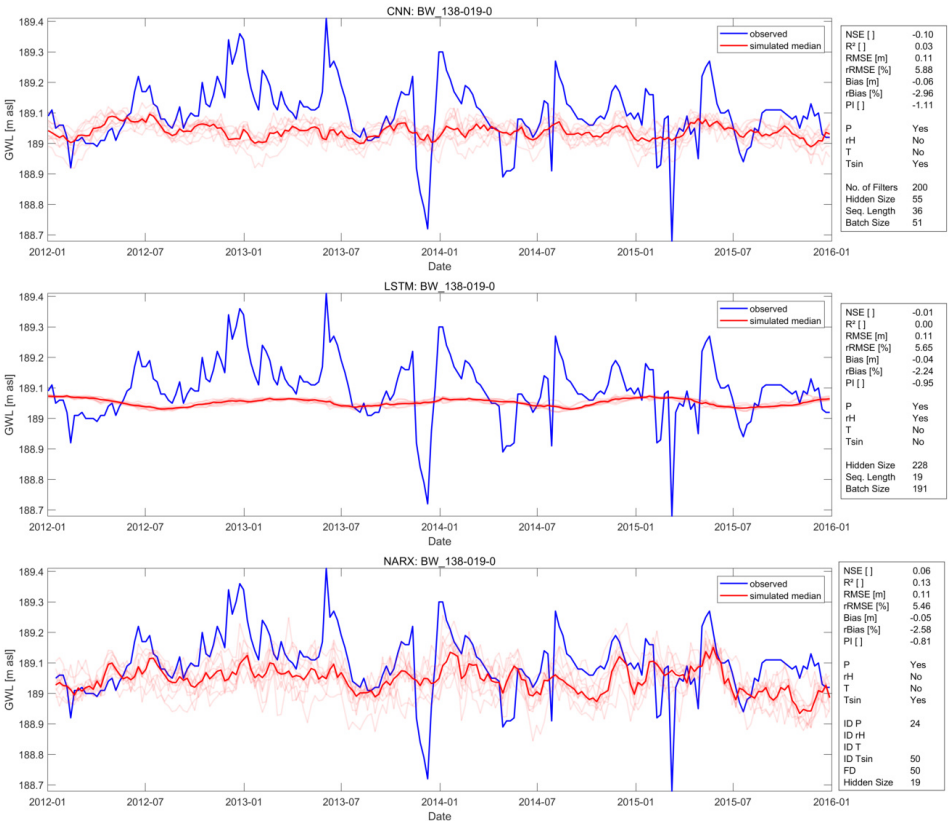

Figure S5: Seq2Val test results for well BW_138-019-0

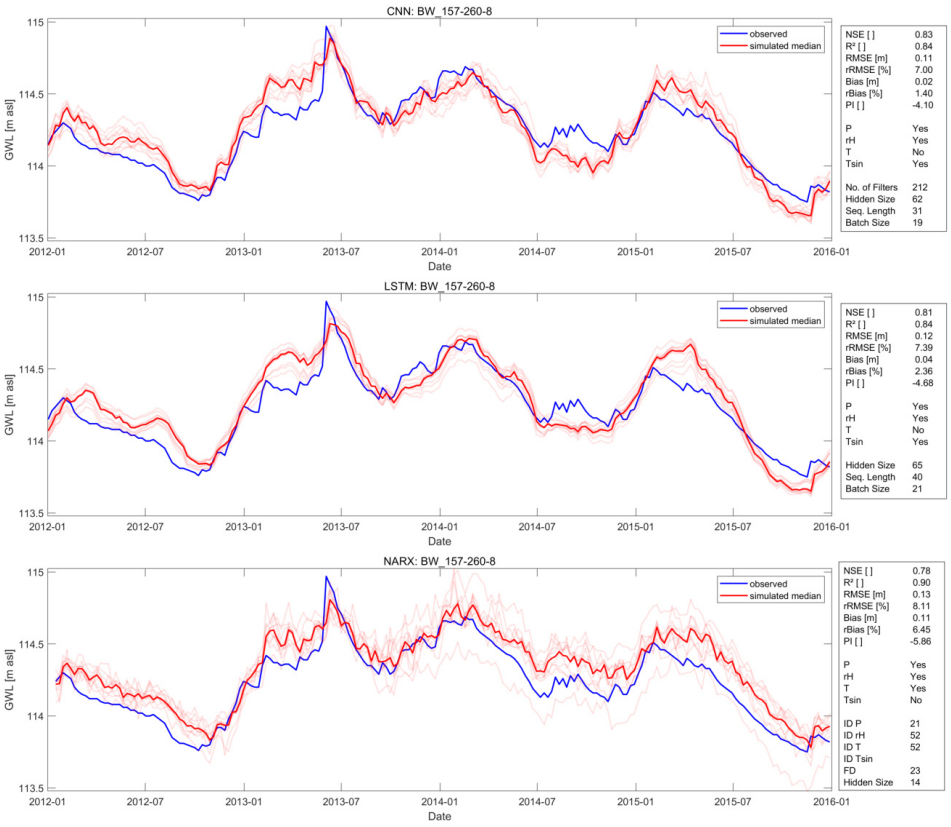

Figure S6: Seq2Val test results for well BW_157-260-8

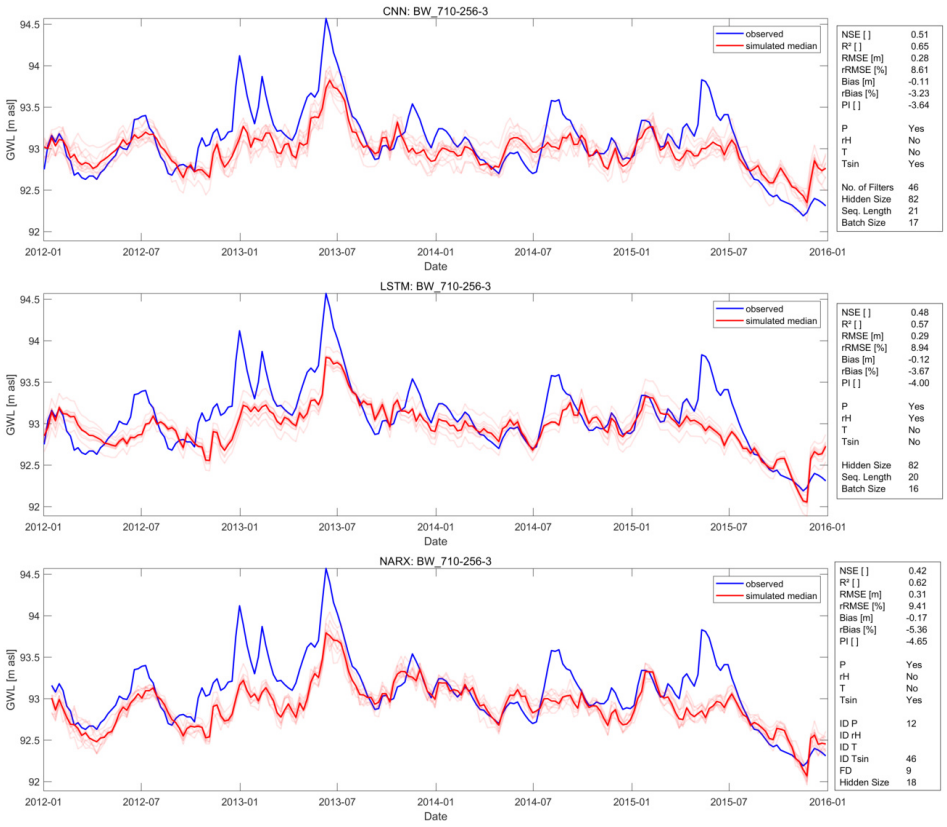

Figure S7: Seq2Val test results for well BW_710-256-3

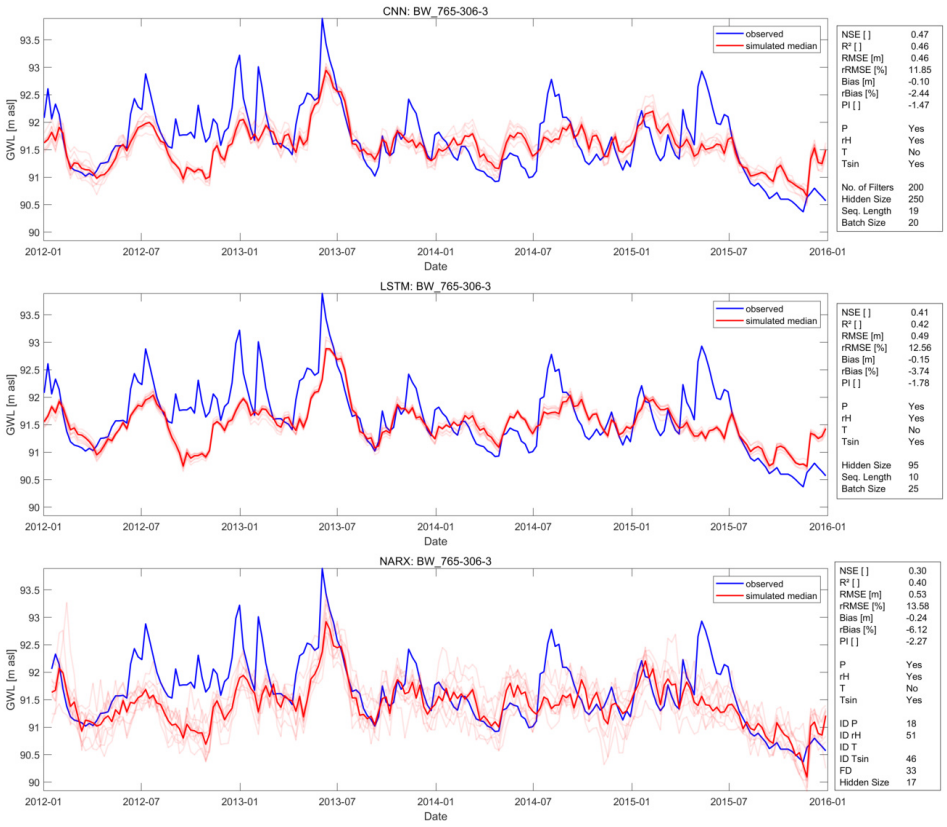

Figure S8: Seq2Val test results for well BW_765-306-3

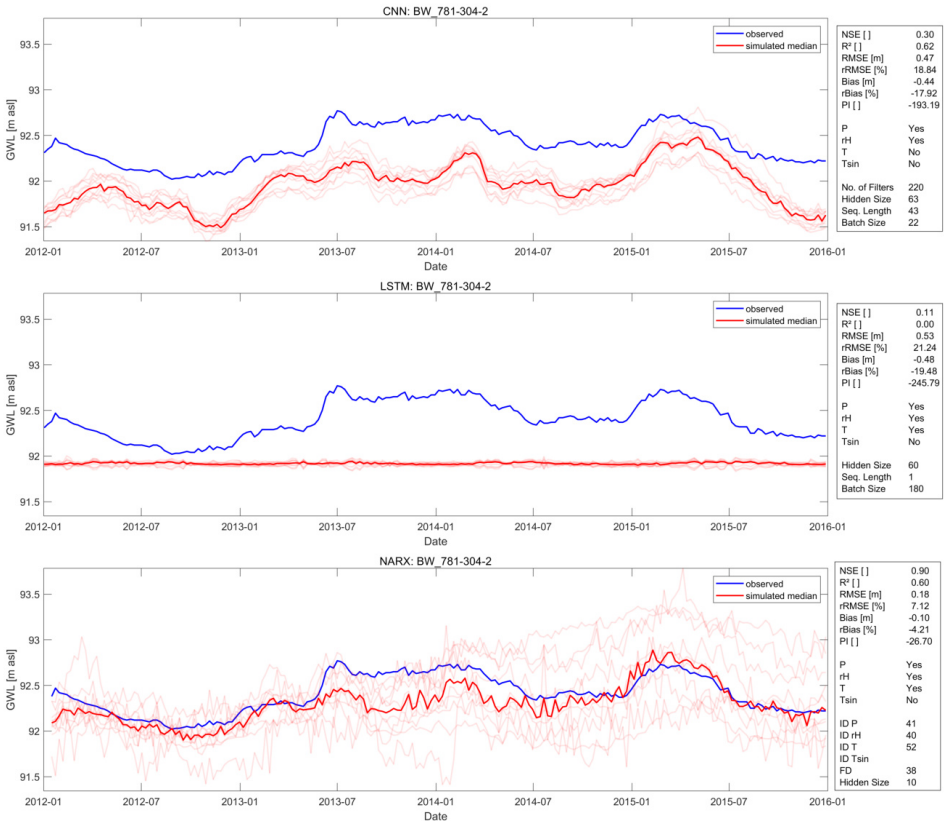

Figure S9: Seq2Val test results for well BW_781-304-2

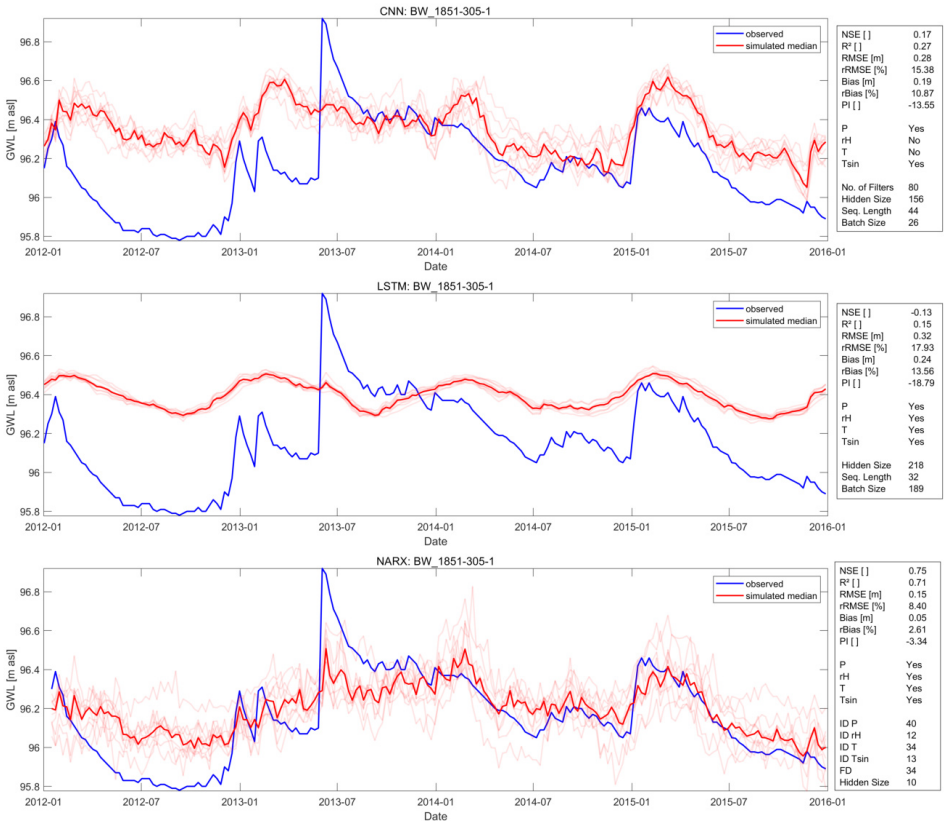

Figure S10: Seq2Val test results for well BW_1851-305-1

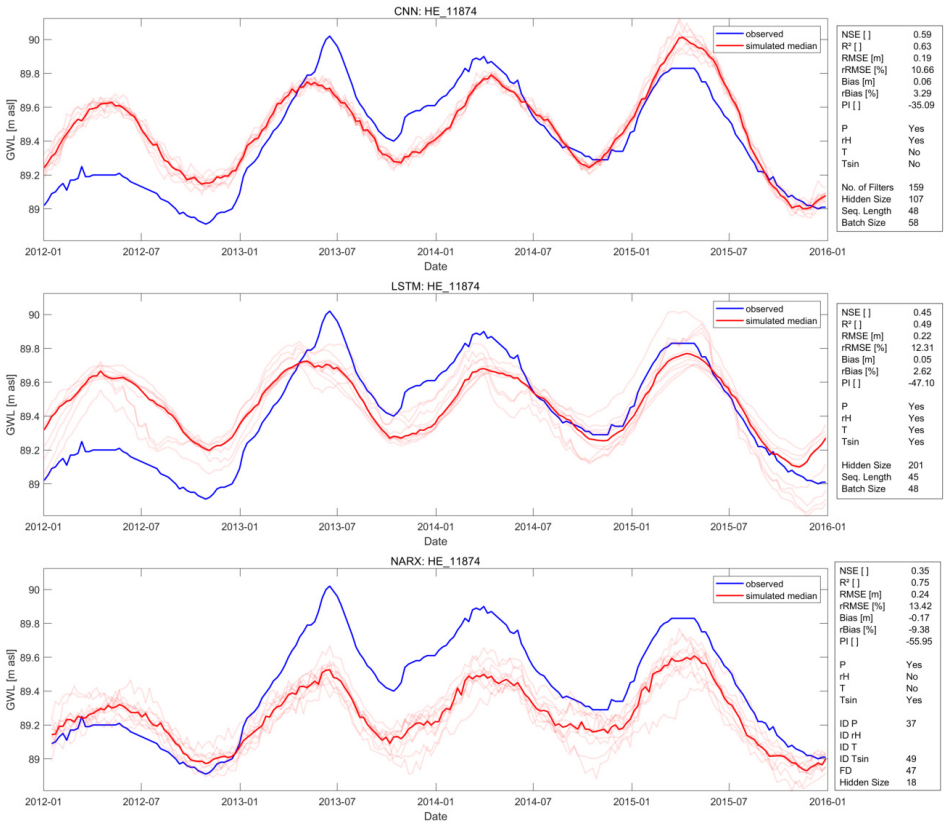

Figure S11: Seq2Val test results for well HE_11874

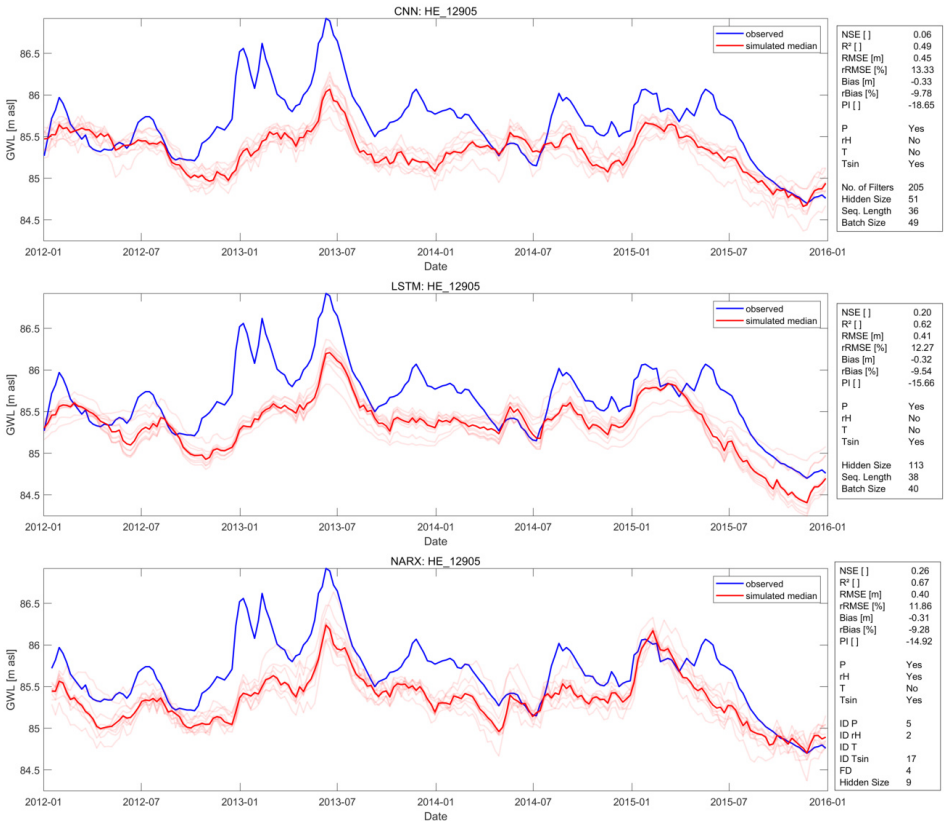

Figure S12: Seq2Val test results for well HE_12905

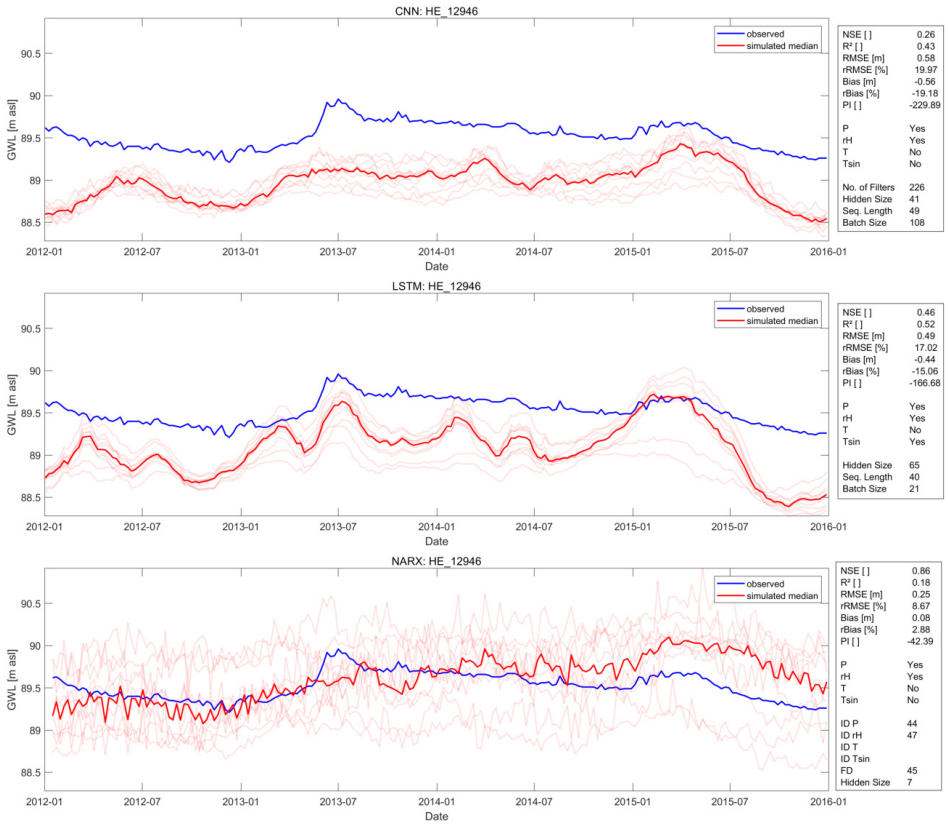

Figure S13: Seq2Val test results for well HE_12946

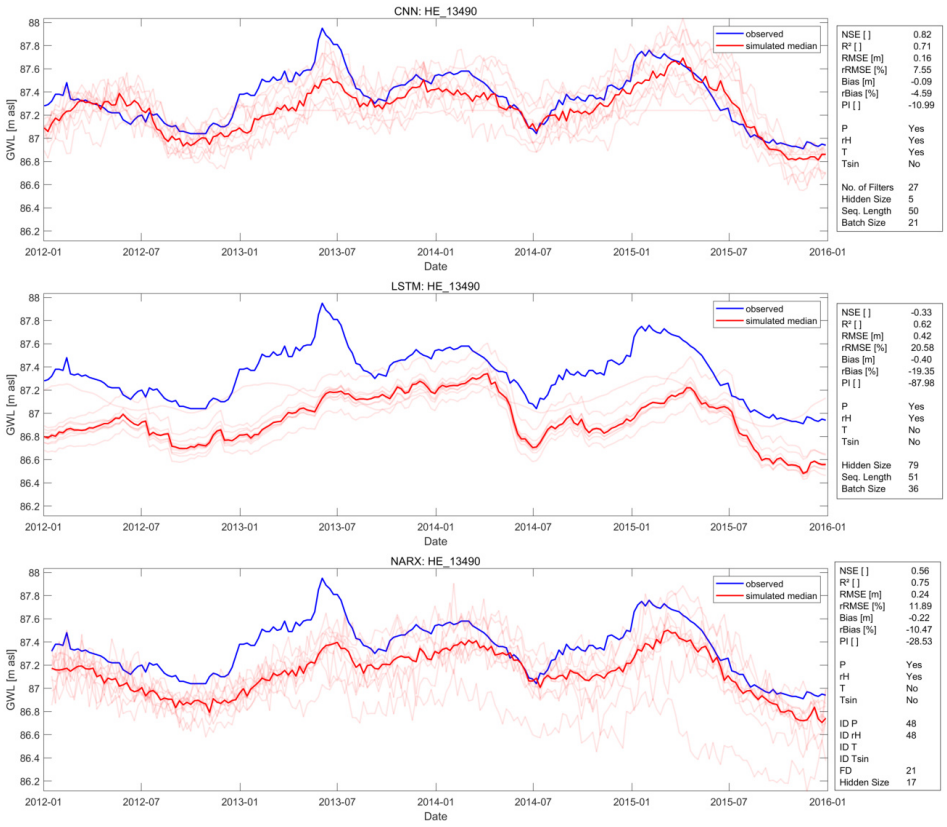

Figure S14: Seq2Val test results for well HE_13490

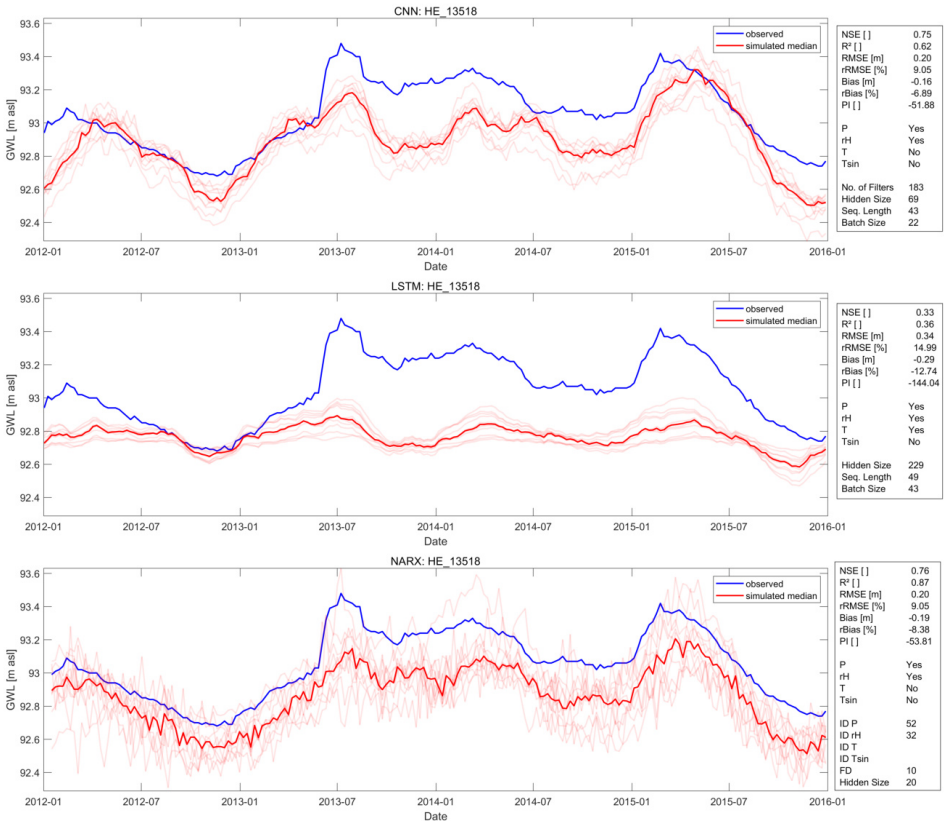

Figure S15: Seq2Val test results for well HE_13518

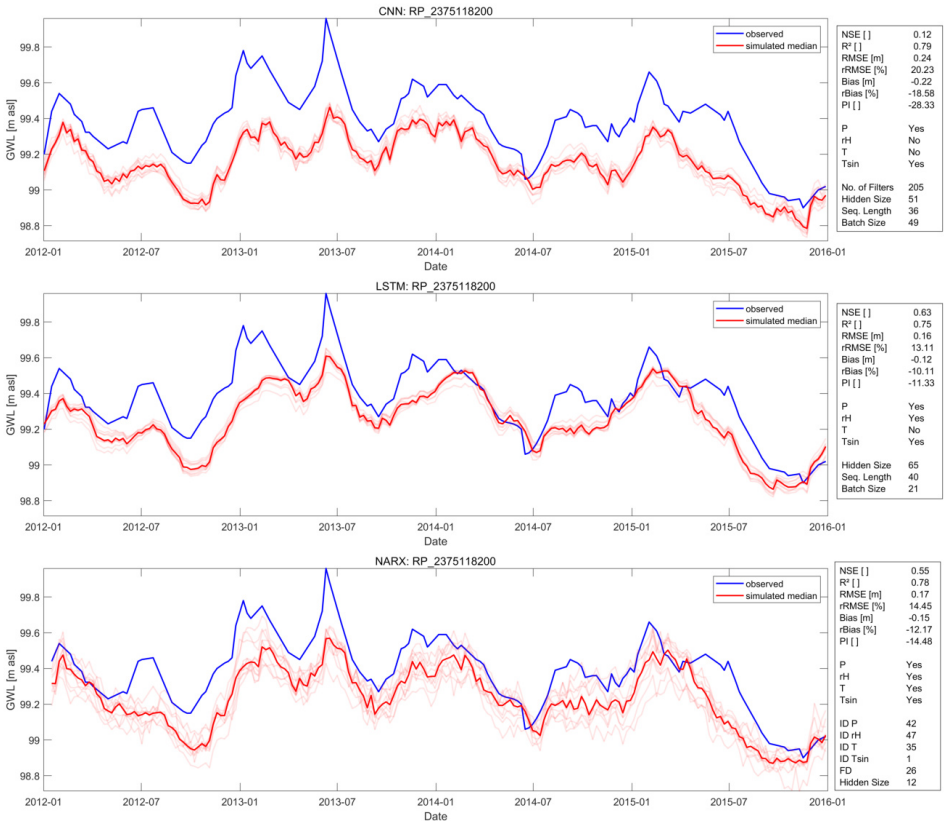

Figure S16: Seq2Val test results for well RP_2375118200

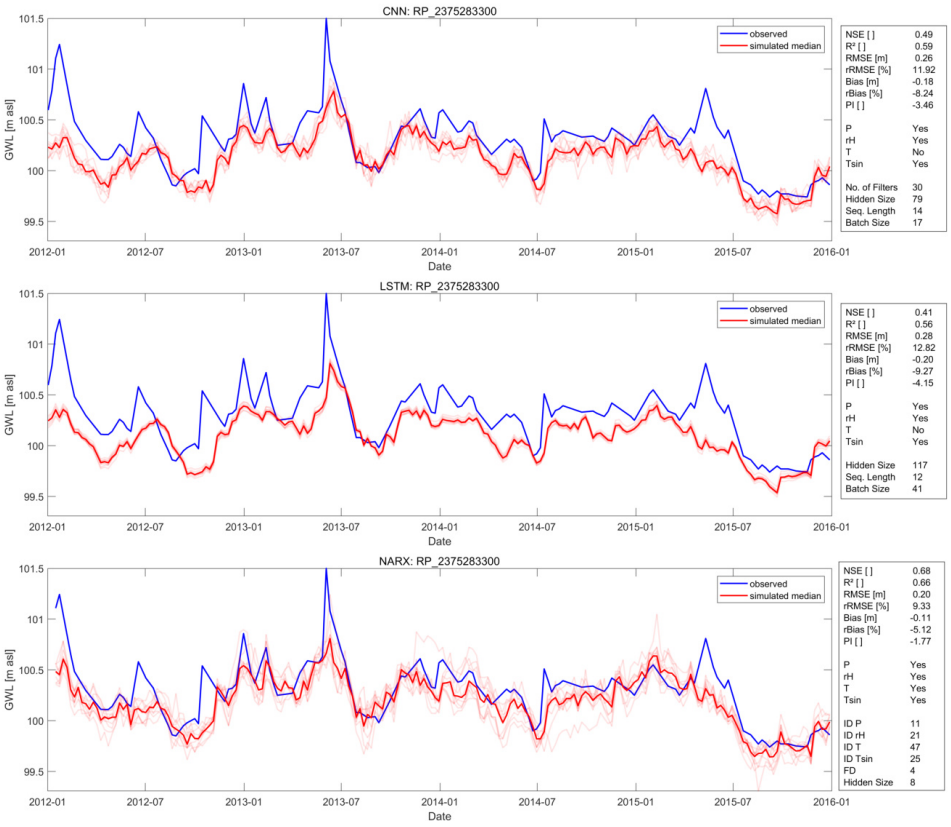

Figure S17: Seq2Val test results for well RP_2375283300

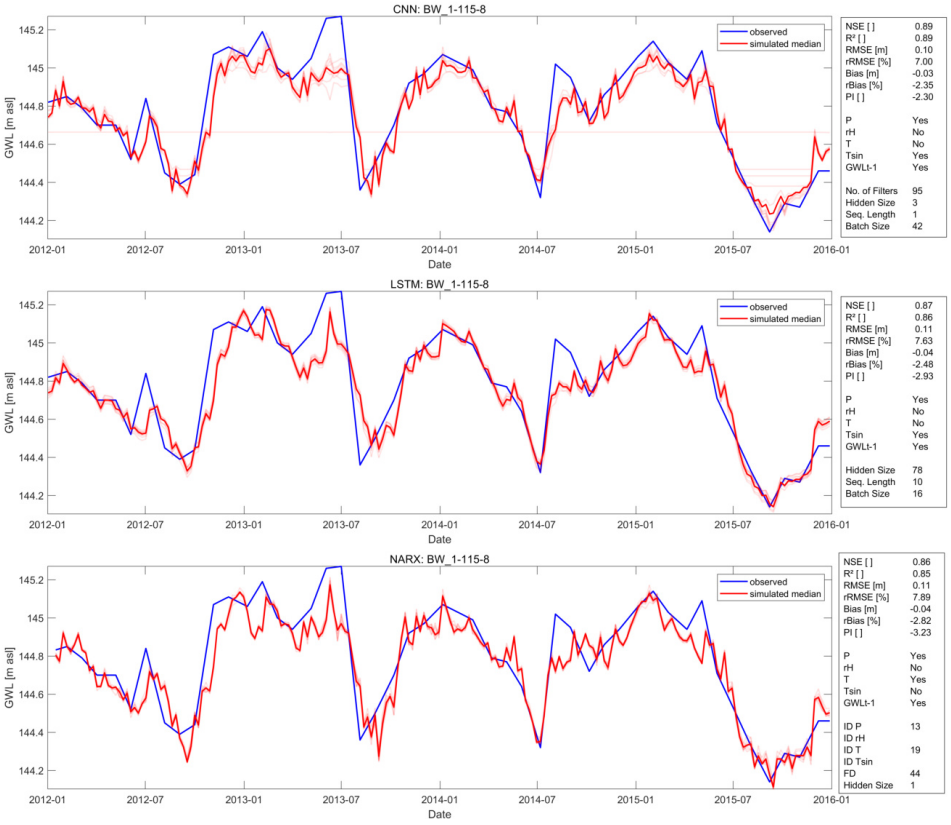

Figure S18: Seq2Val GWL_{t-1} test results for well BW_1-115-8

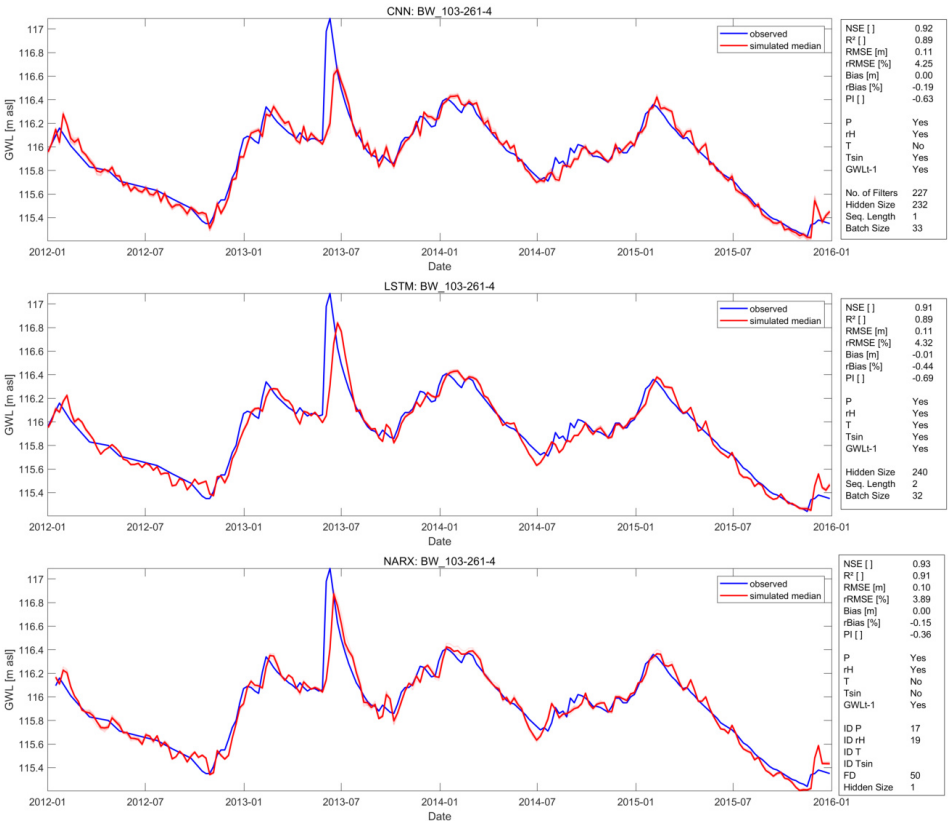

Figure S19: Seq2Val GWL_{t-1} test results for well BW_103-261-4

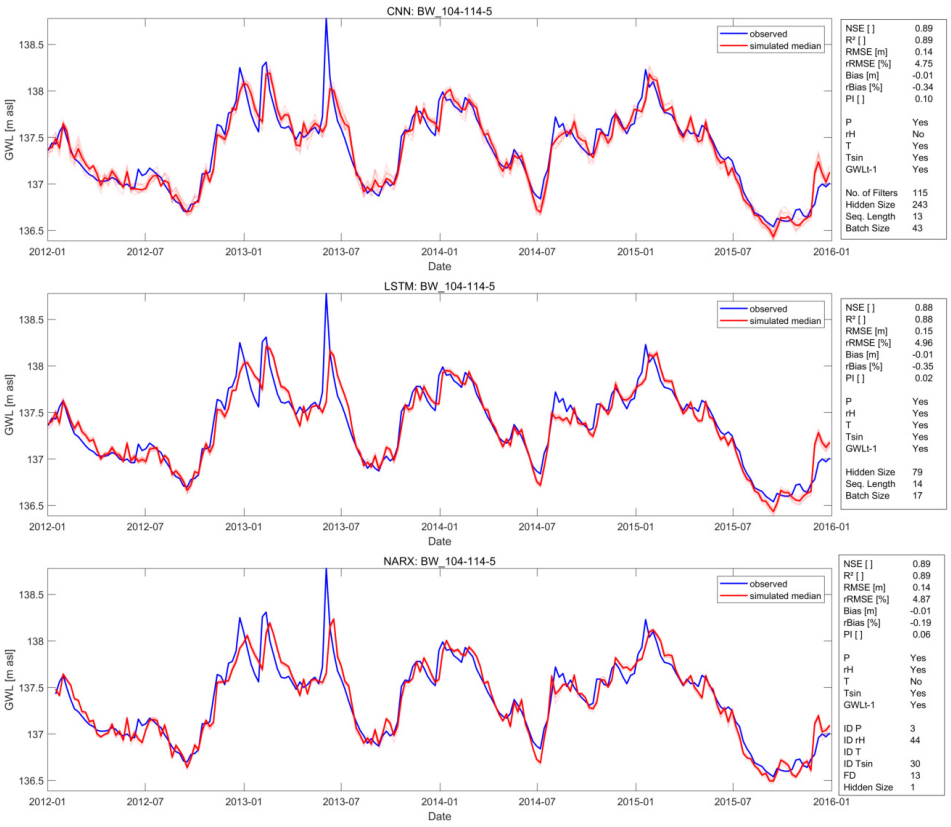

Figure S20: Seq2Val GWL_{t-1} test results for well BW_104-114-5

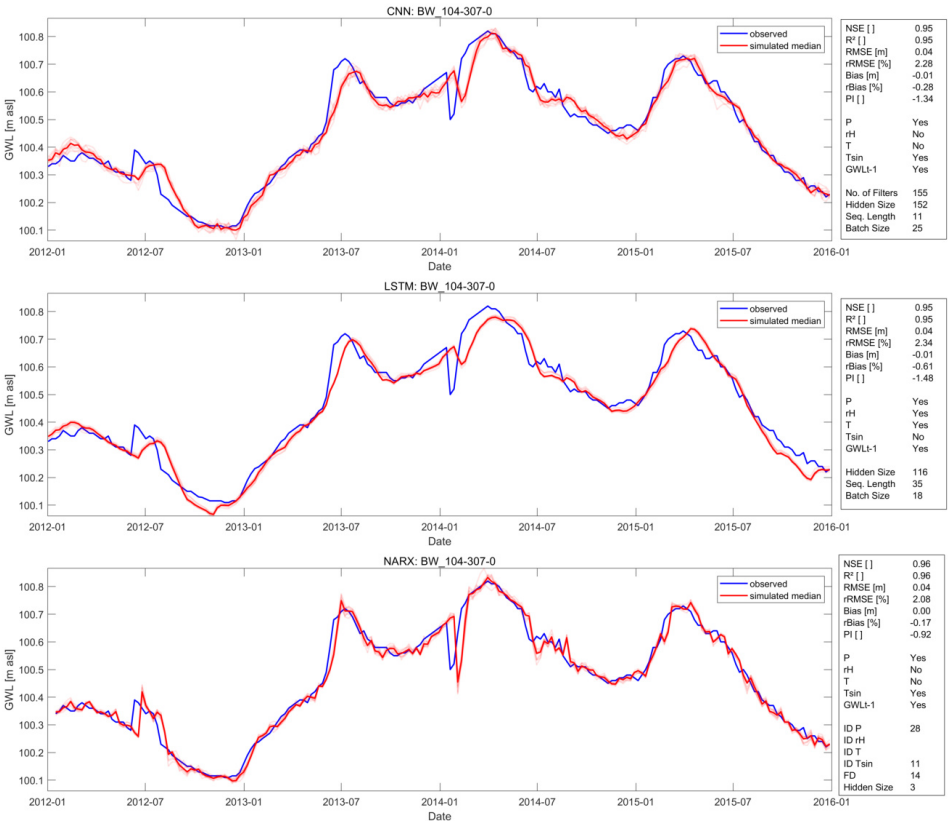

Figure S21: Seq2Val GWL_{t-1} test results for well BW_104-307-0

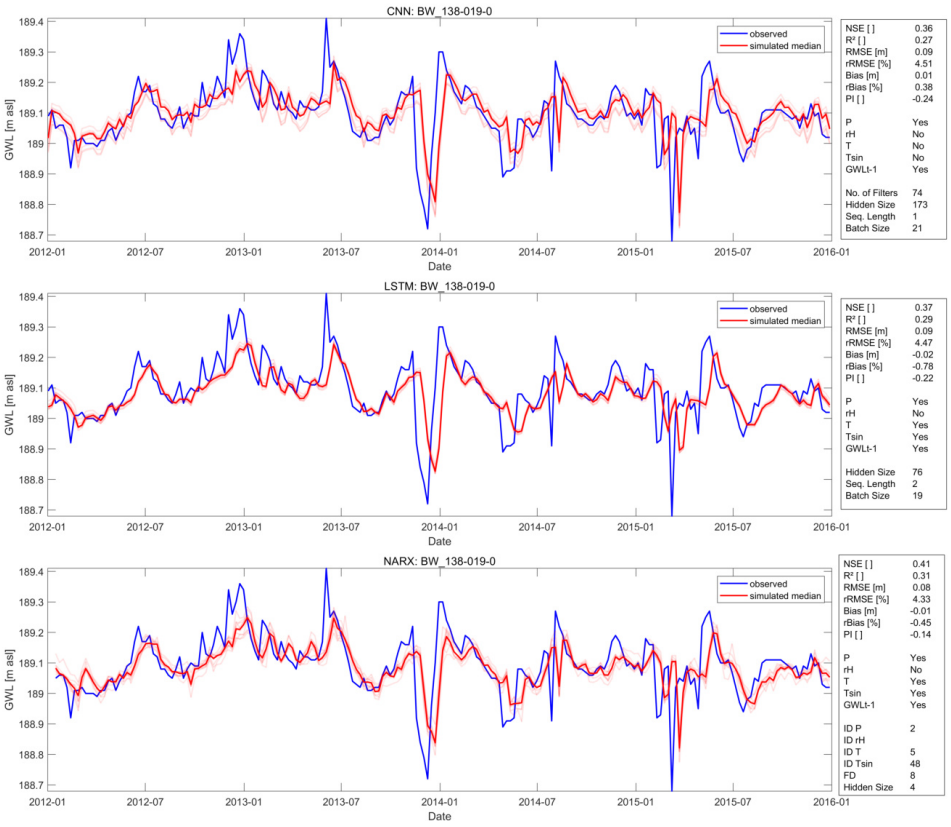

Figure S22: Seq2Val GWL_{t-1} test results for well BW_138-019-0

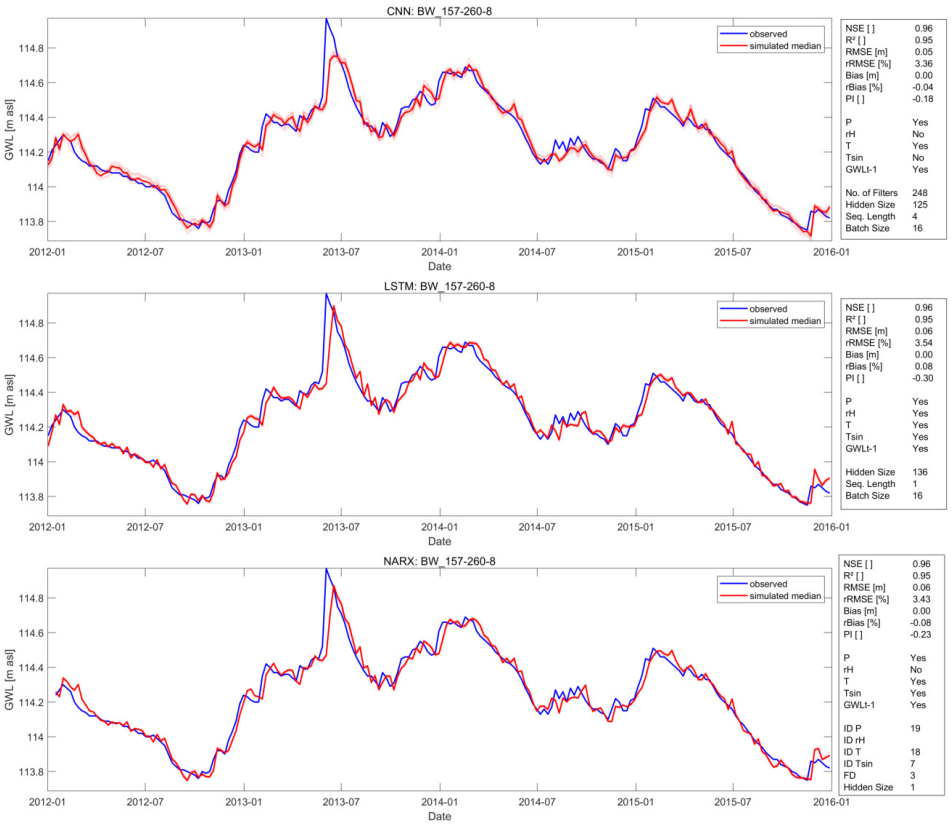

Figure S23: Seq2Val GWL_{t-1} test results for well BW_157-260-8

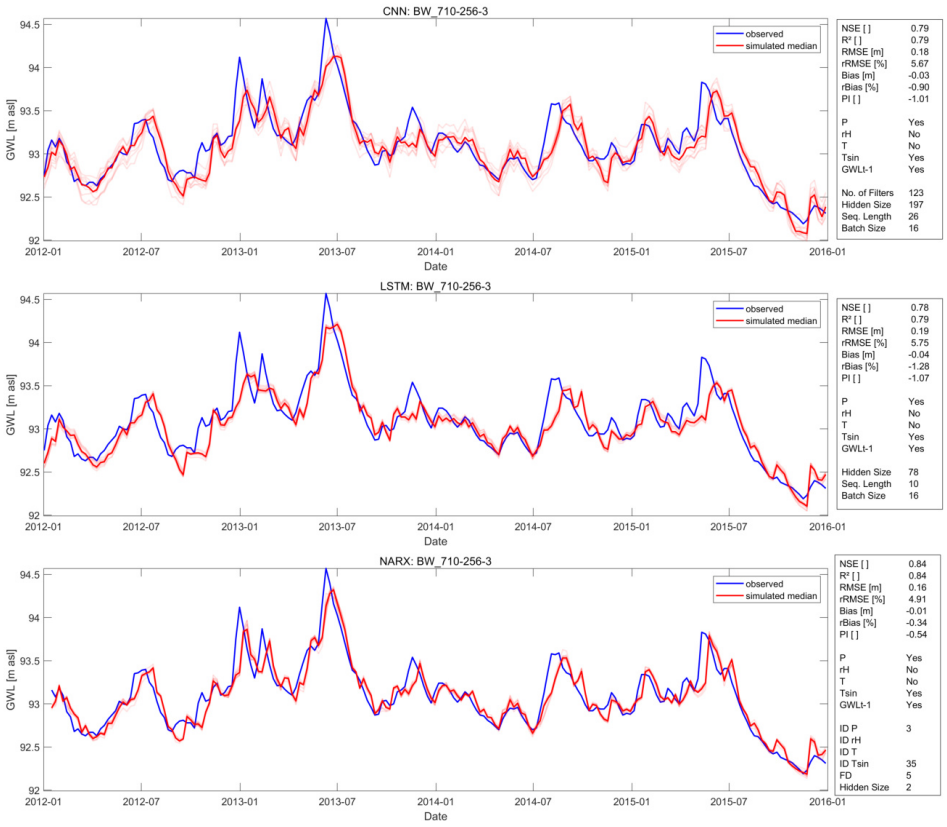

Figure S24: Seq2Val GWL_{t-1} test results for well BW_710-256-3

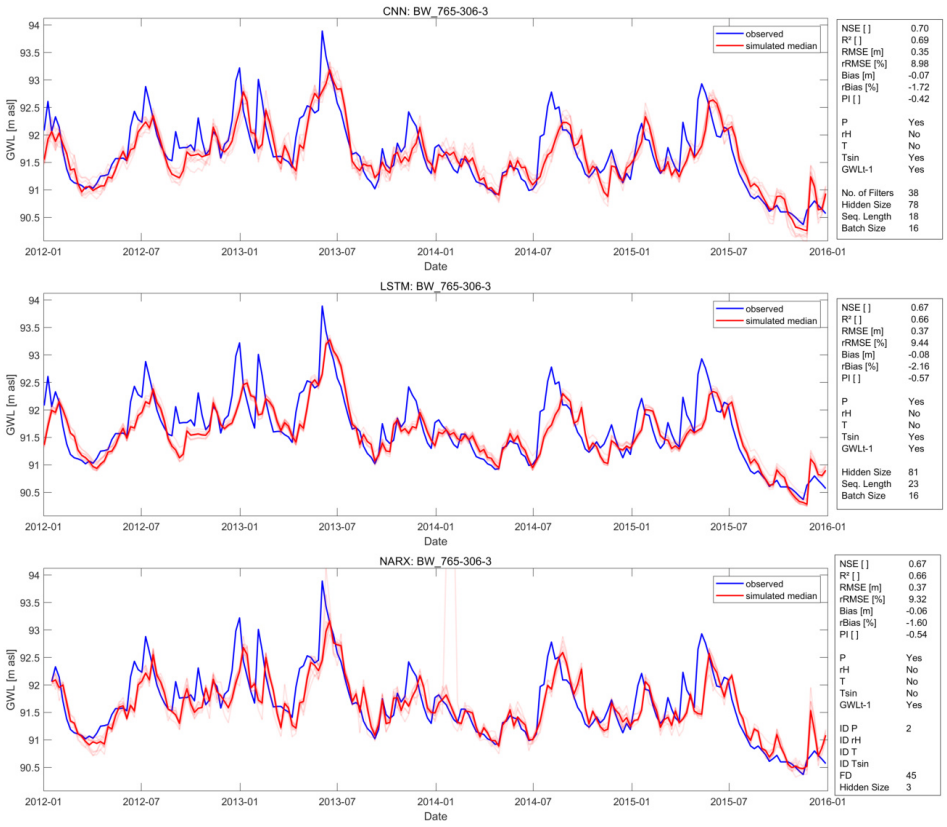

Figure S25: Seq2Val GWL_{t-1} test results for well BW_765-306-3

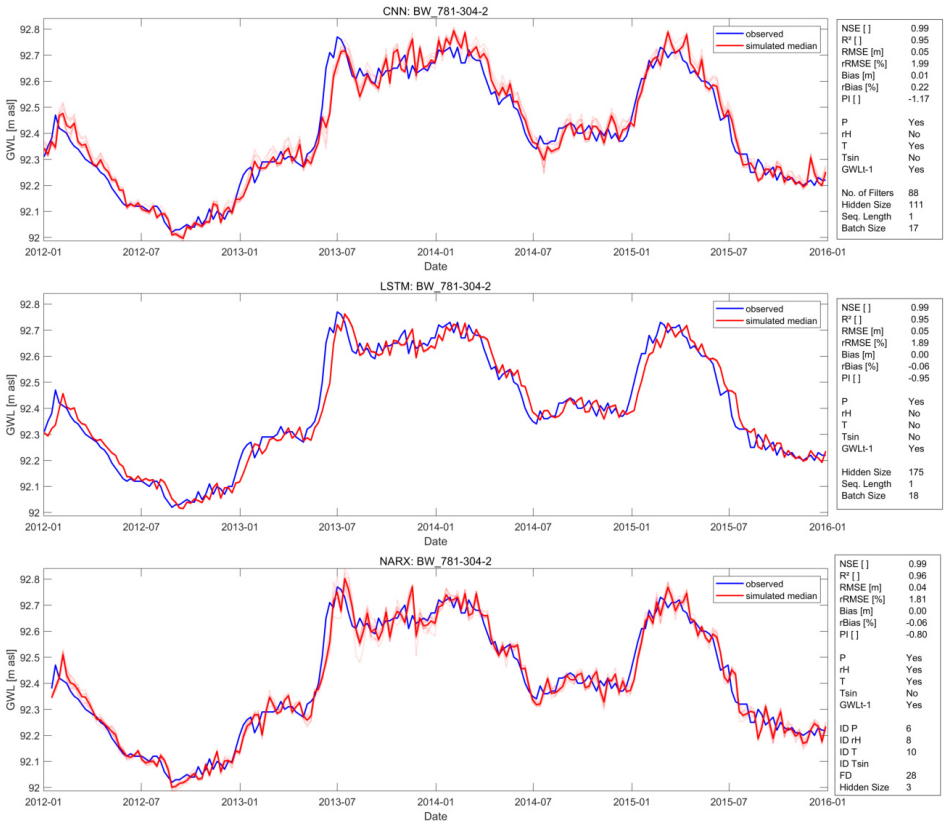

Figure S26: Seq2Val GWL_{t-1} test results for well BW_781-304-2

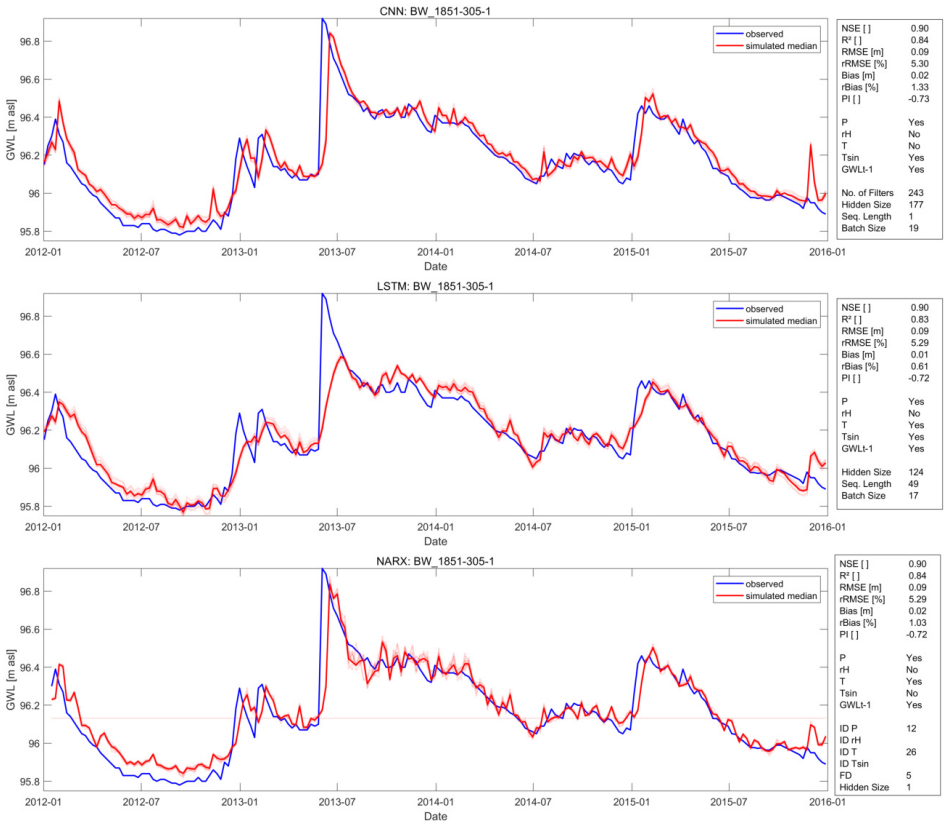

Figure S27: Seq2Val GWL_{t-1} test results for well BW_1851-305-1

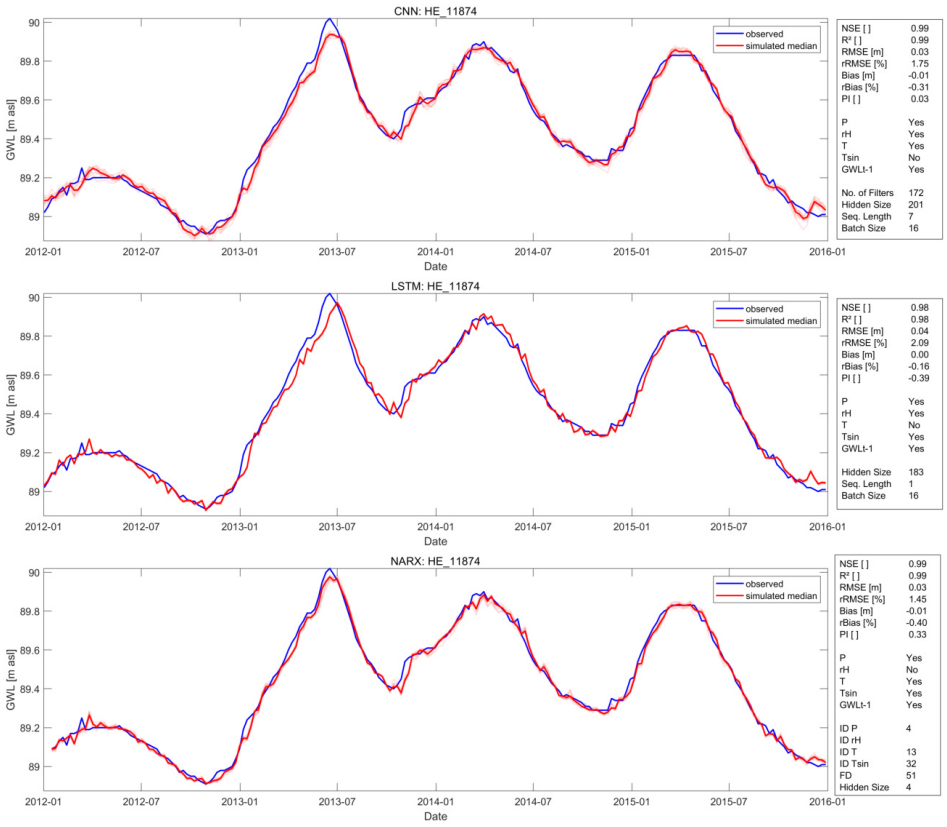

Figure S28: Seq2Val GWL_{t-1} test results for well HE_11874

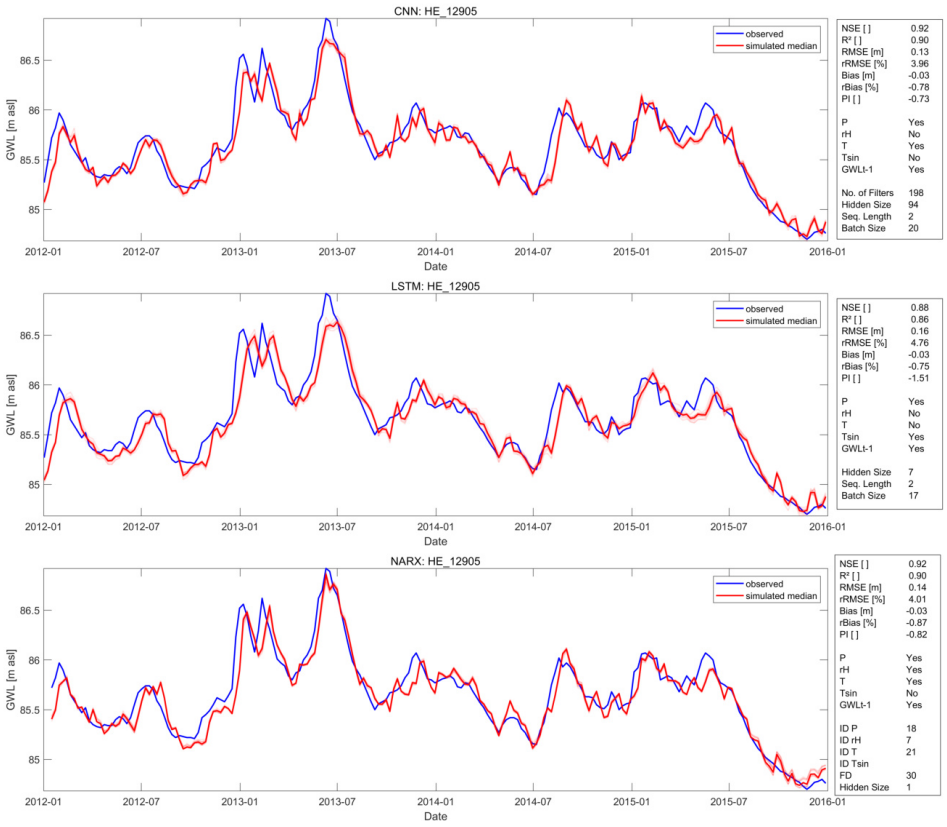

Figure S29: Seq2Val GWL_{t-1} test results for well HE_12905

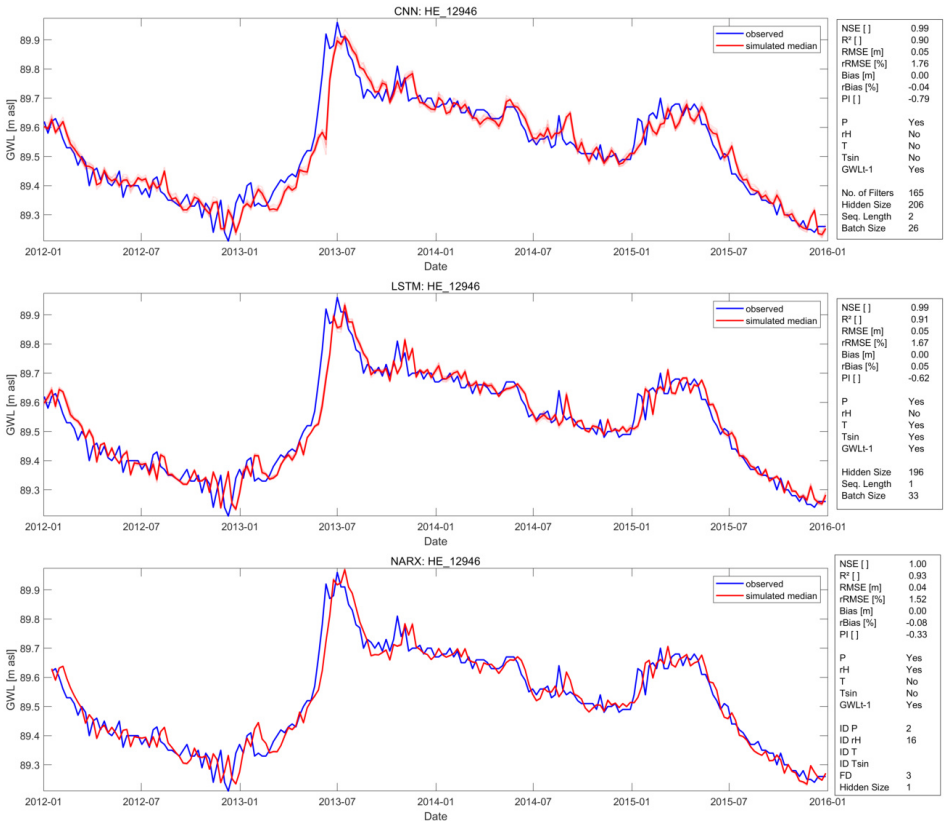

Figure S30: Seq2Val GWL_{t-1} test results for well HE_12946

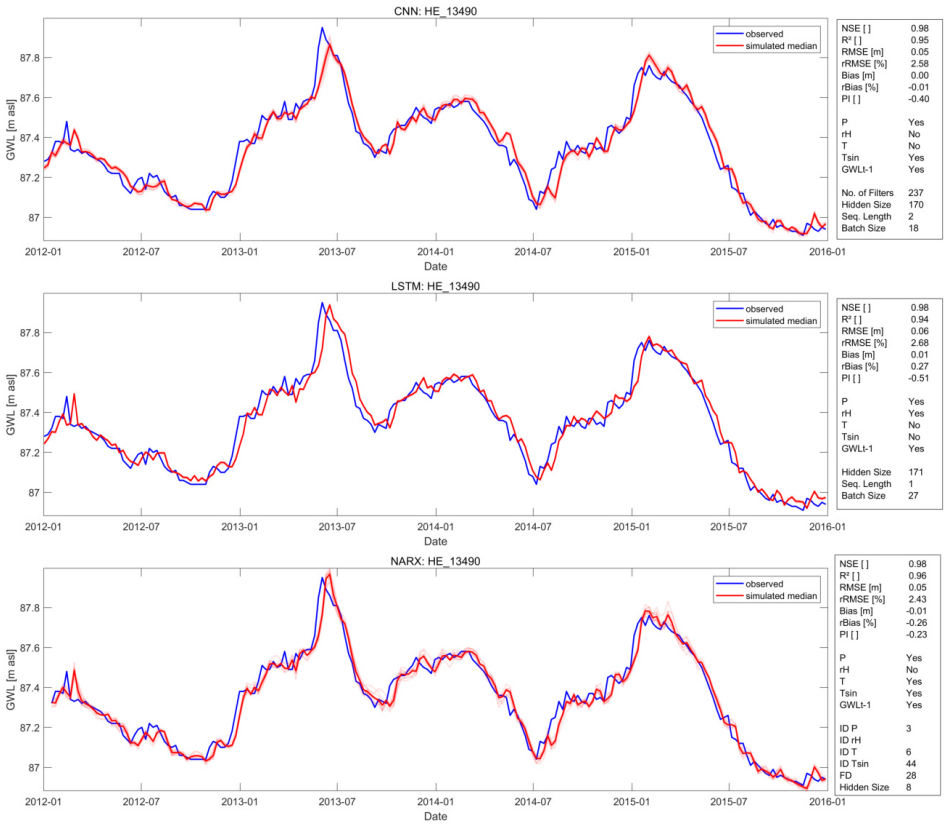

Figure S31: Seq2Val GWL_{t-1} test results for well HE_13490

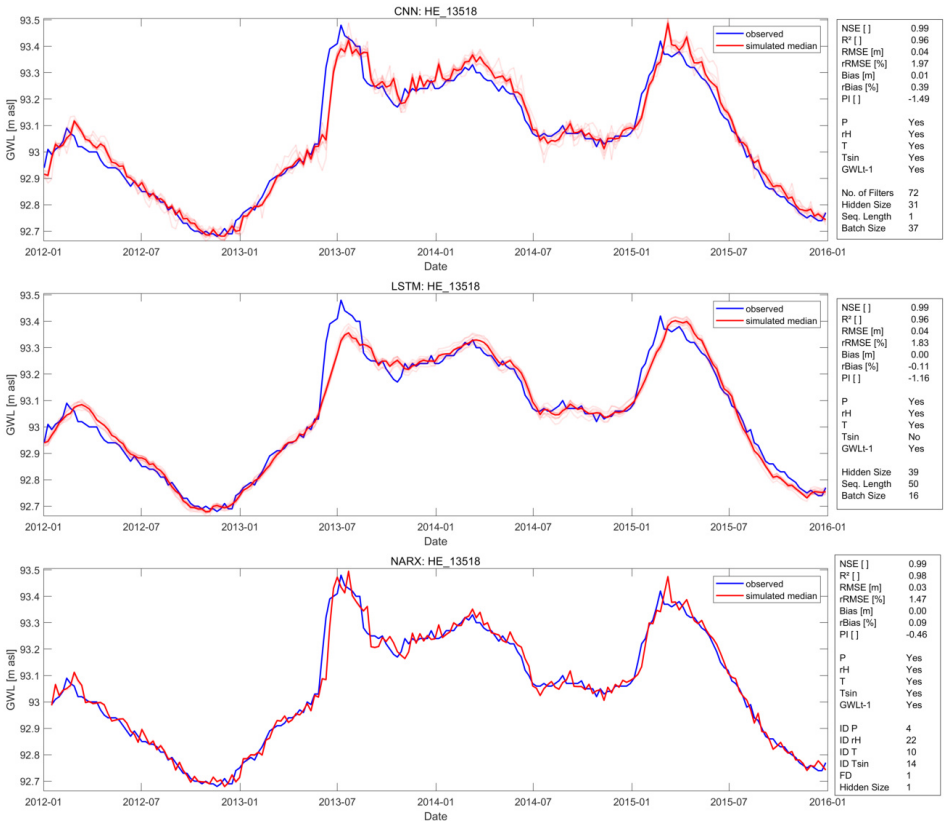

Figure S32: Seq2Val GWL_{t-1} test results for well HE_13518

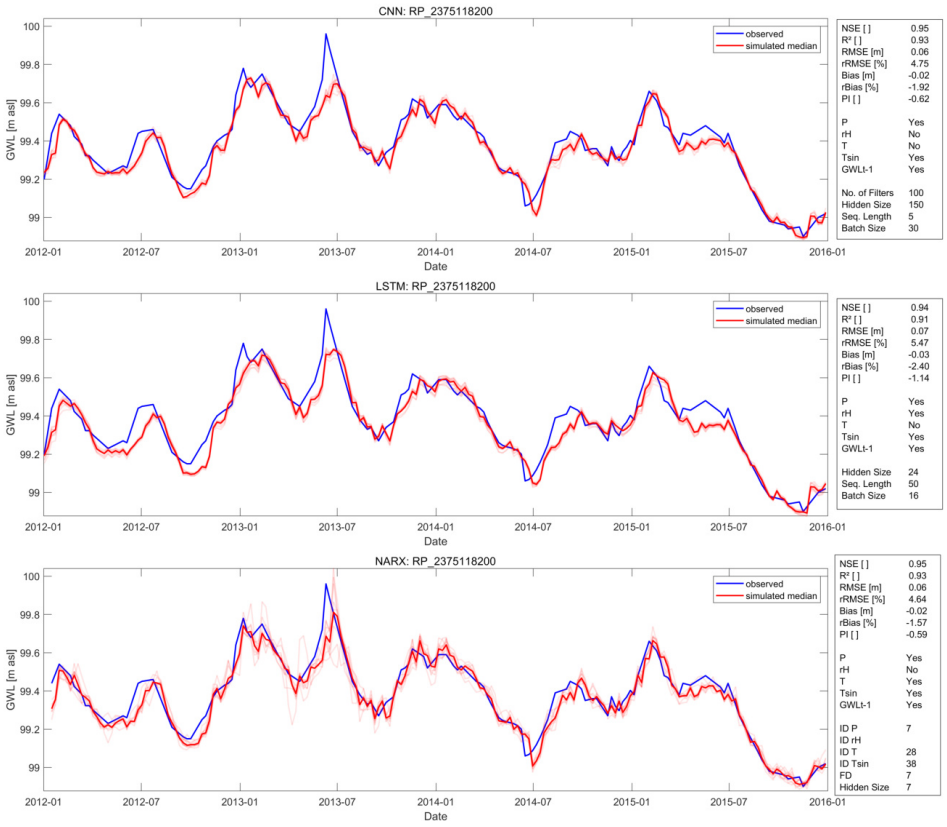

Figure S33: Seq2Val GWL_{t-1} test results for well RP_2375118200

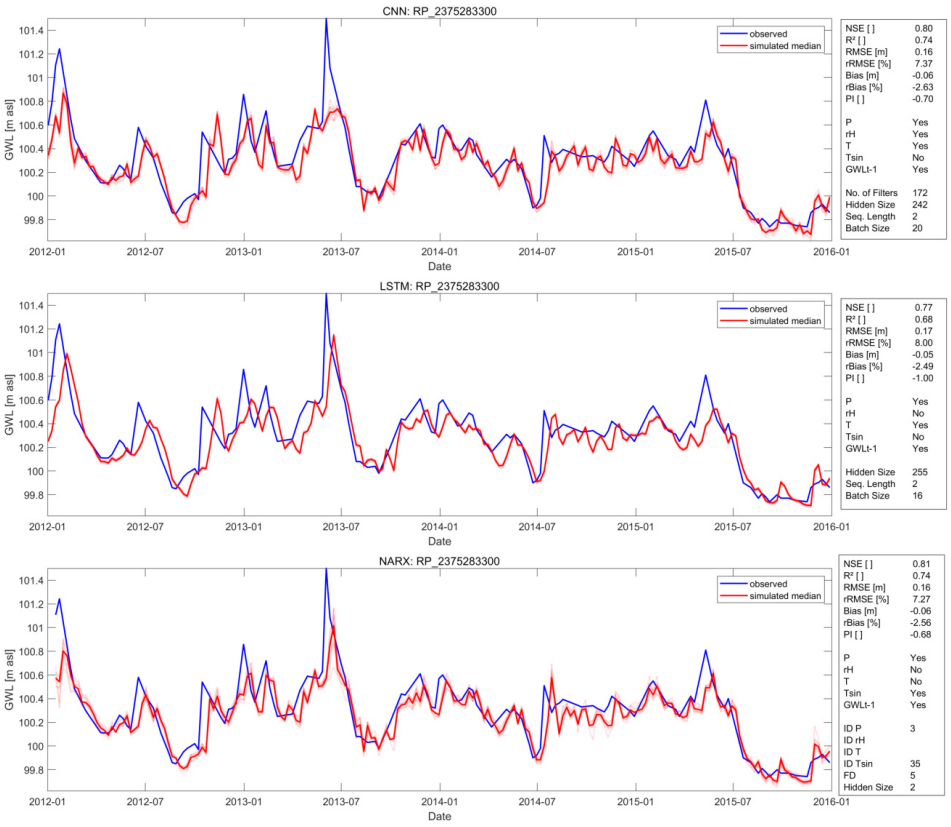

Figure S34: Seq2Val GWL_{t-1} test results for well RP_2375283300

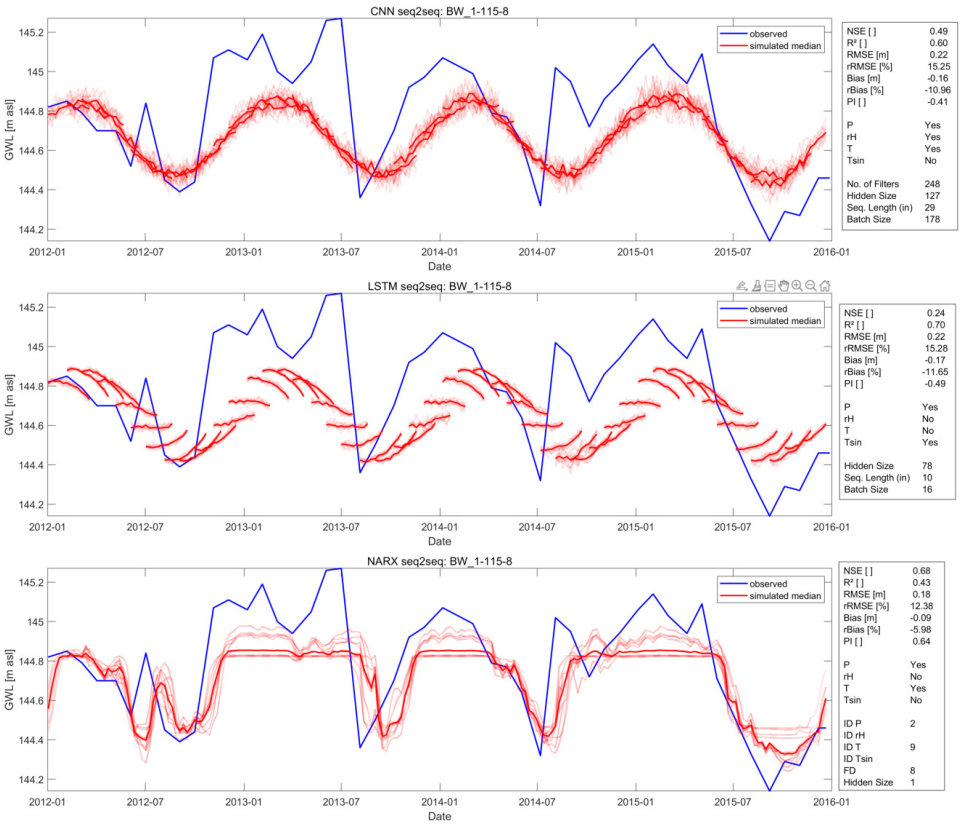

Figure S35: Seq2Seq test results for well BW_1-115-8

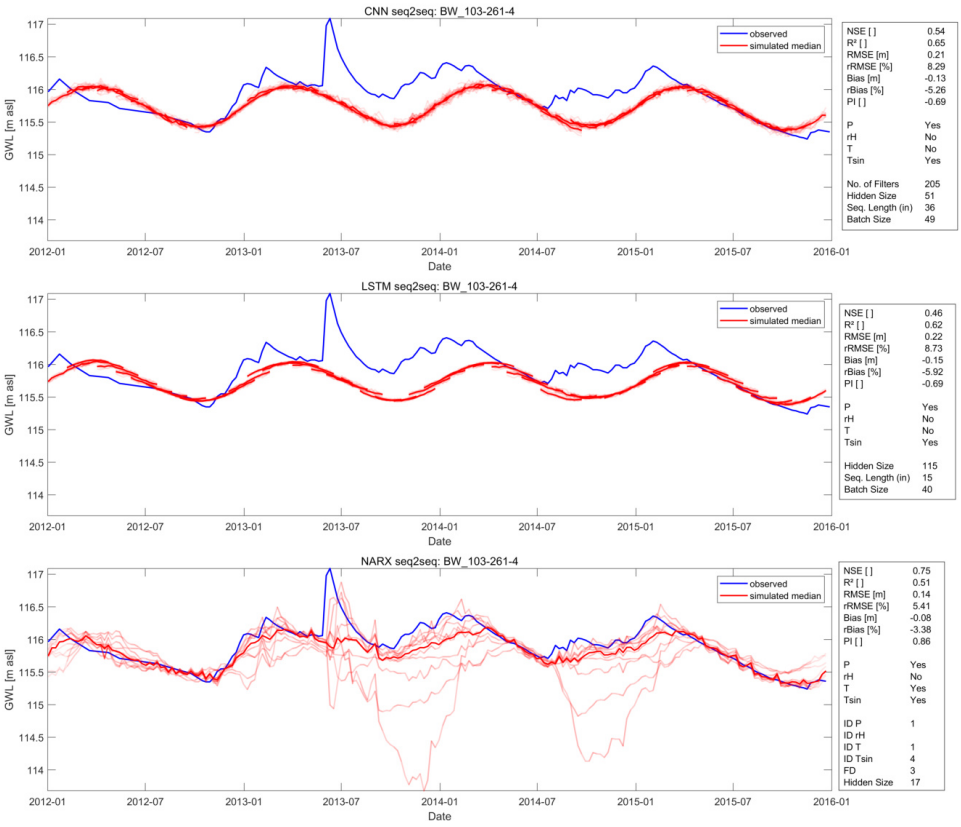

Figure S36: Seq2Seq test results for well BW_103-261-4

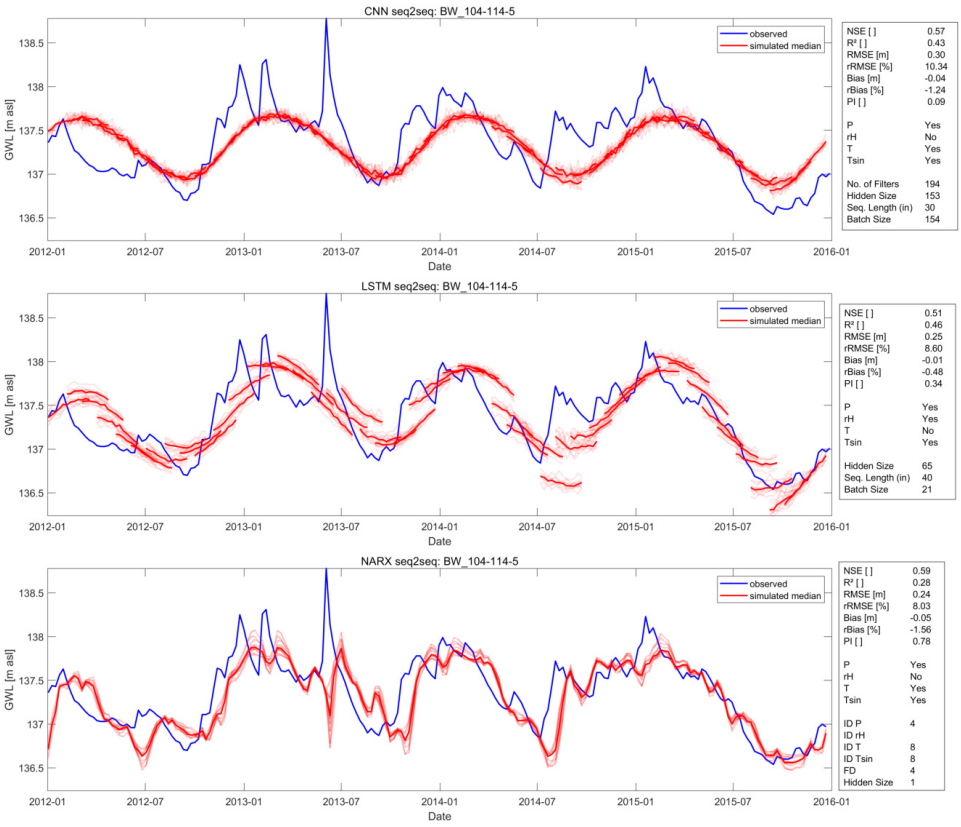

Figure S37: Seq2Seq test results for well BW_104-114-5

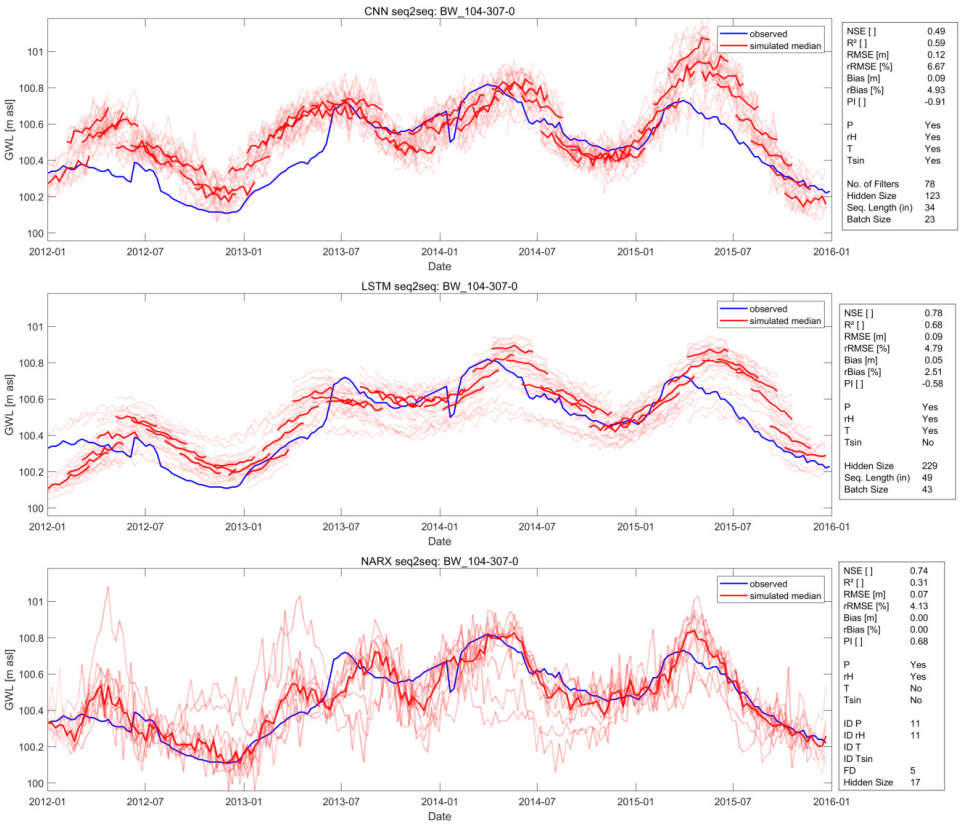

Figure S38: Seq2Seq test results for well BW_104-307-0

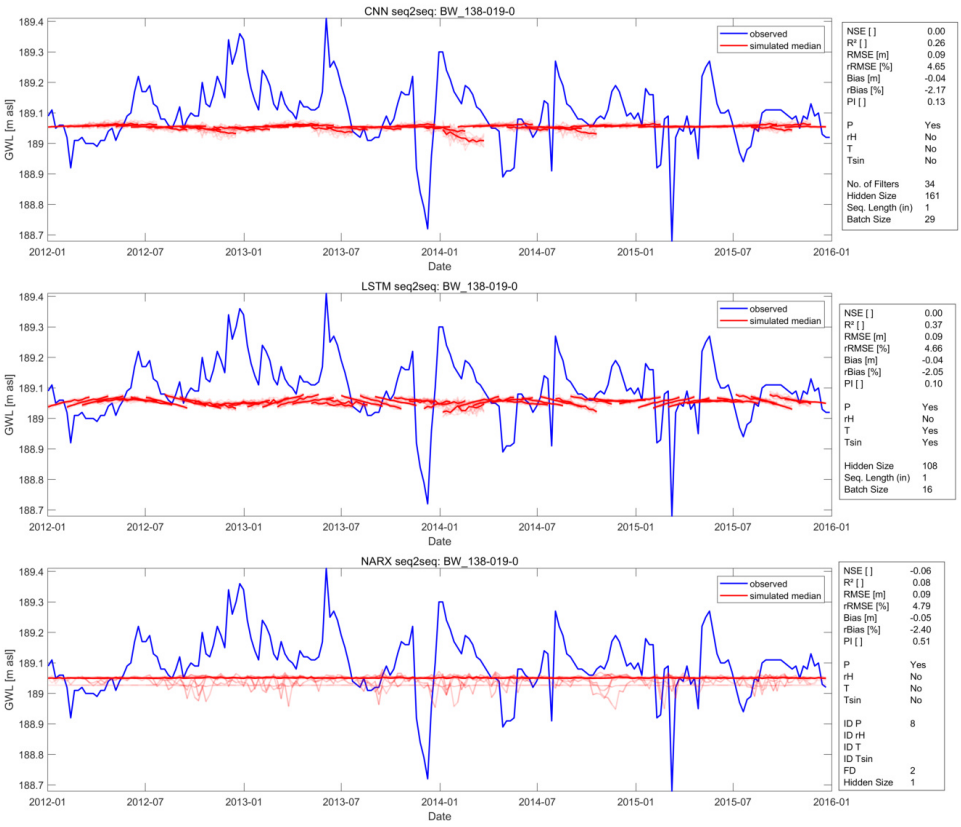

Figure S39: Seq2Seq test results for well BW_138-019-0

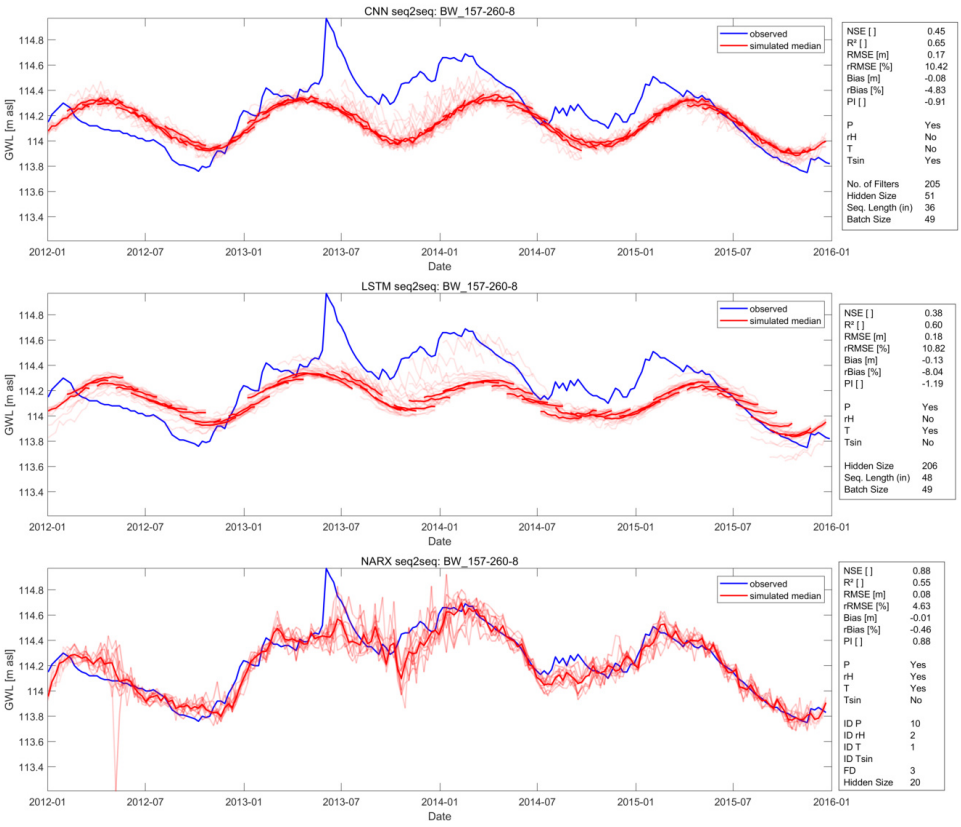

Figure S40: Seq2Seq test results for well BW_157-260-8

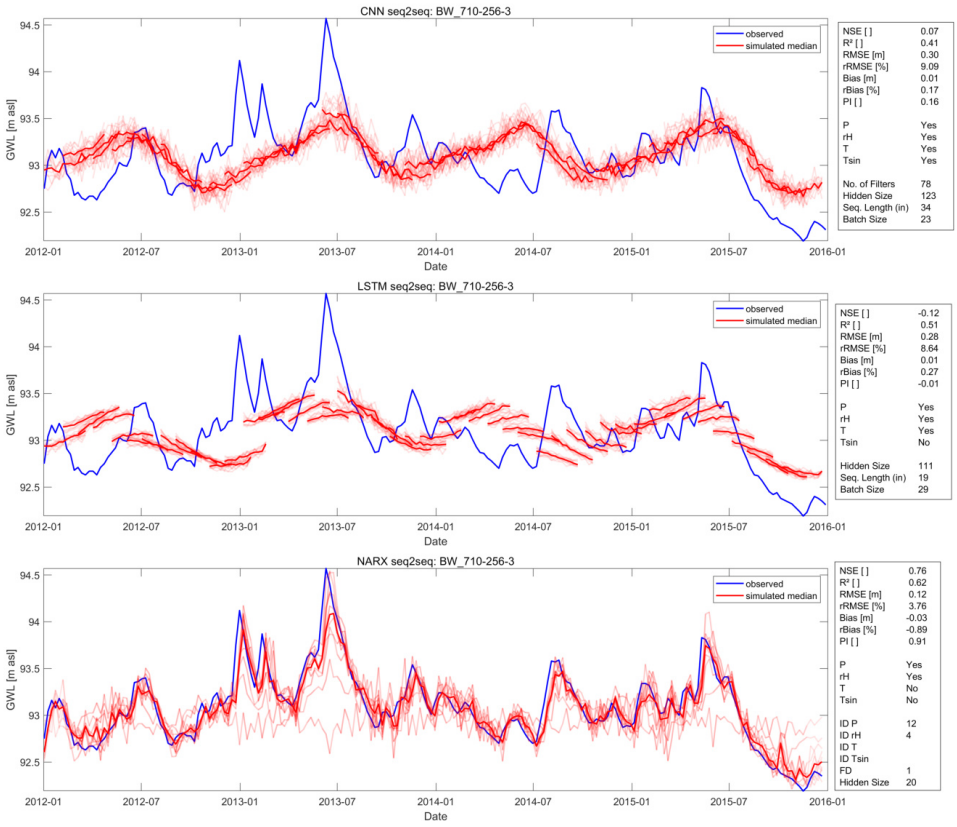

Figure S41: Seq2Seq test results for well BW_710-256-3

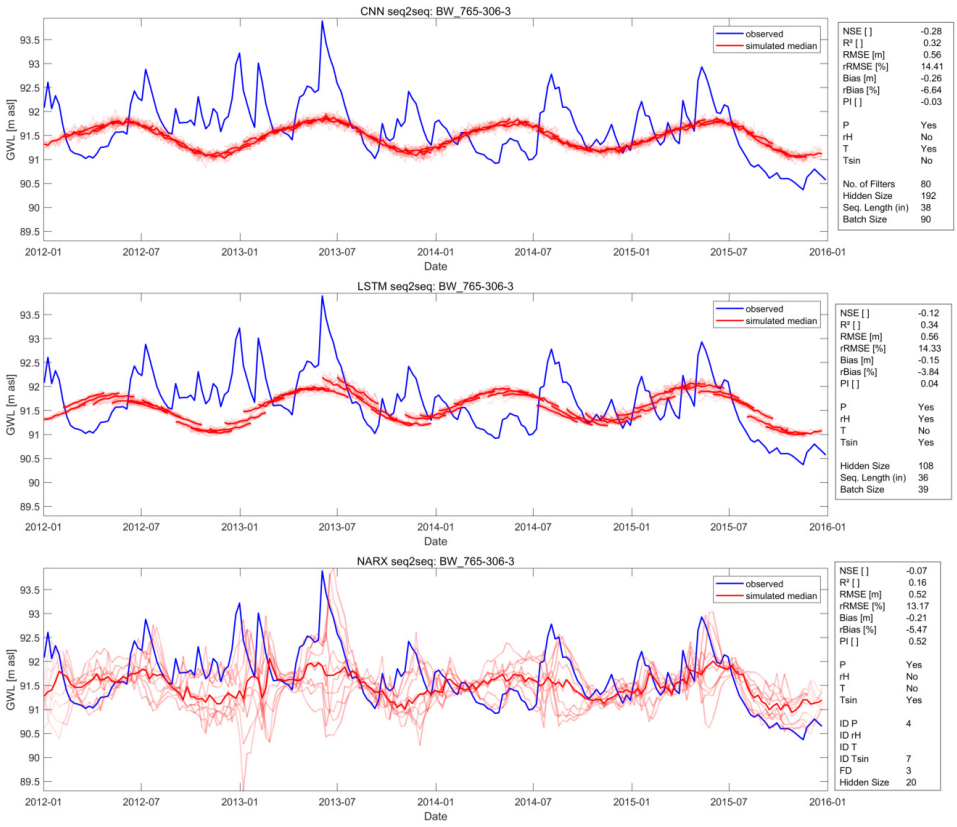

Figure S42: Seq2Seq test results for well BW_765-306-3

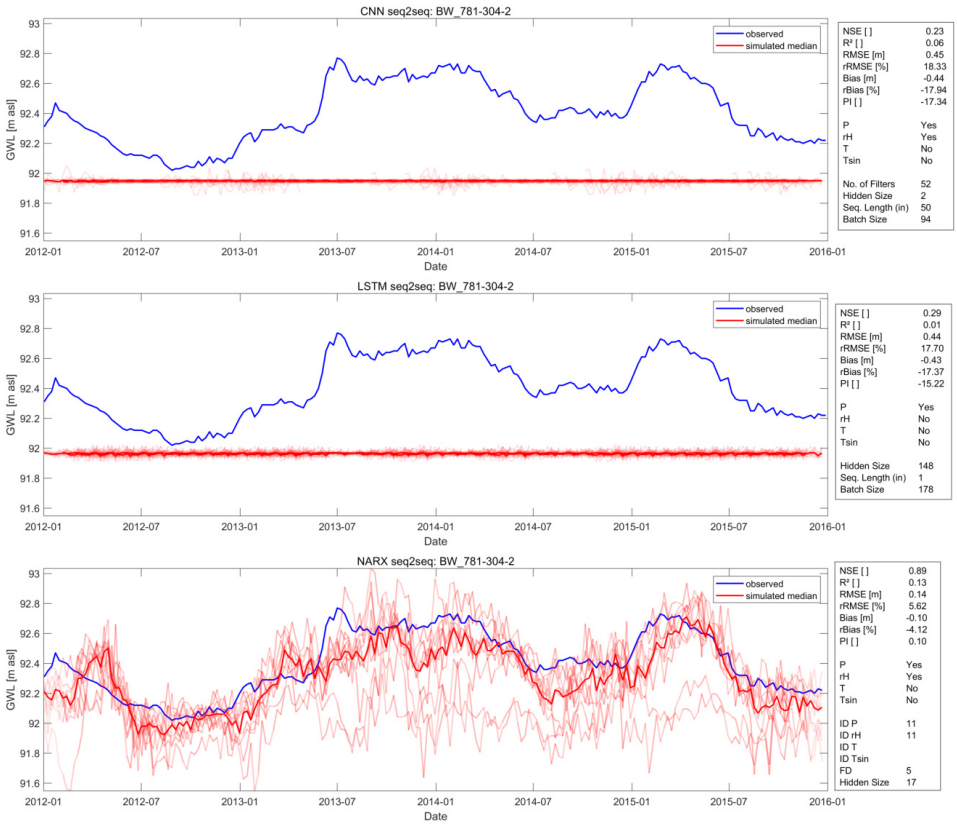

Figure S43: Seq2Seq test results for well BW_781-304-2

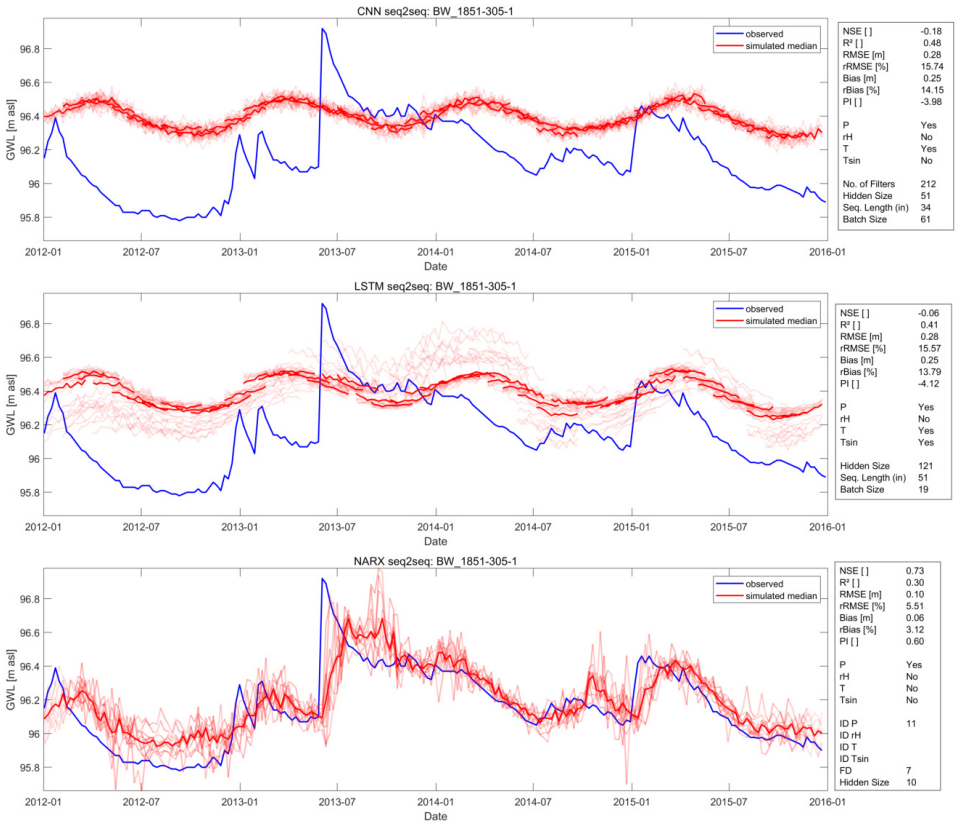

Figure S44: Seq2Seq test results for well BW_1851-305-1

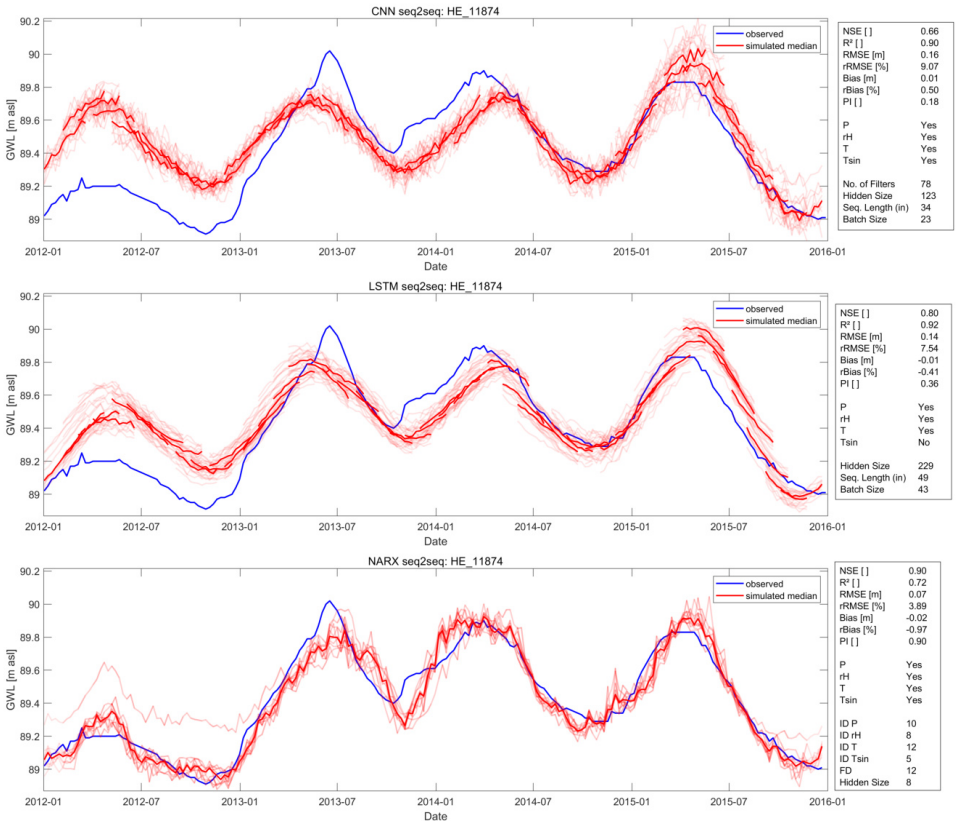

Figure S45: Seq2Seq test results for well HE_11874

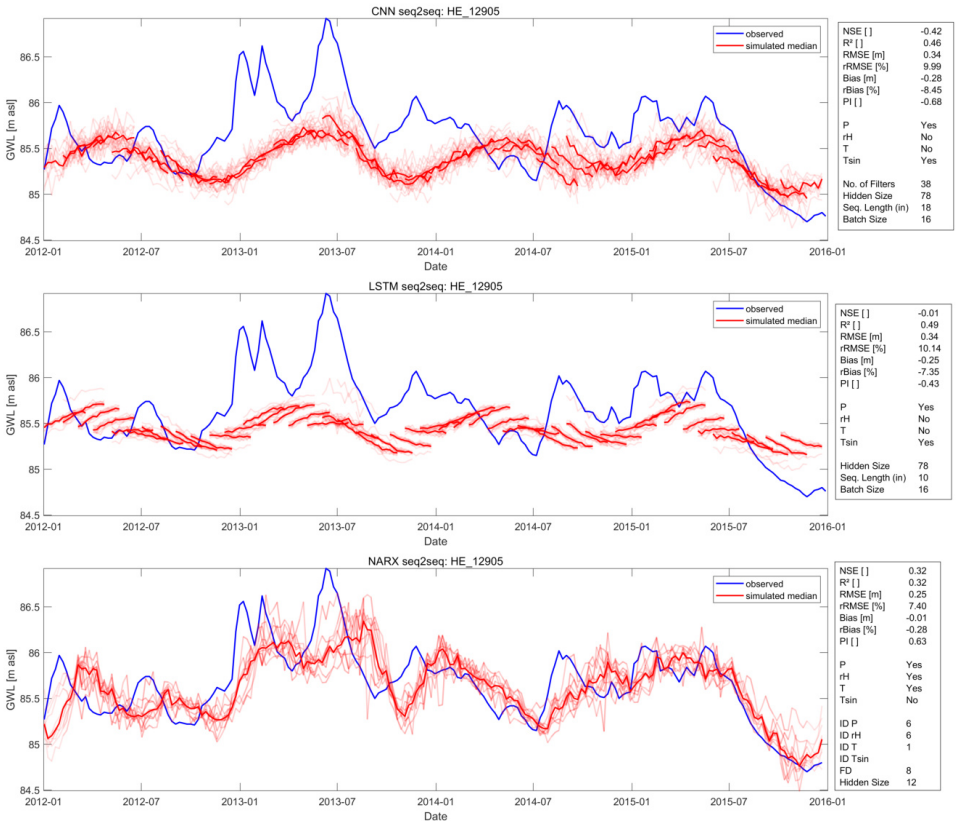

Figure S46: Seq2Seq test results for well HE_12905

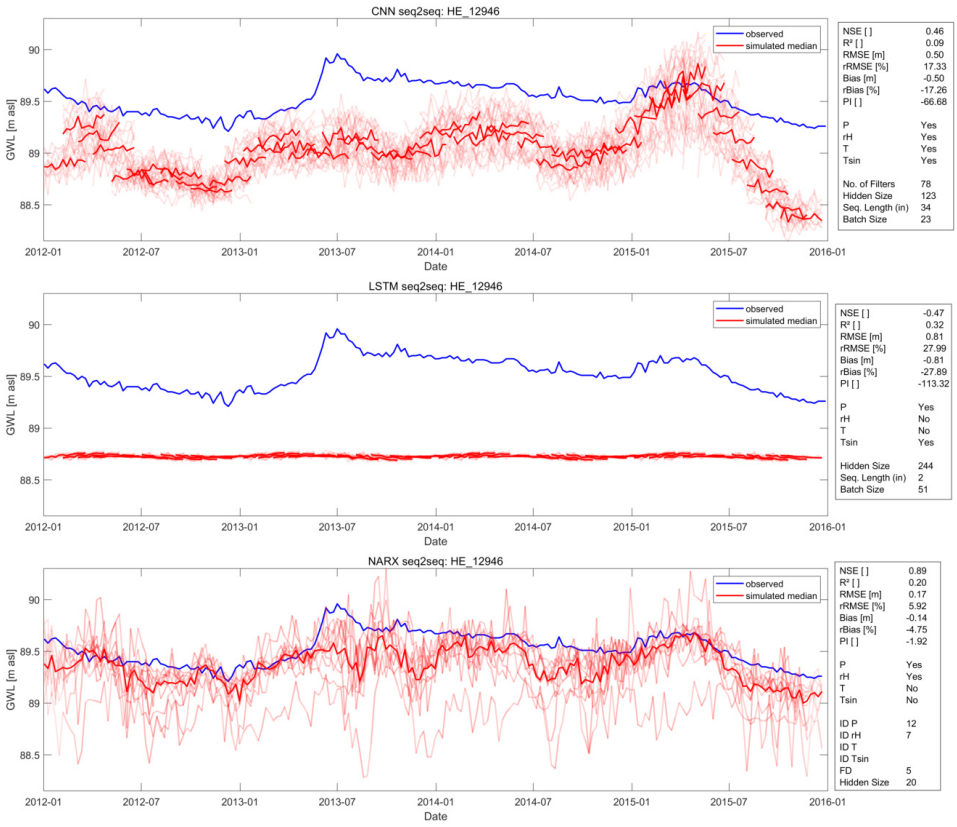

Figure S47: Seq2Seq test results for well HE_12946

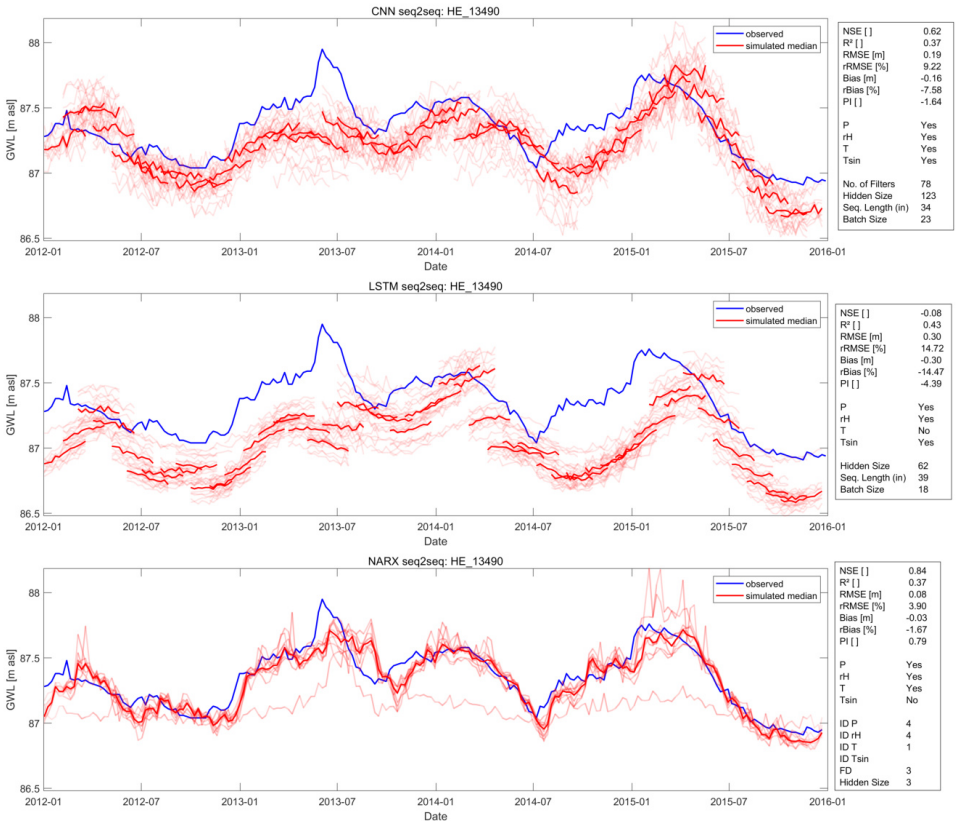

Figure S48: Seq2Seq test results for well HE_13490

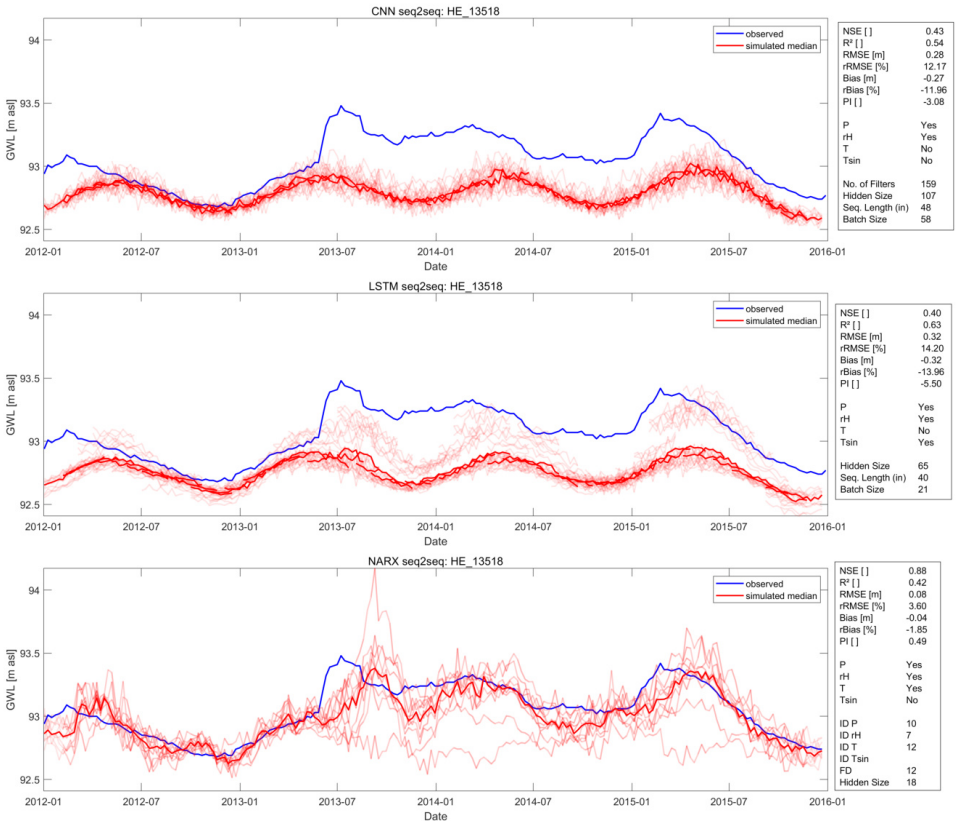

Figure S49: Seq2Seq test results for well HE_13518

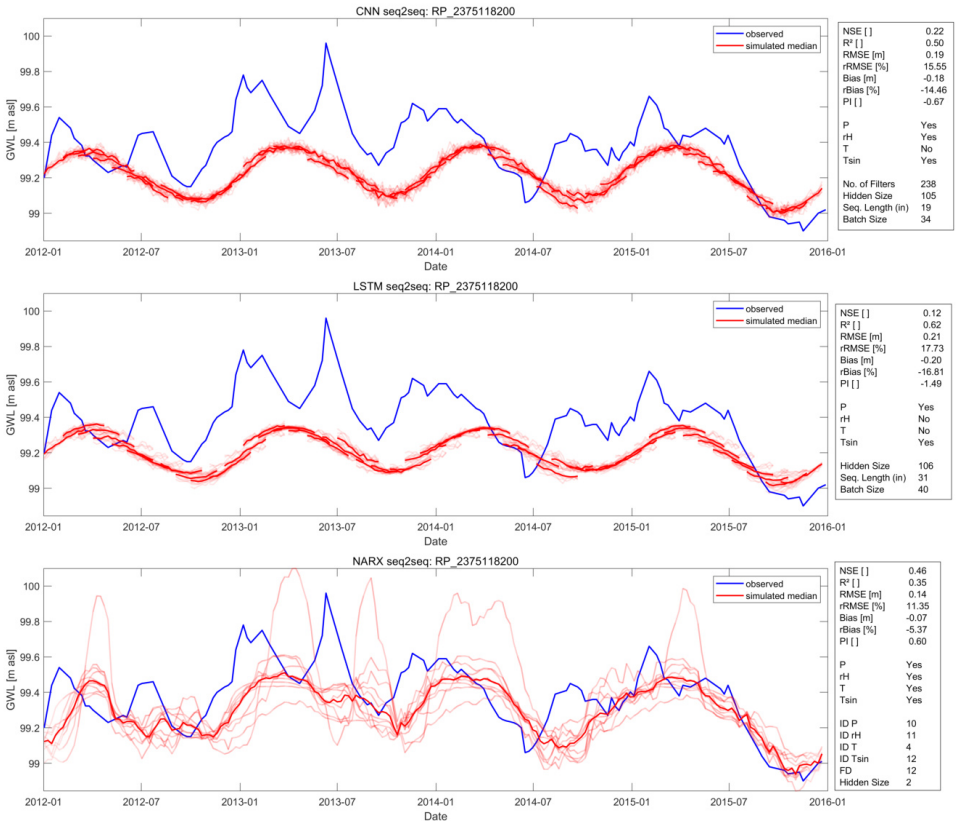

Figure S50: Seq2Seq test results for well RP_2375118200

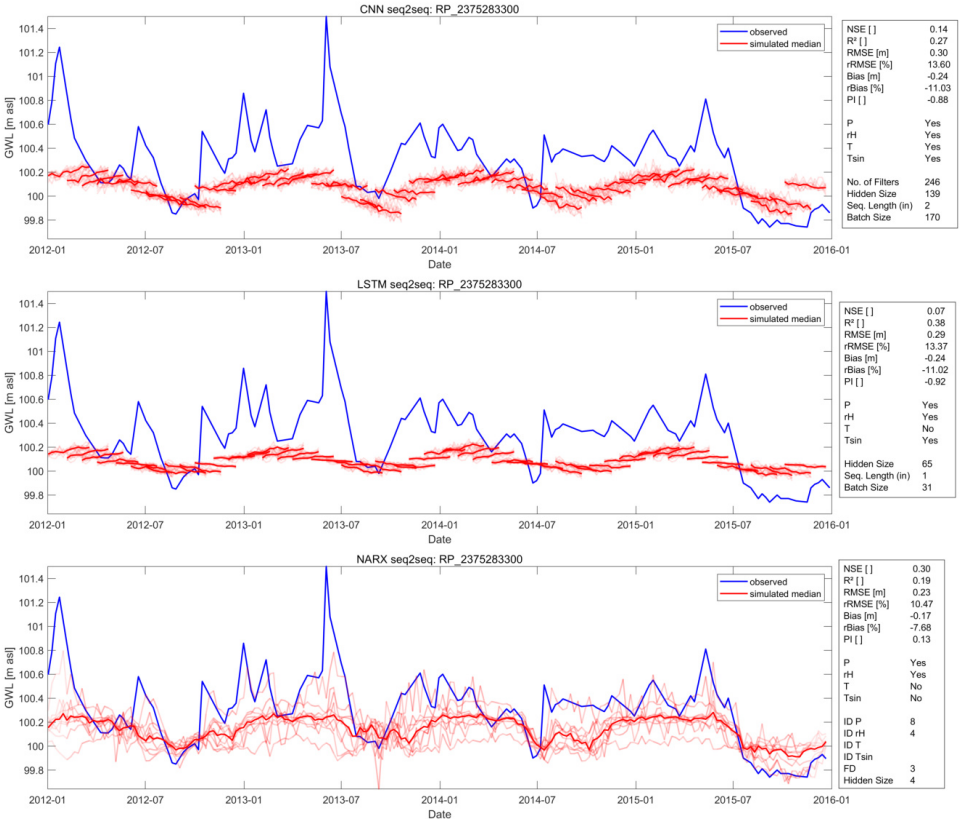

Figure S51: Seq2Seq test results for well RP_2375283300

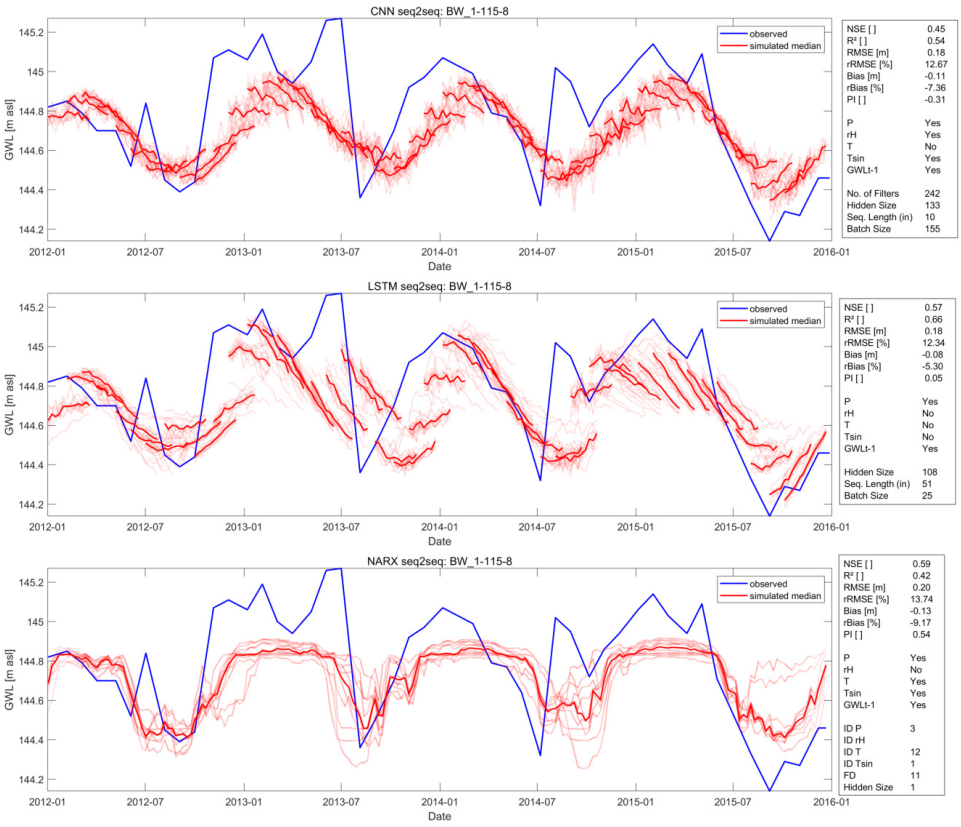

Figure S52: Seq2Seq GWL_{t-1} test results for well BW_1-115-8

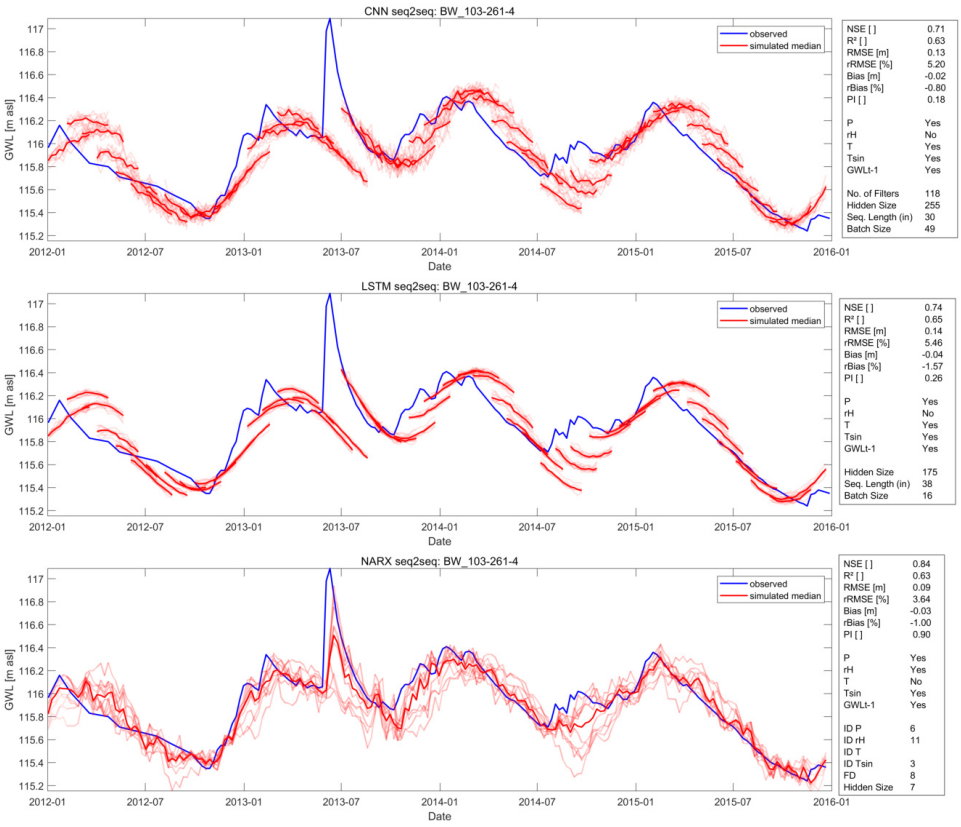

Figure S53: Seq2Seq GWL_{t-1} test results for well BW_103-261-4

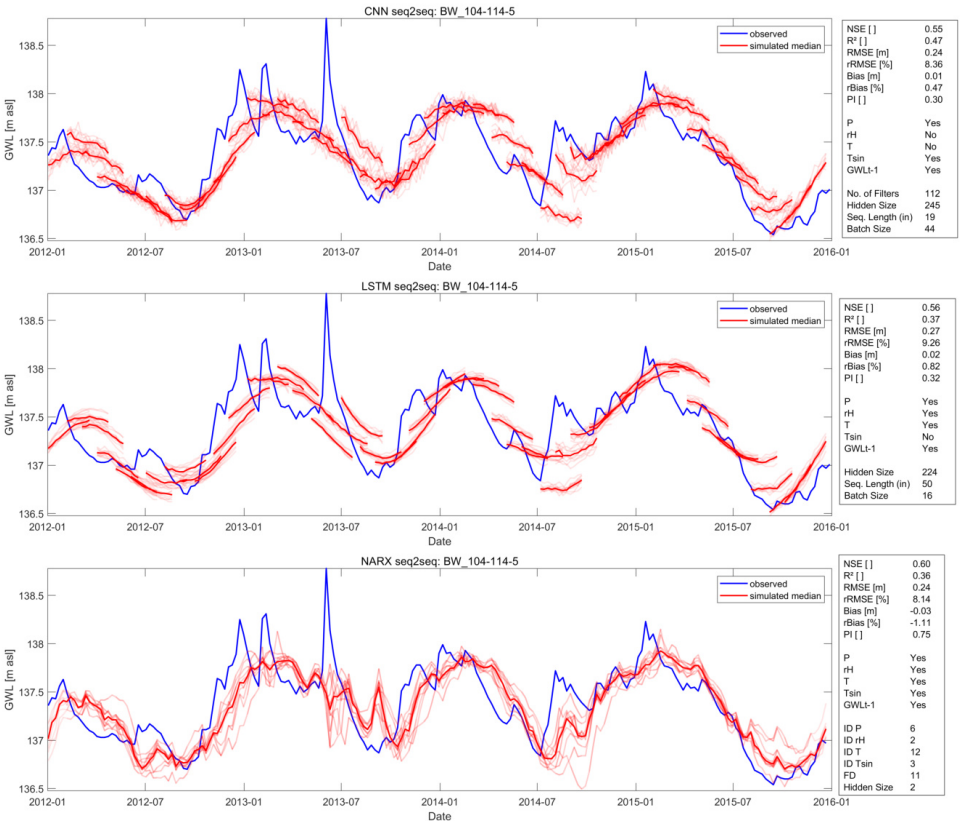

Figure S54: Seq2Seq GWL_{t-1} test results for well BW_104-114-5

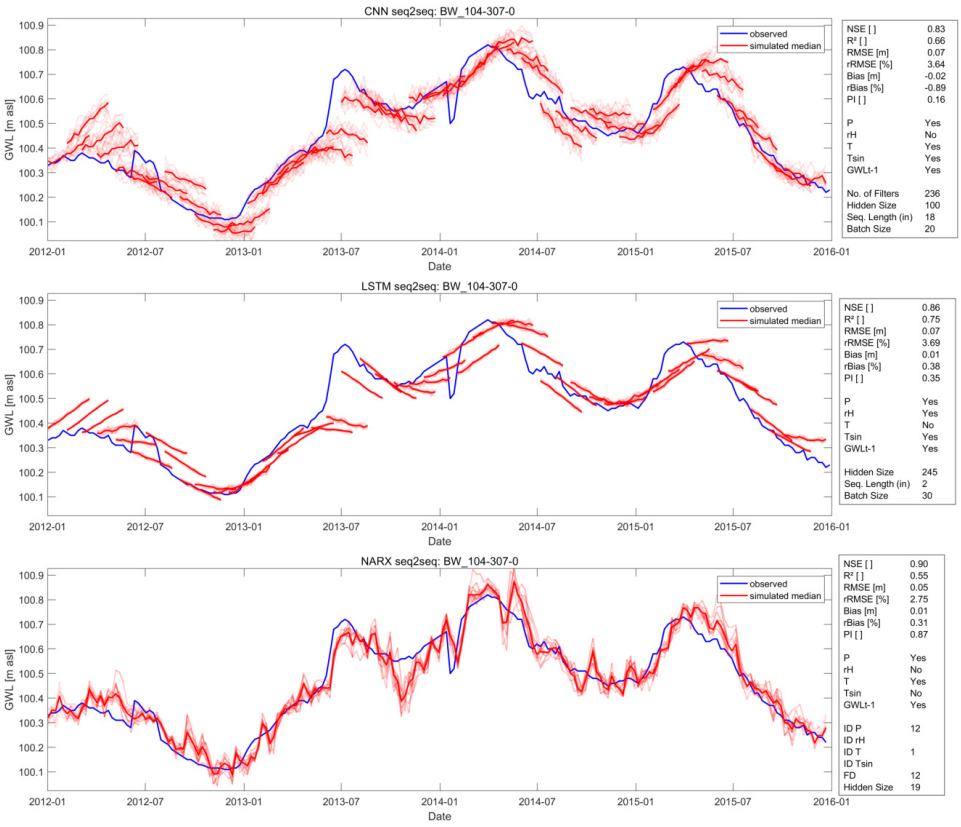

Figure S55: Seq2Seq GWL_{t-1} test results for well BW_104-307-0

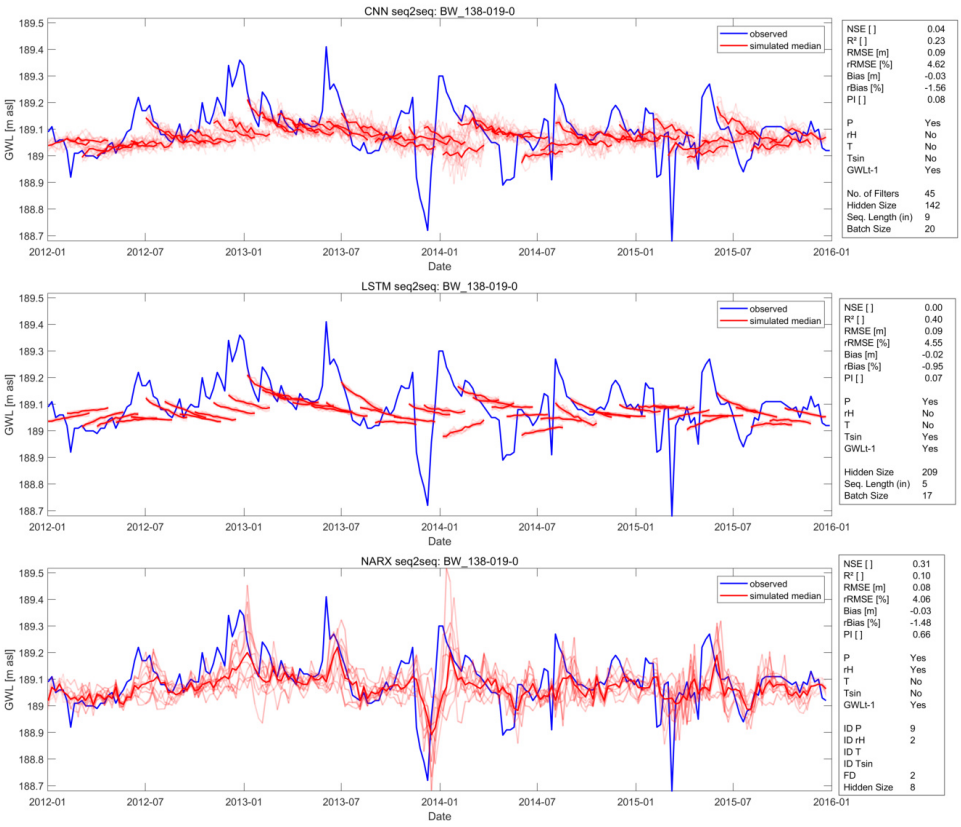

Figure S56: Seq2Seq GWL_{t-1} test results for well BW_138-019-0

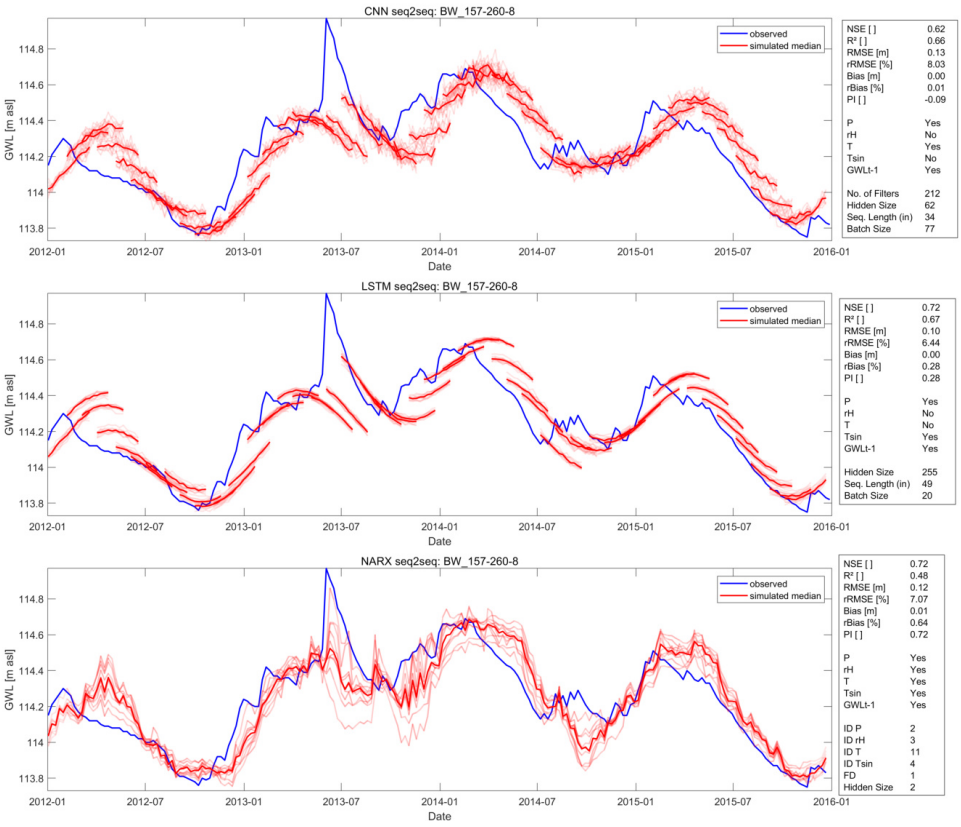

Figure S57: Seq2Seq GWL_{t-1} test results for well BW_157-260-8

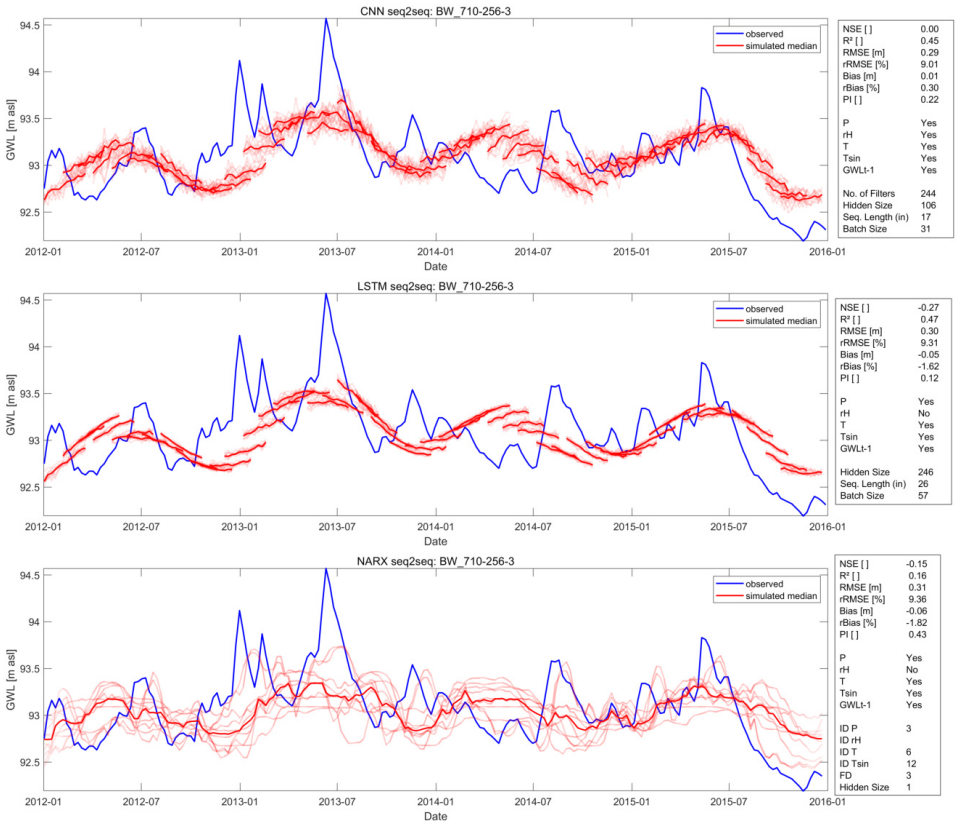

Figure S58: Seq2Seq GWL_{t-1} test results for well BW_710-256-3

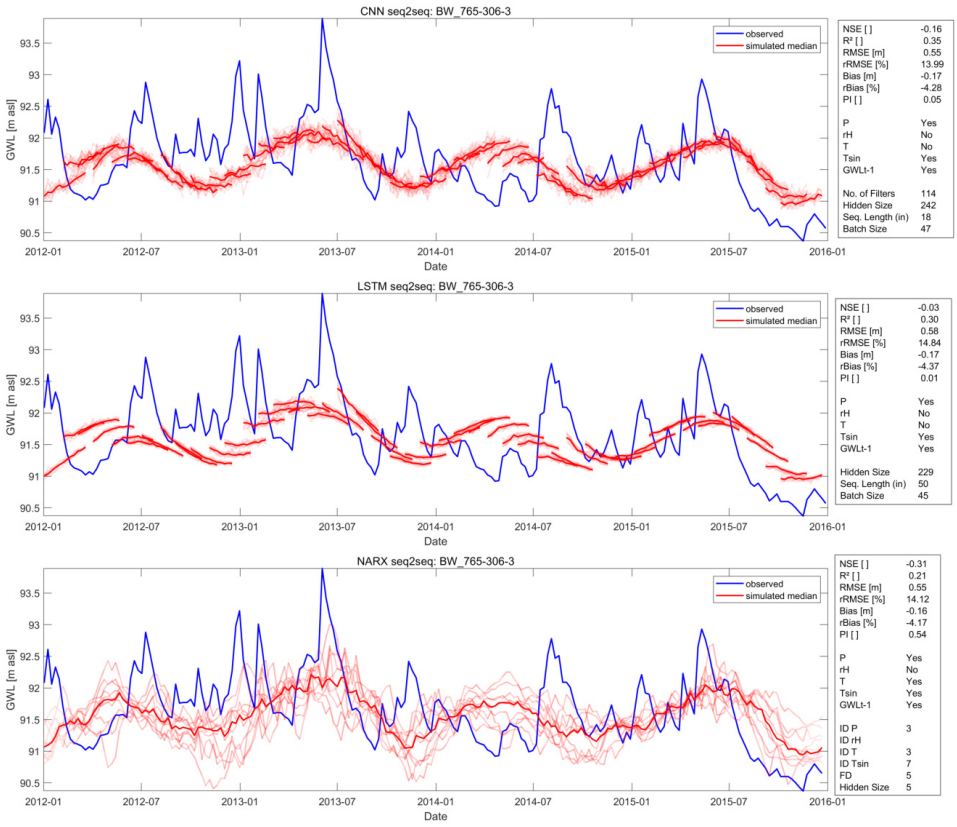

Figure S59: Seq2Seq GWL_{t-1} test results for well BW_765-306-3

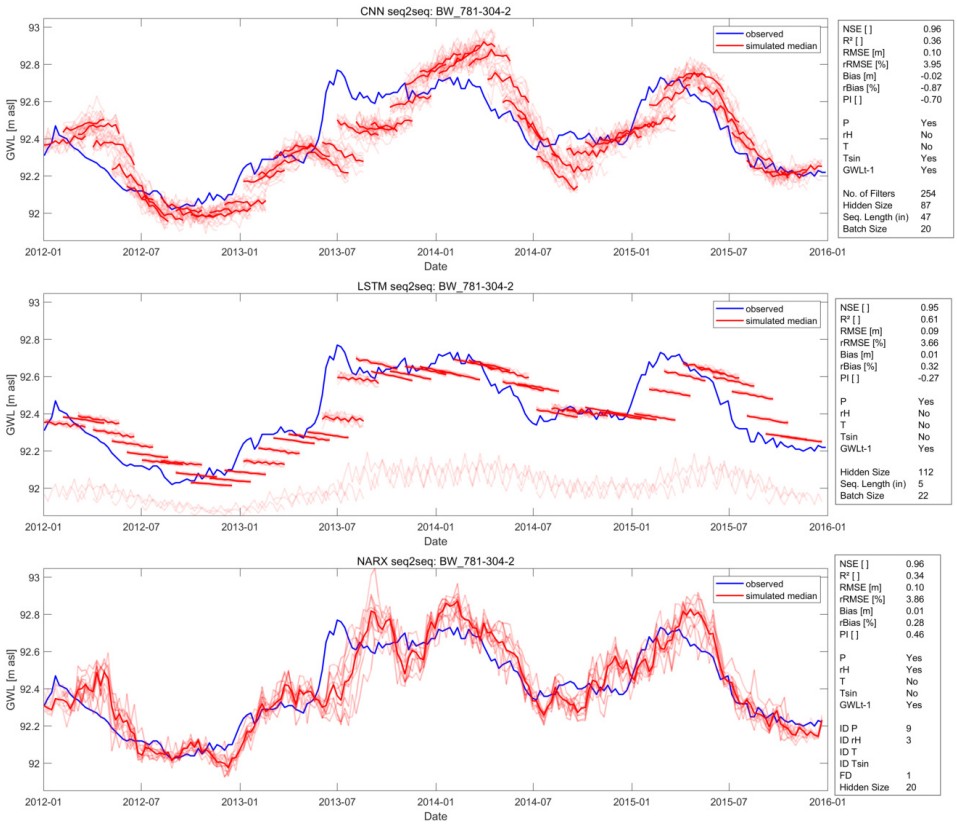

Figure S60: Seq2Seq GWL_{t-1} test results for well BW_781-304-2

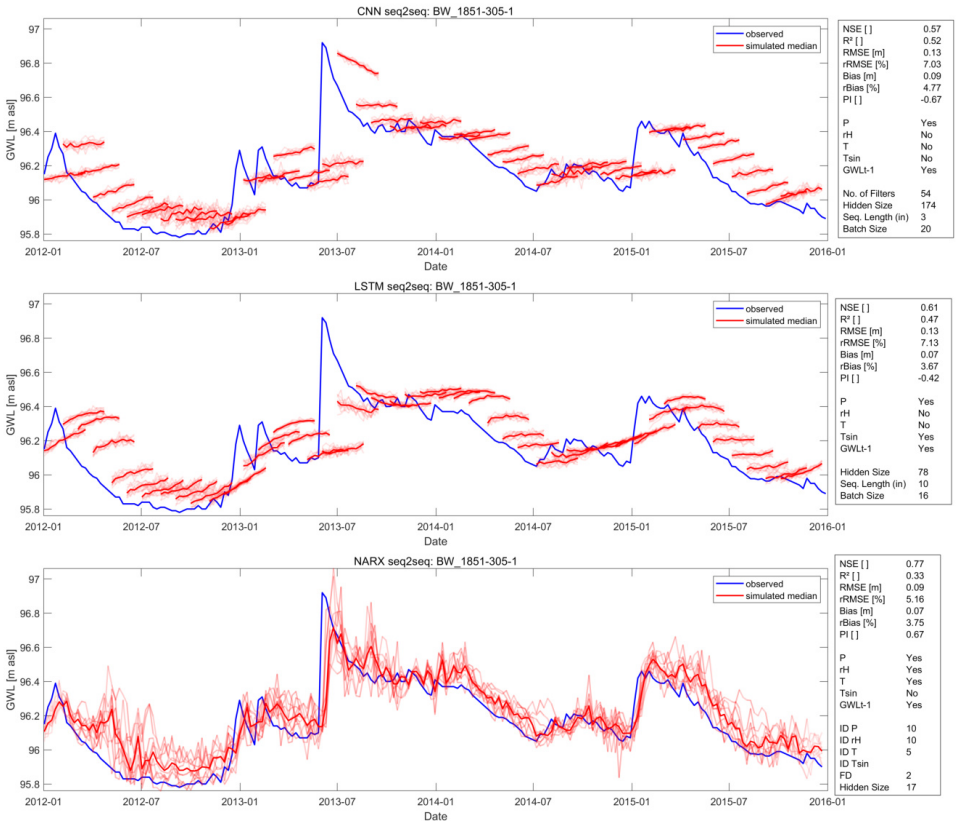

Figure S61: Seq2Seq GWL_{t-1} test results for well BW_1851-305-1

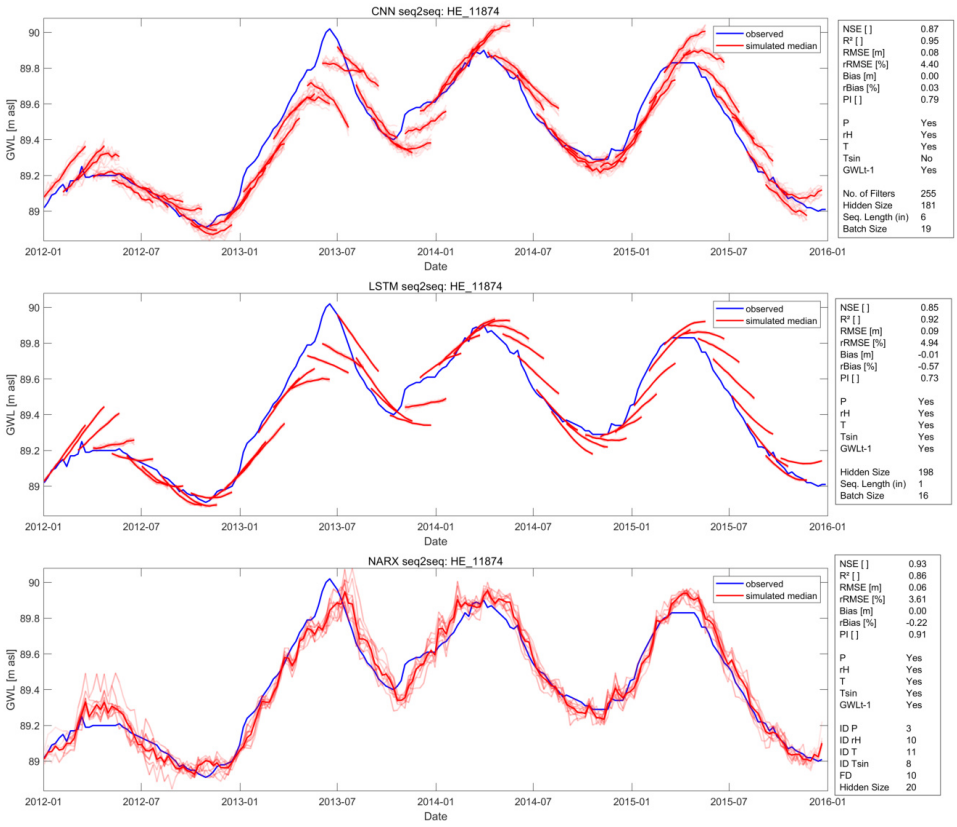

Figure S62: Seq2Seq GWL_{t-1} test results for well HE_11874

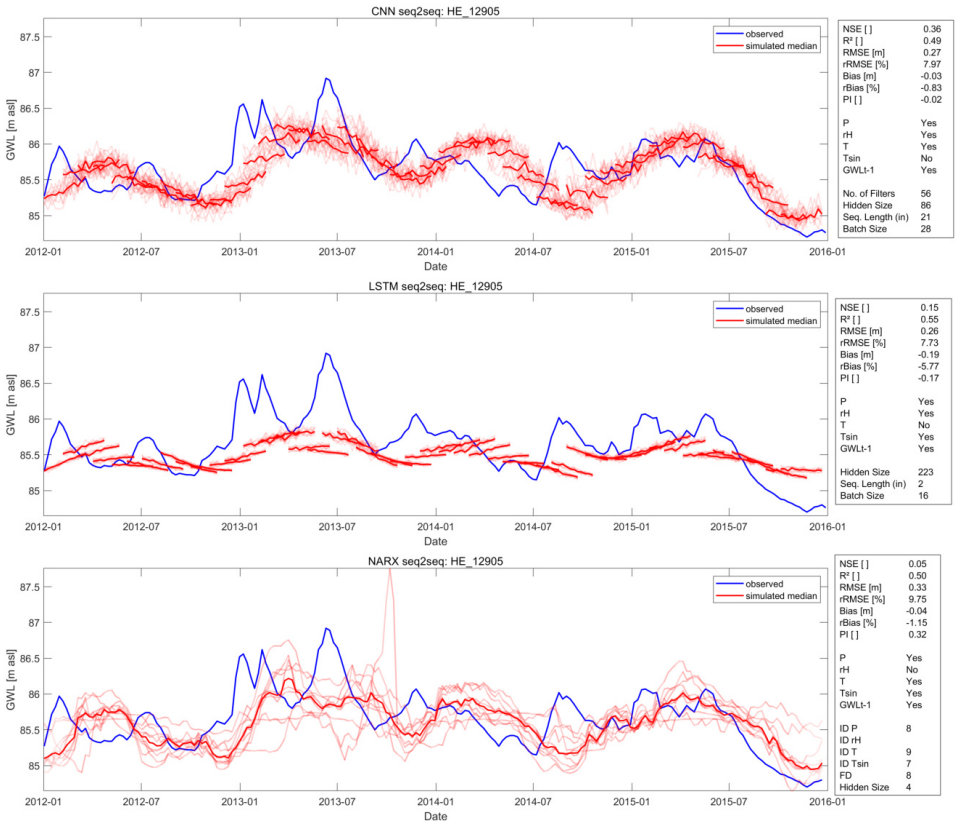

Figure S63: Seq2Seq GWL_{t-1} test results for well HE_12905

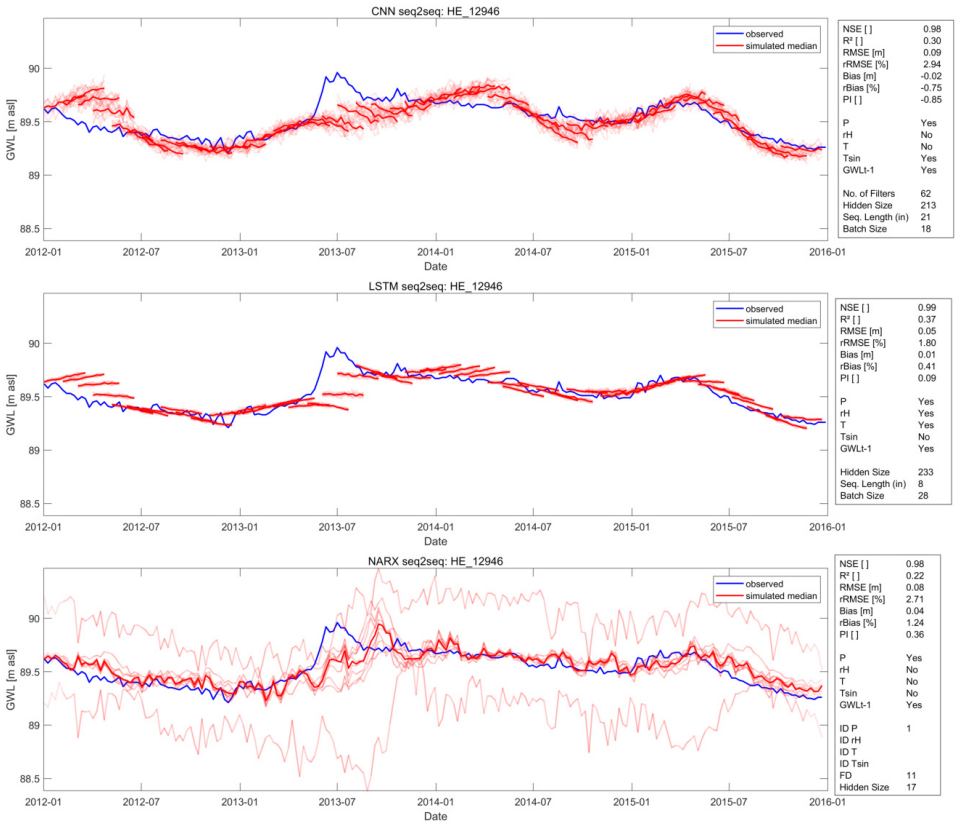

Figure S64: Seq2Seq GWL_{t-1} test results for well HE_12946

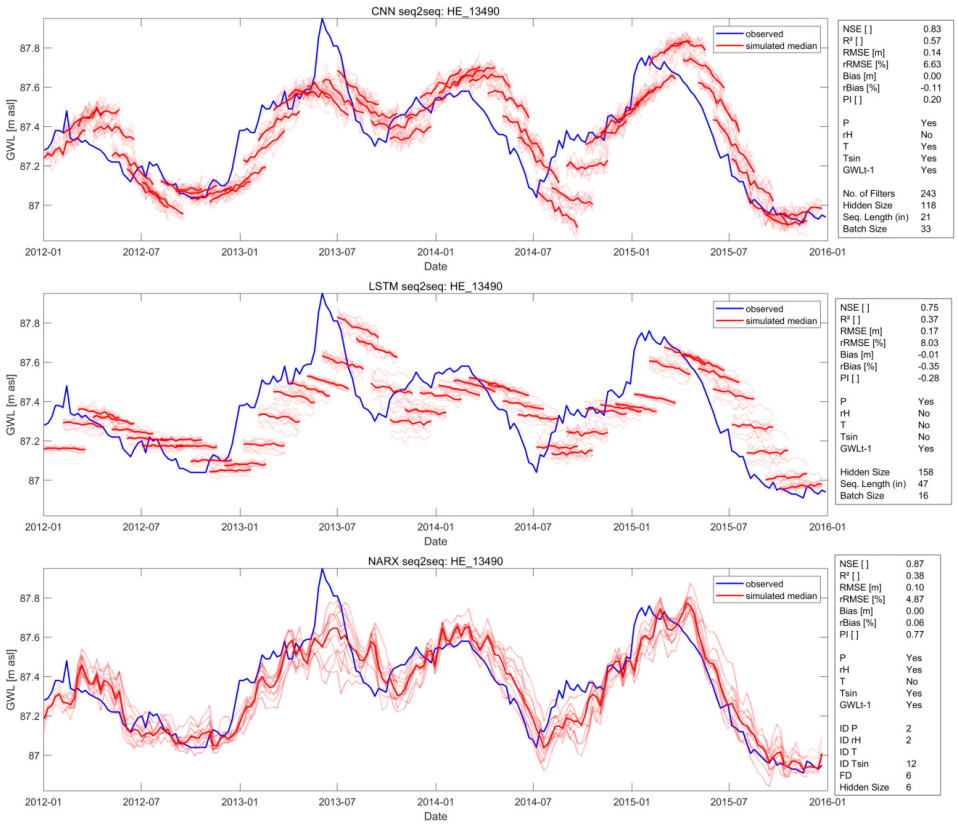

Figure S65: Seq2Seq GWL_{t-1} test results for well HE_13490

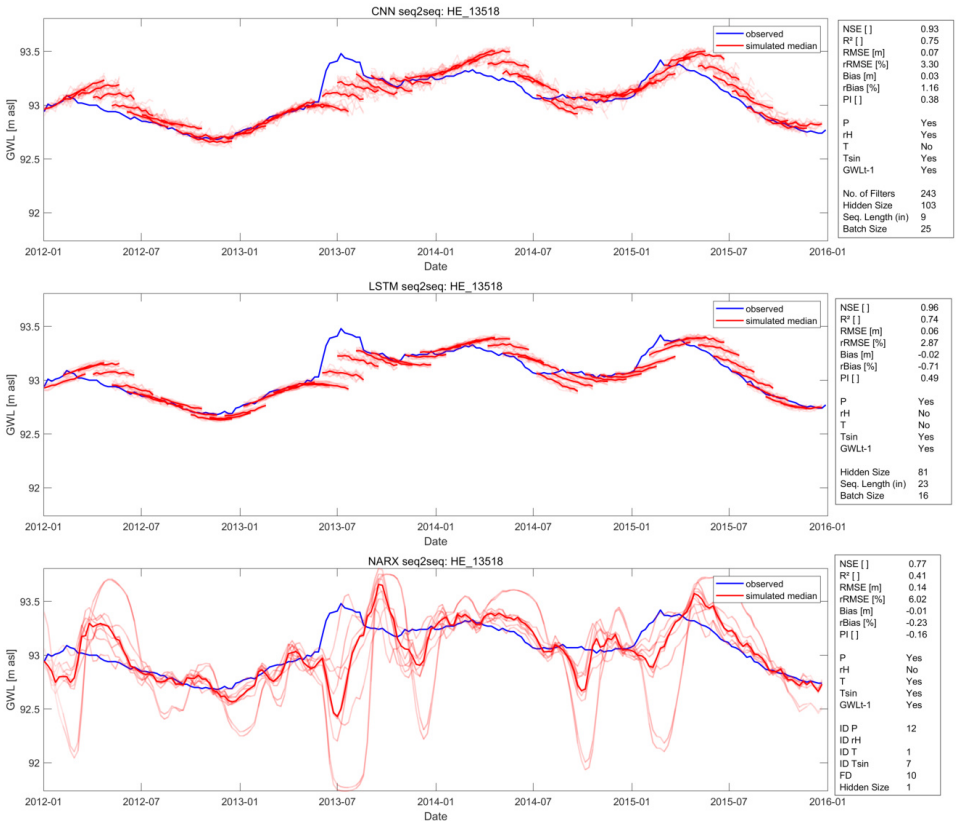

Figure S66: Seq2Seq GWL_{t-1} test results for well HE_13518

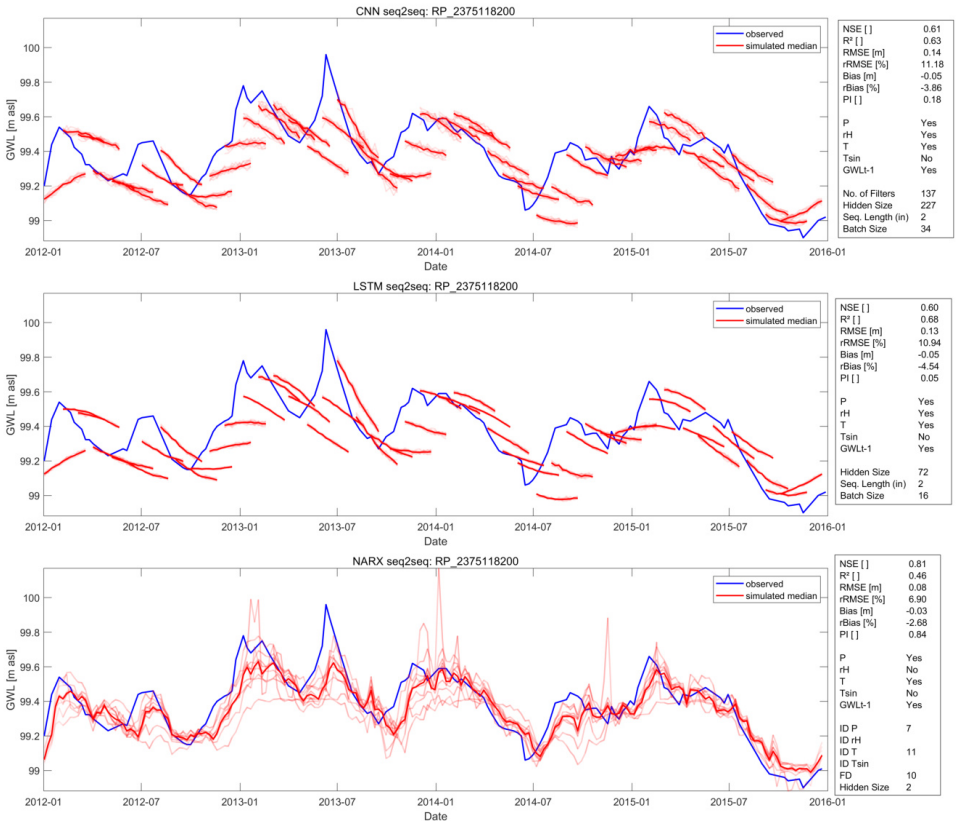

Figure S67: Seq2Seq GWL_{t-1} test results for well RP_2375118200

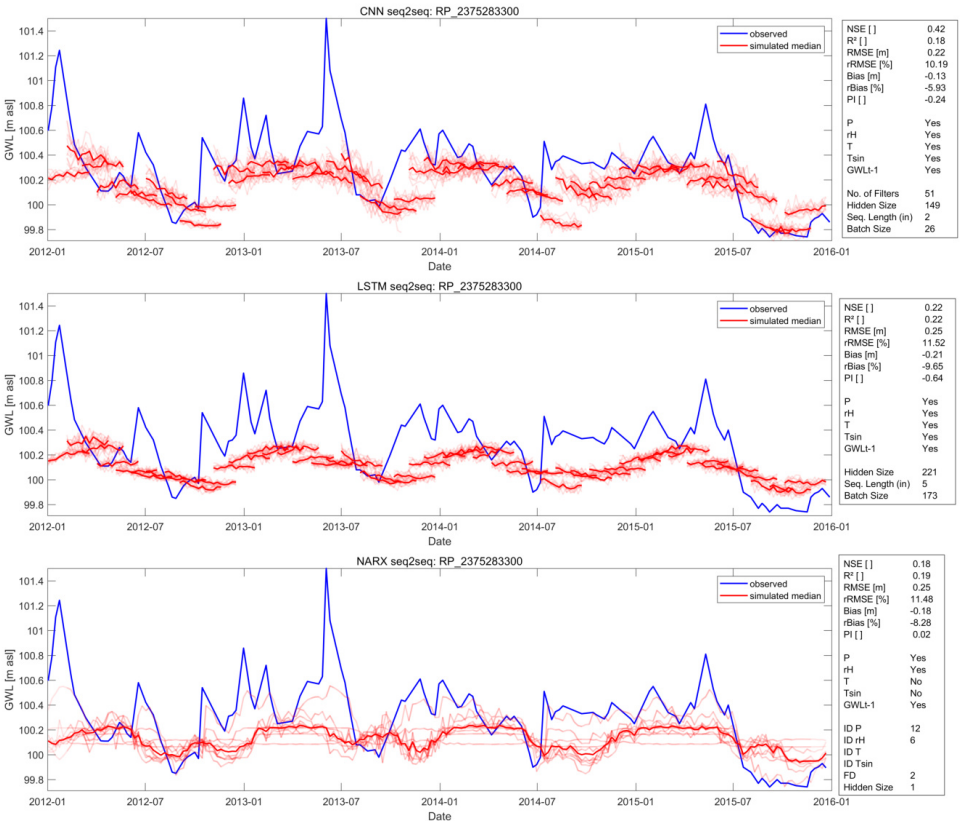

Figure S68: Seq2Seq GWL_{t-1} test results for well RP_2375283300

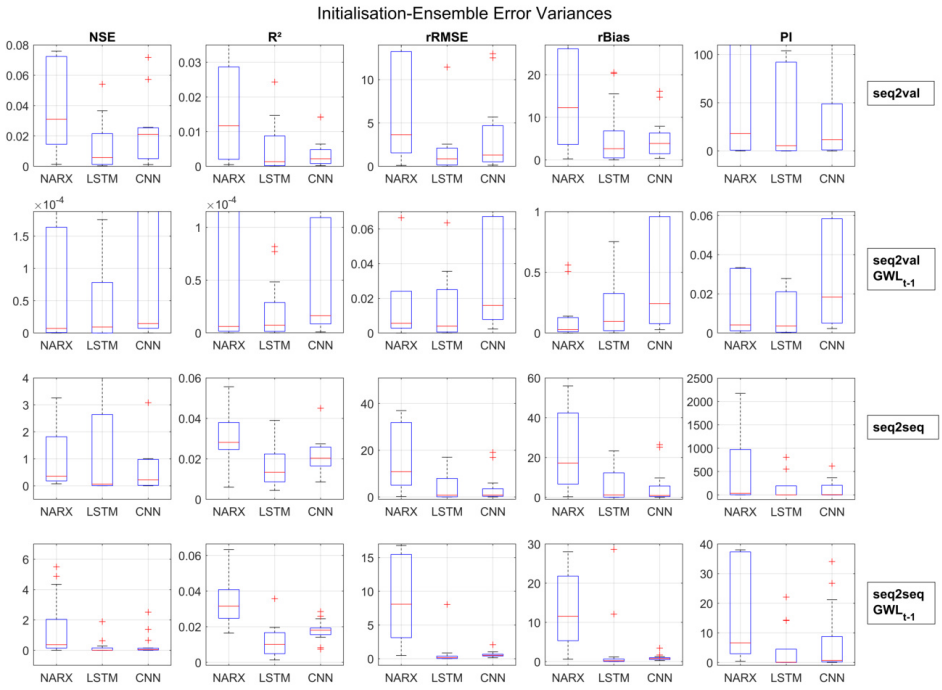

Figure S69: Error Variance of Initialization Ensemble Members

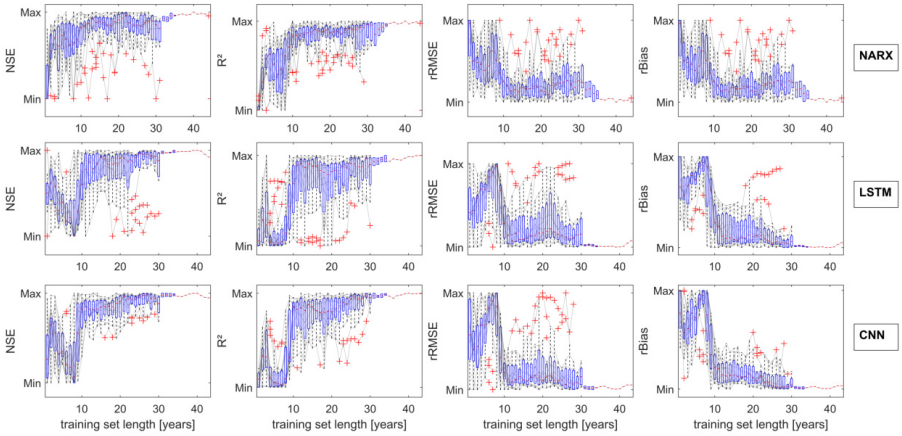

Figure S70: Influence of the available amount of training data on seq2val model performance based on meteorological inputs.

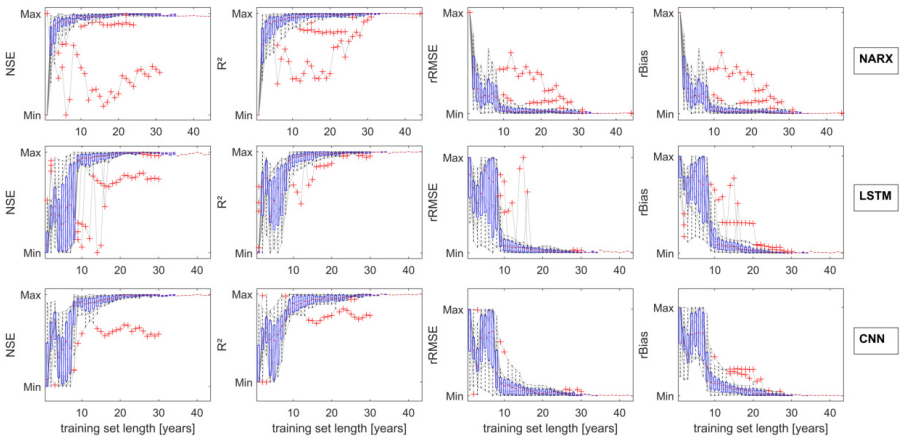

Figure S71: Influence of the available amount of training data on seq2val model performance based on meteorological inputs and past groundwater levels.

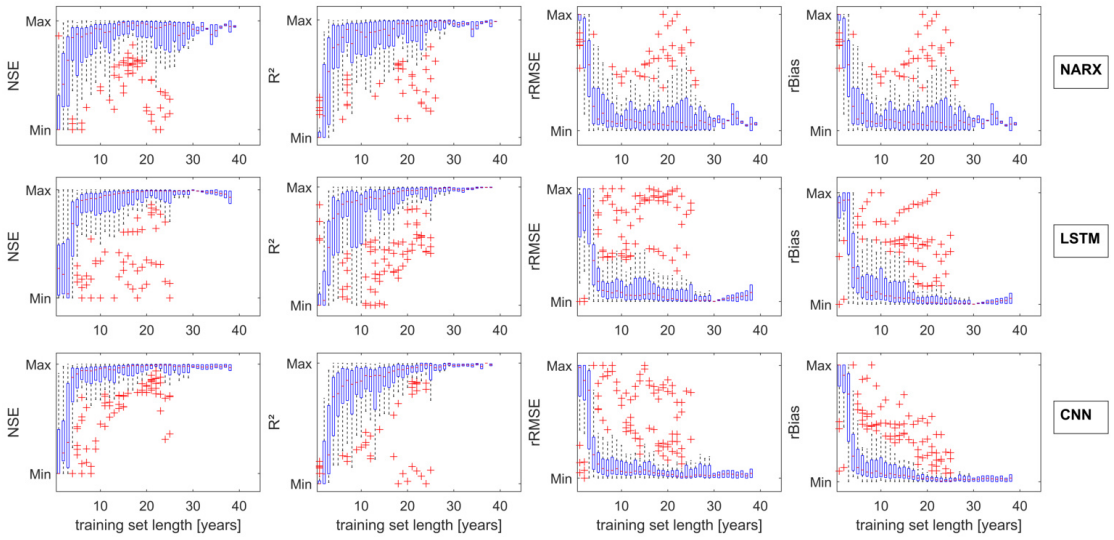

Figure S72: Influence of the available amount of training data on all seq2val model performance with training ending in 2007 instead of 2012

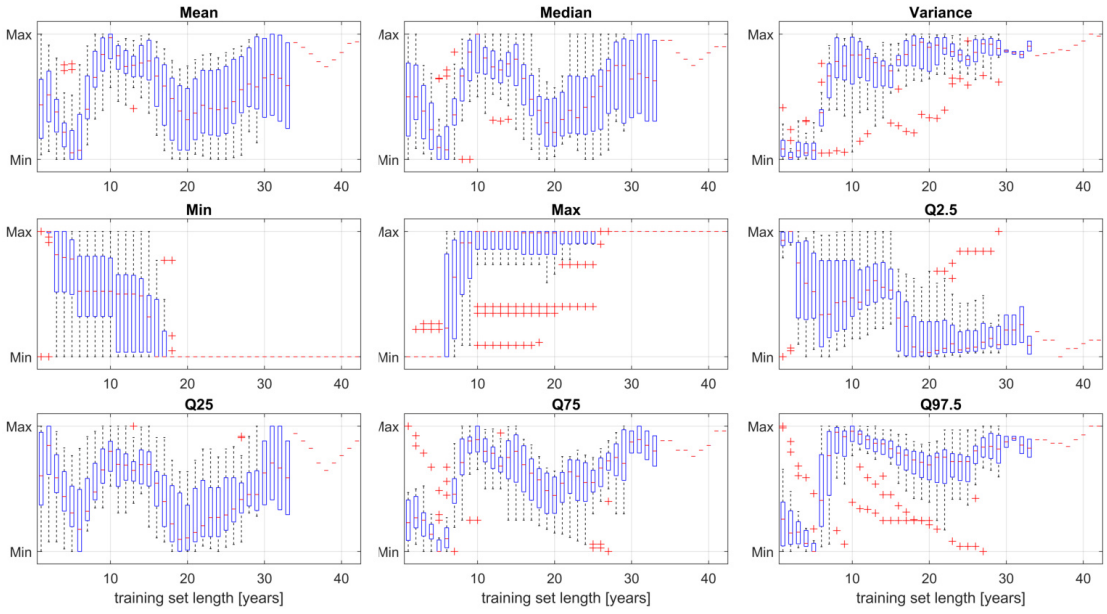

Figure S73: Development of several statistic measures with yearly expanding time series length from 2012 on backwards (Q: Quantile).

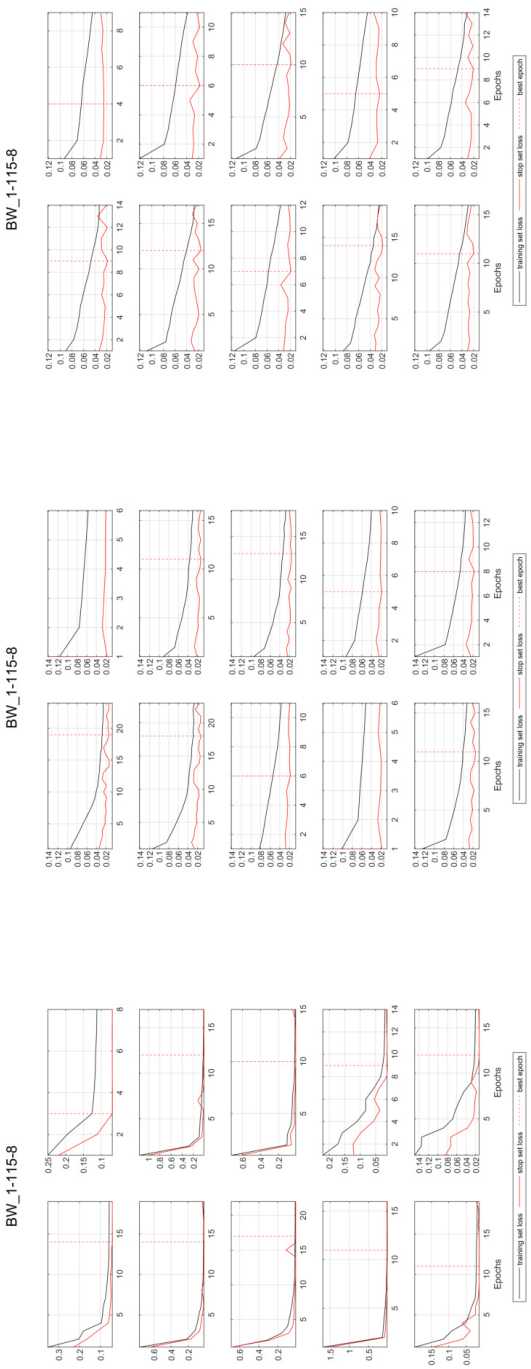

Figure S74: Seq2Val training and early stopping loss (MSE) for all 10 model initializations for well BW_1-115-8: NARX (top), LSTM (middle), CNN (bottom)

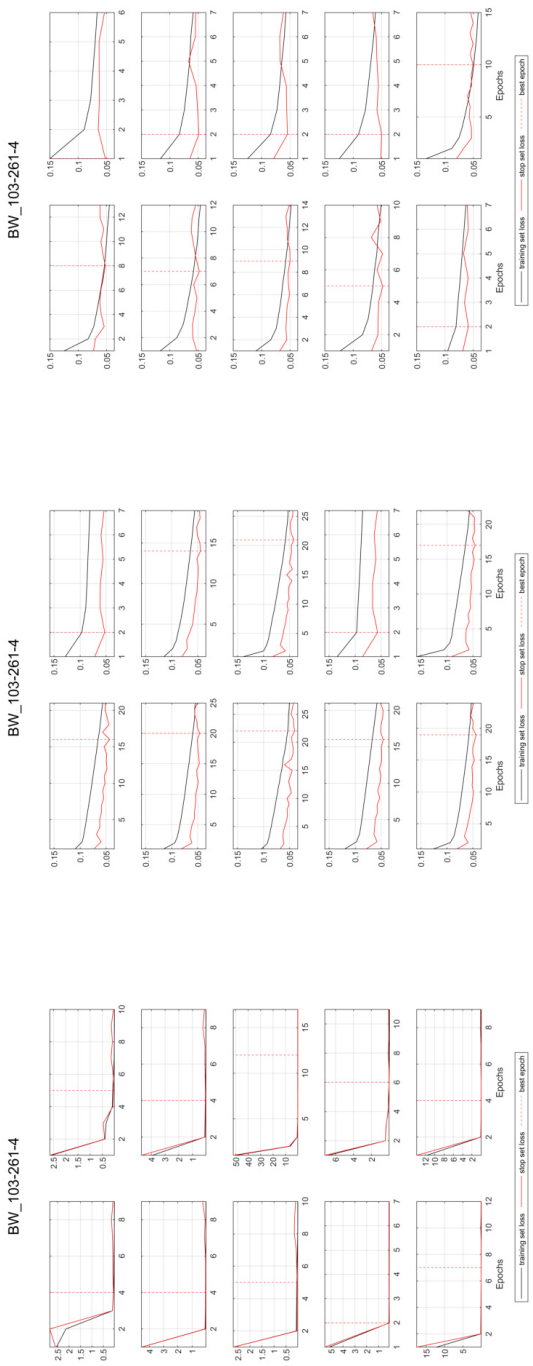

Figure S75: Seq2Val training and early stopping loss (MSE) for all 10 model initializations for well BW_103-261-4: NARX (top), LSTM (middle), CNN (bottom)

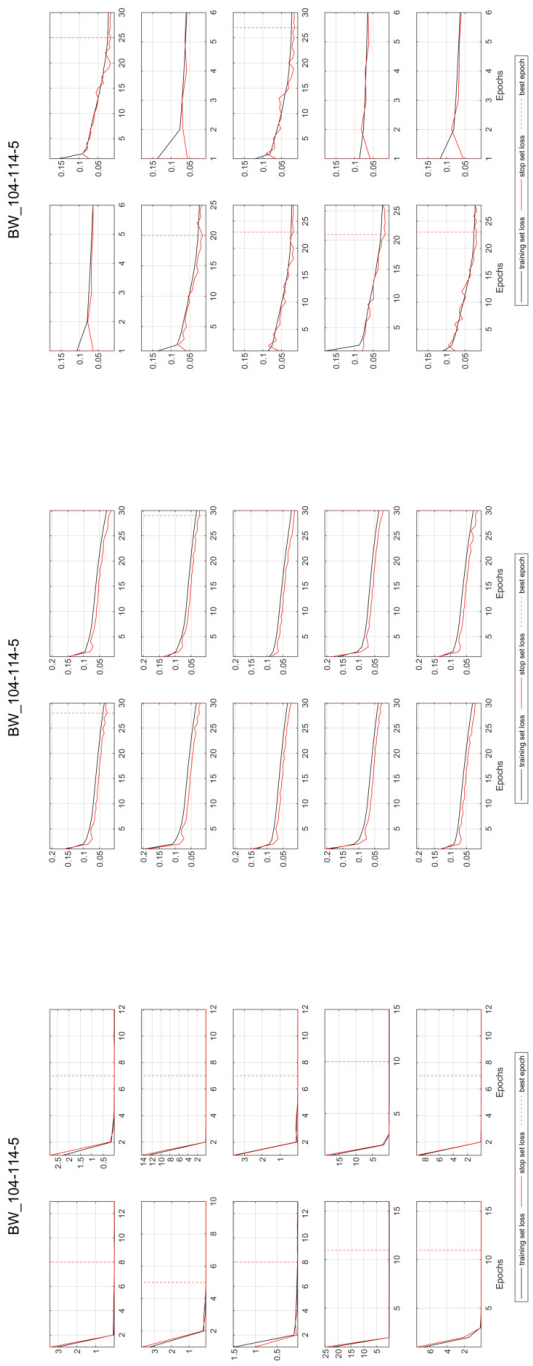

Figure S76: Seq2Val training and early stopping loss (MSE) for all 10 model initializations for well BW_104-114-5: NARX (top), LSTM (middle), CNN (bottom)

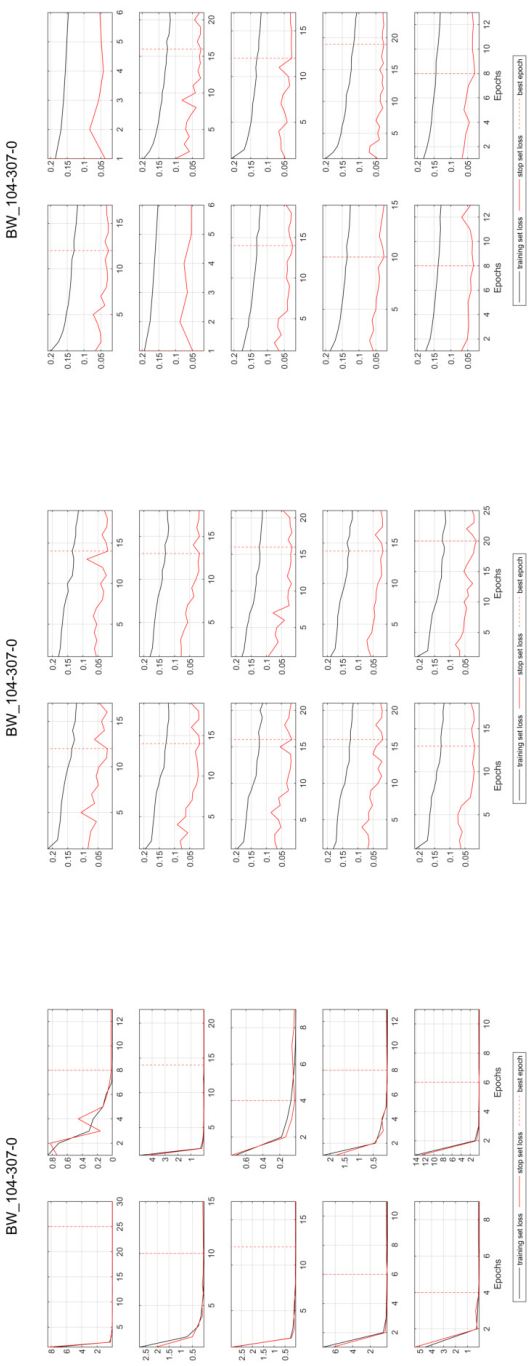

Figure S77: Seq2Val training and early stopping loss (MSE) for all 10 model initializations for well BW_104-307-0: NARX (top), LSTM (middle), CNN (bottom)

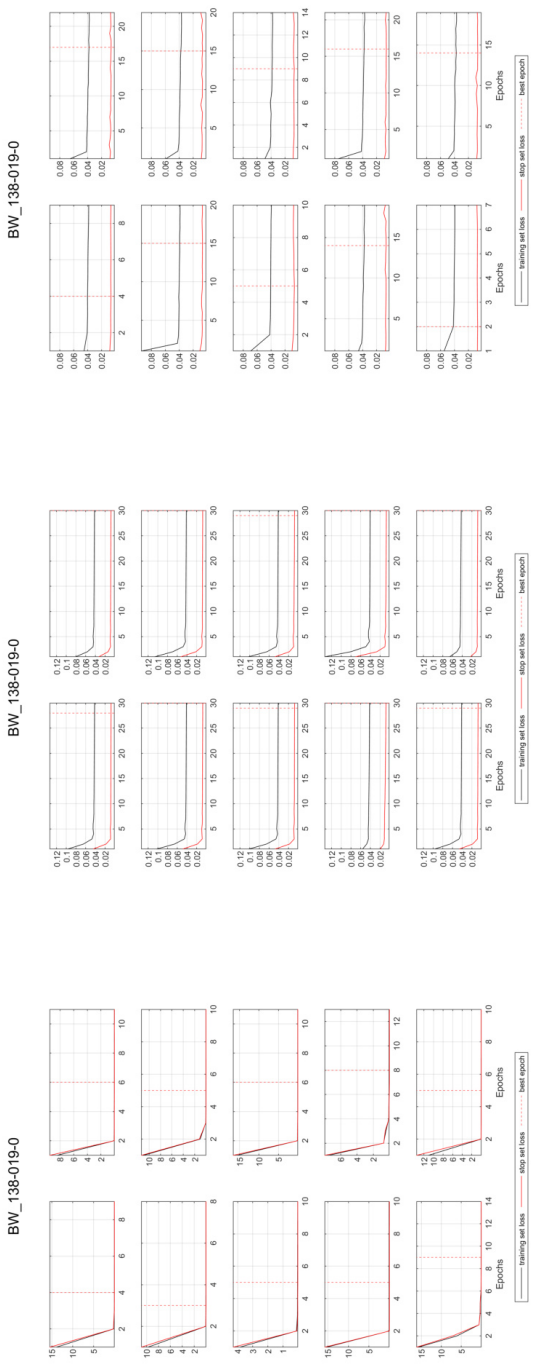

Figure S78: Seq2Val training and early stopping loss (MSE) for all 10 model initializations for well BW_138-019-0: NARX (top), LSTM (middle), CNN (bottom)

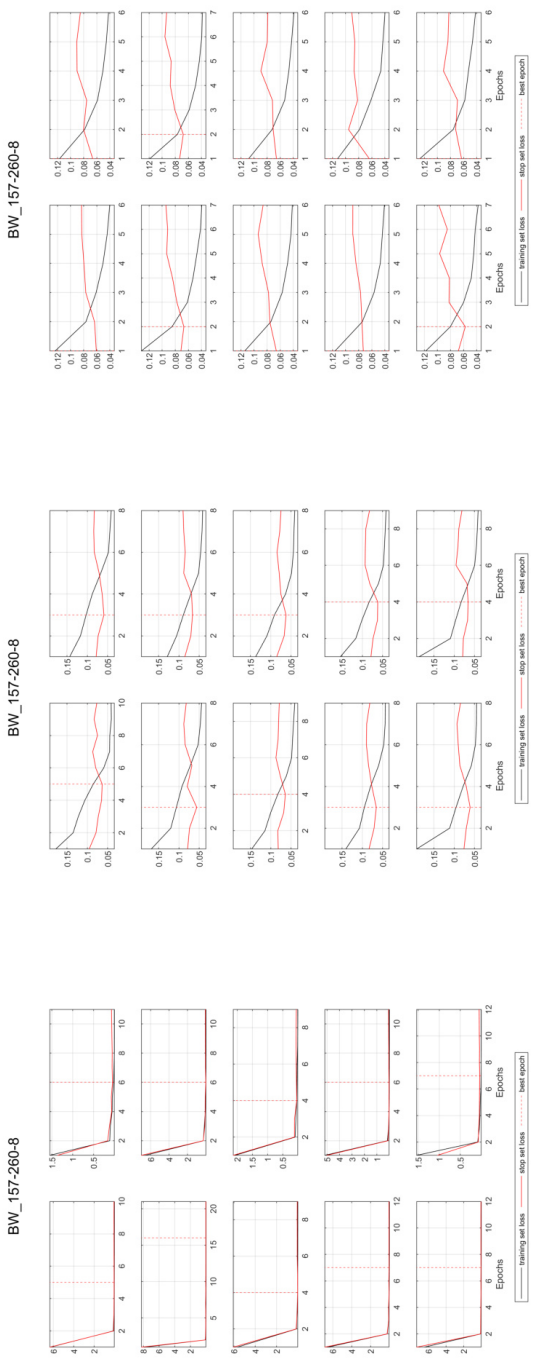

Figure S79: Seq2Val training and early stopping loss (MSE) for all 10 model initializations for well BW_157-260-8: NARX (top), LSTM (middle), CNN (bottom)

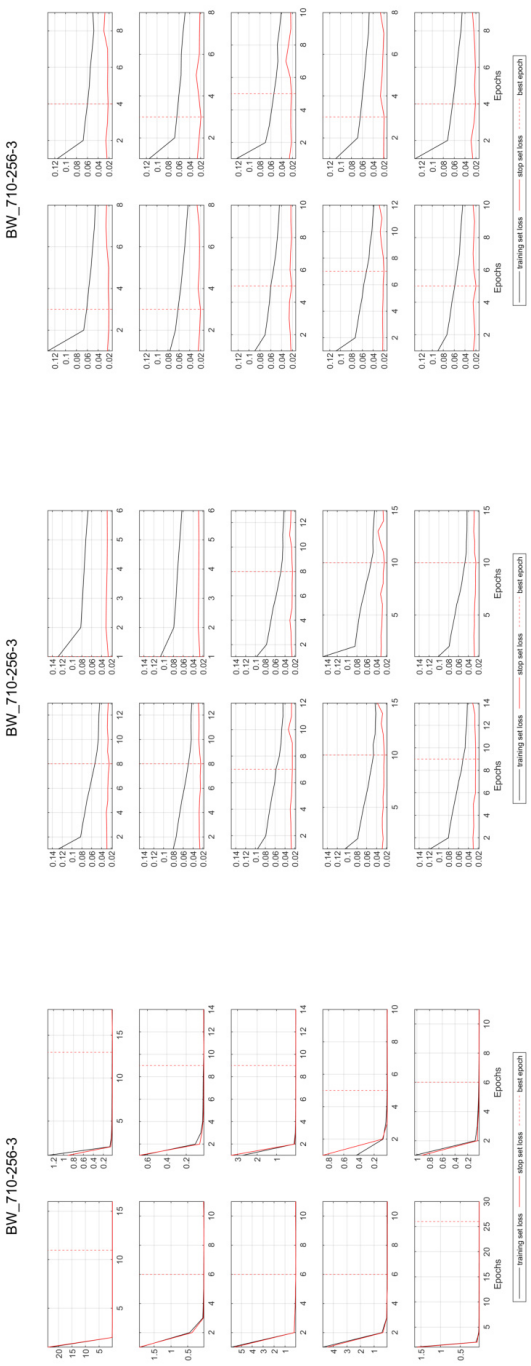

Figure S80: Seq2Val training and early stopping loss (MSE) for all 10 model initializations for well BW_710-256-3: NARX (top), LSTM (middle), CNN (bottom)

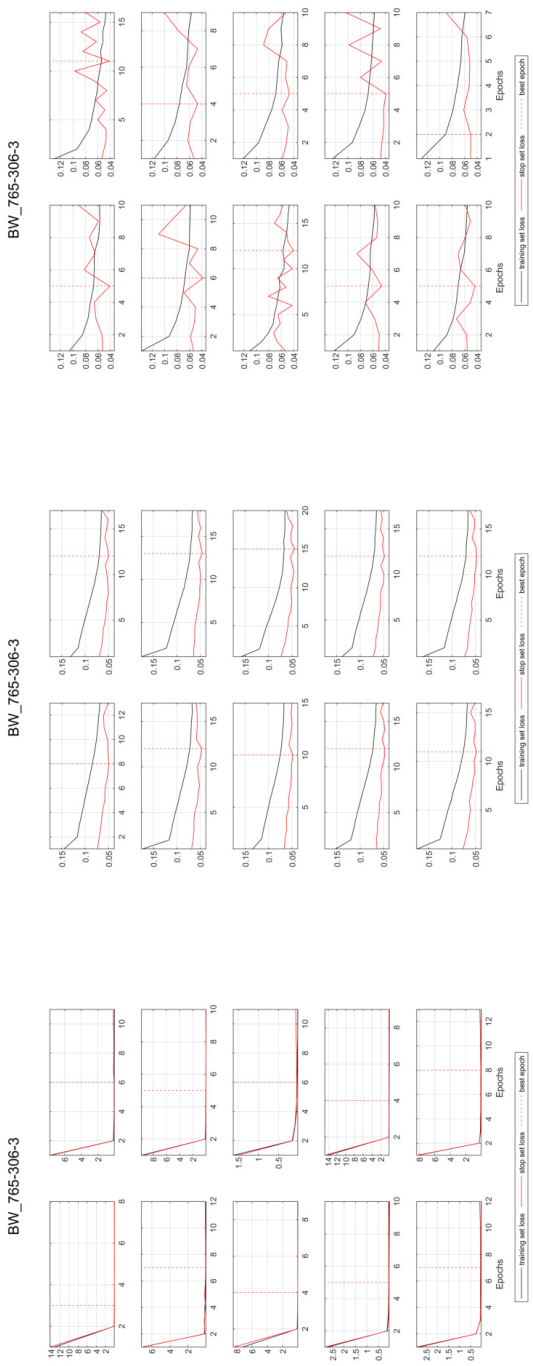

Figure S81: Seq2Val training and early stopping loss (MSE) for all 10 model initializations for well BW_765-306-3: NARX (top), LSTM (middle), CNN (bottom)

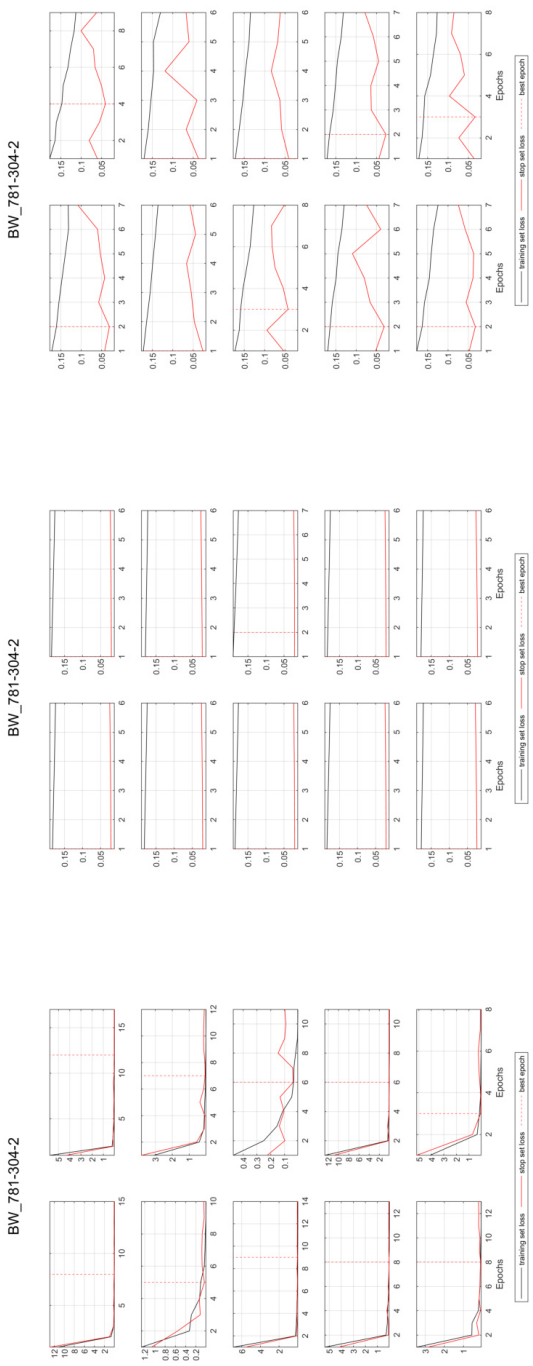

Figure S82: Seq2Val training and early stopping loss (MSE) for all 10 model initializations for well BW_781-304-2: NARX (top), LSTM (middle), CNN (bottom)

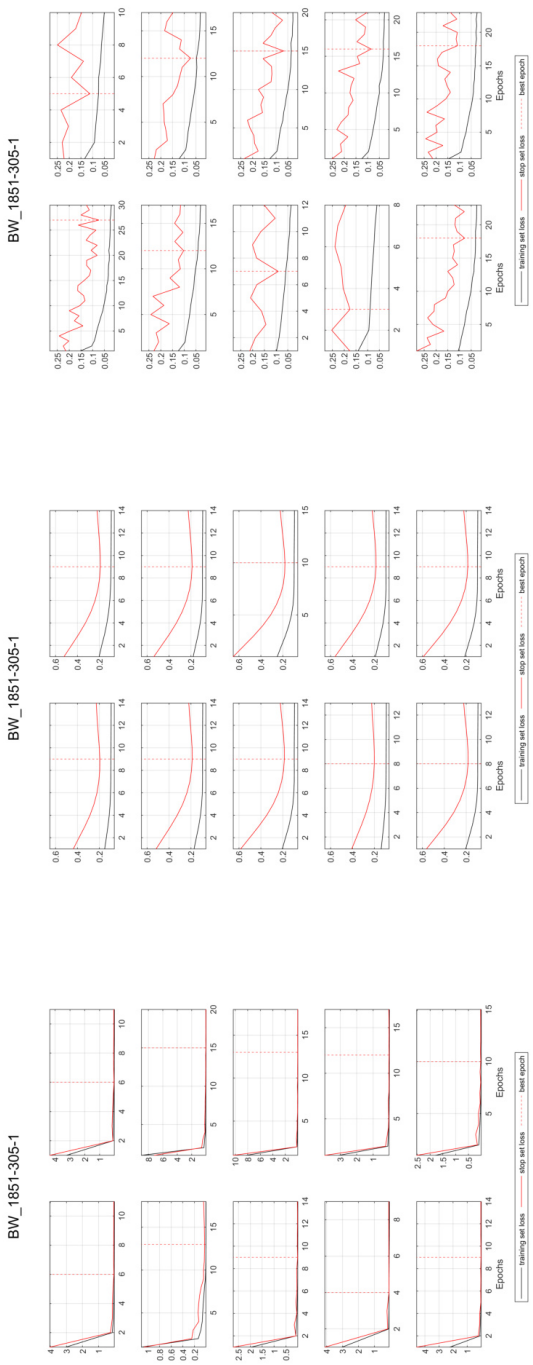

Figure S83: Seq2Val training and early stopping loss (MSE) for all 10 model initializations for well BW_1851-305-1: NARX (top), LSTM (middle), CNN (bottom)

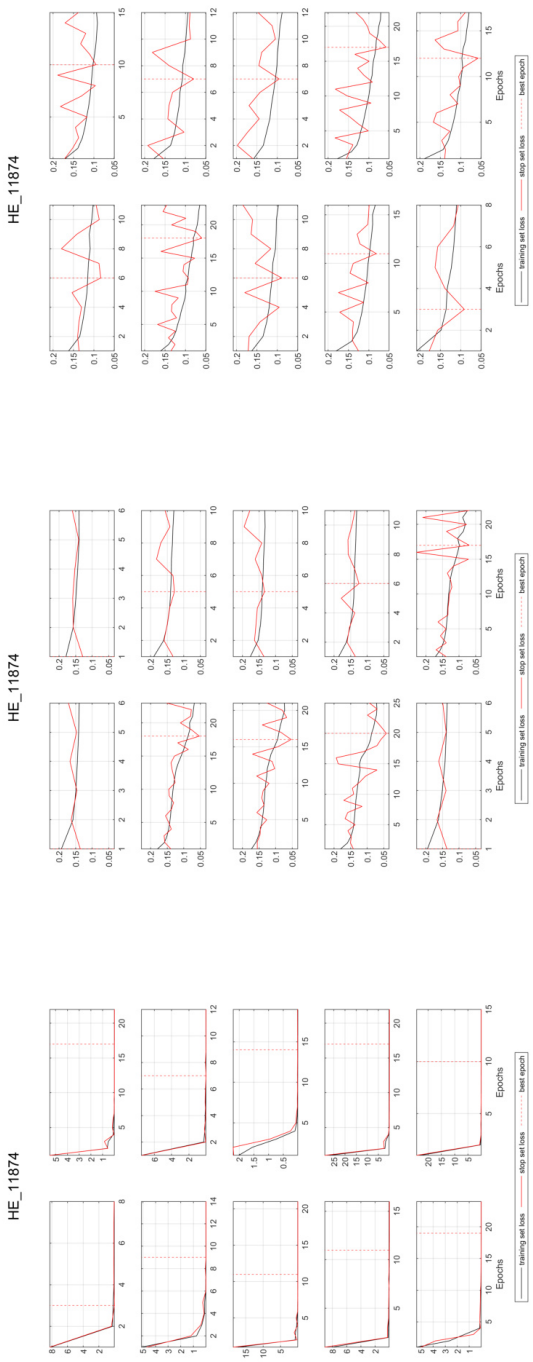

Figure S84: Seq2Val training and early stopping loss (MSE) for all 10 model initializations for well HE_11874: NARX (top), LSTM (middle), CNN (bottom)

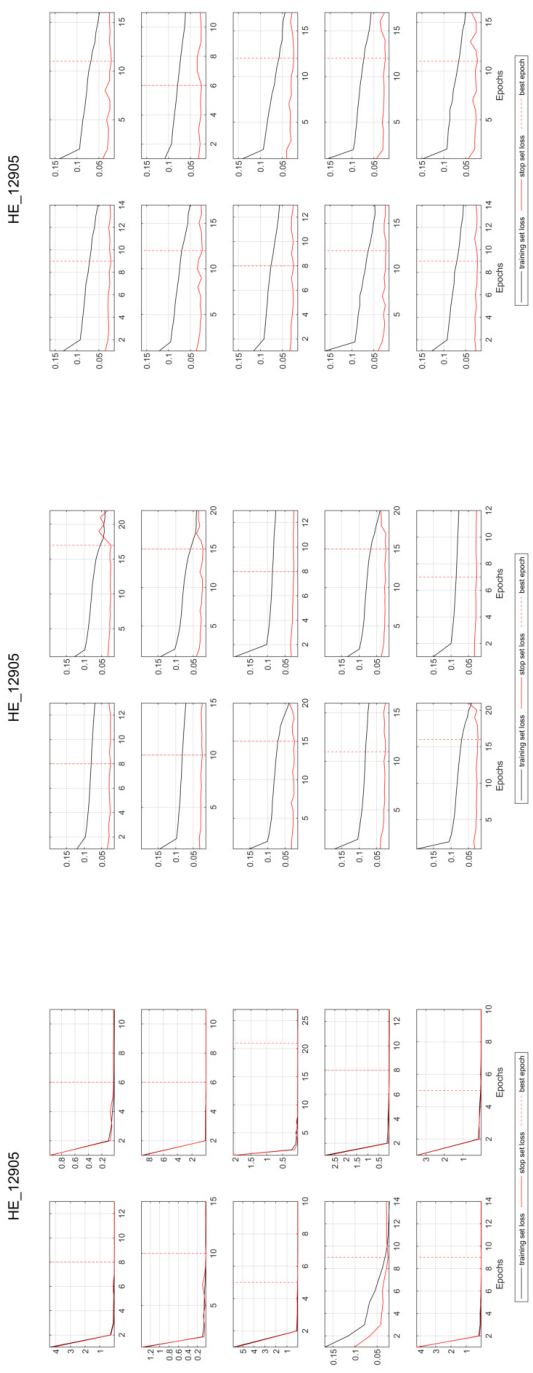

Figure S85: Seq2Val training and early stopping loss (MSE) for all 10 model initializations for well HE_12905: NARX (top), LSTM (middle), CNN (bottom)

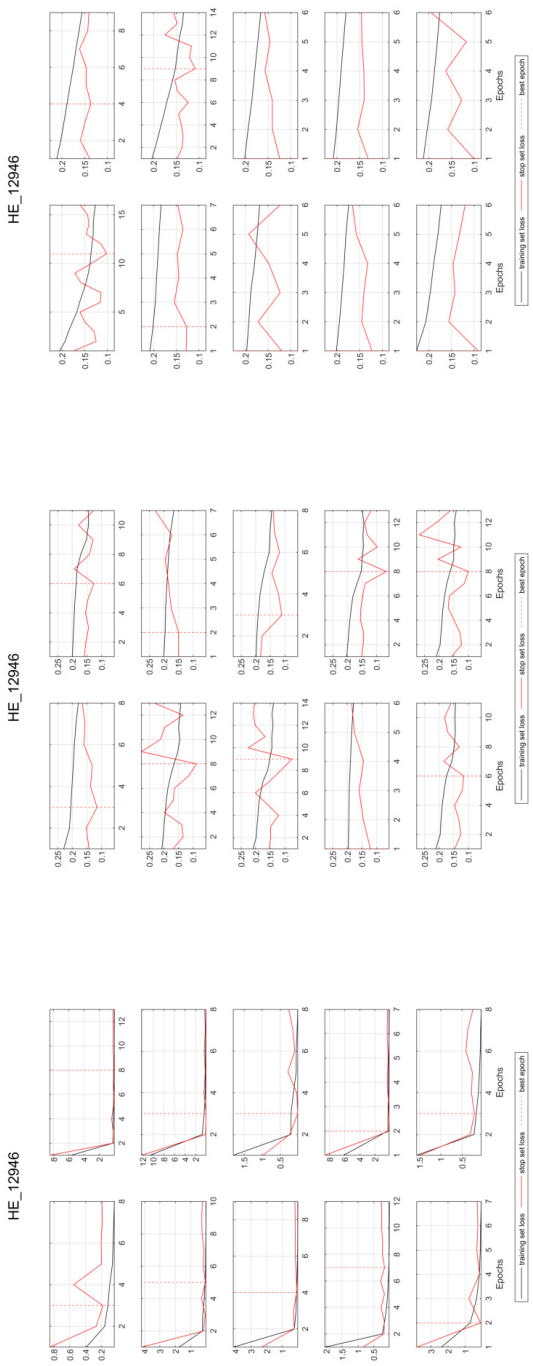

Figure S86: Seq2Val training and early stopping loss (MSE) for all 10 model initializations for well HE_12946: NARX (top), LSTM (middle), CNN (bottom)

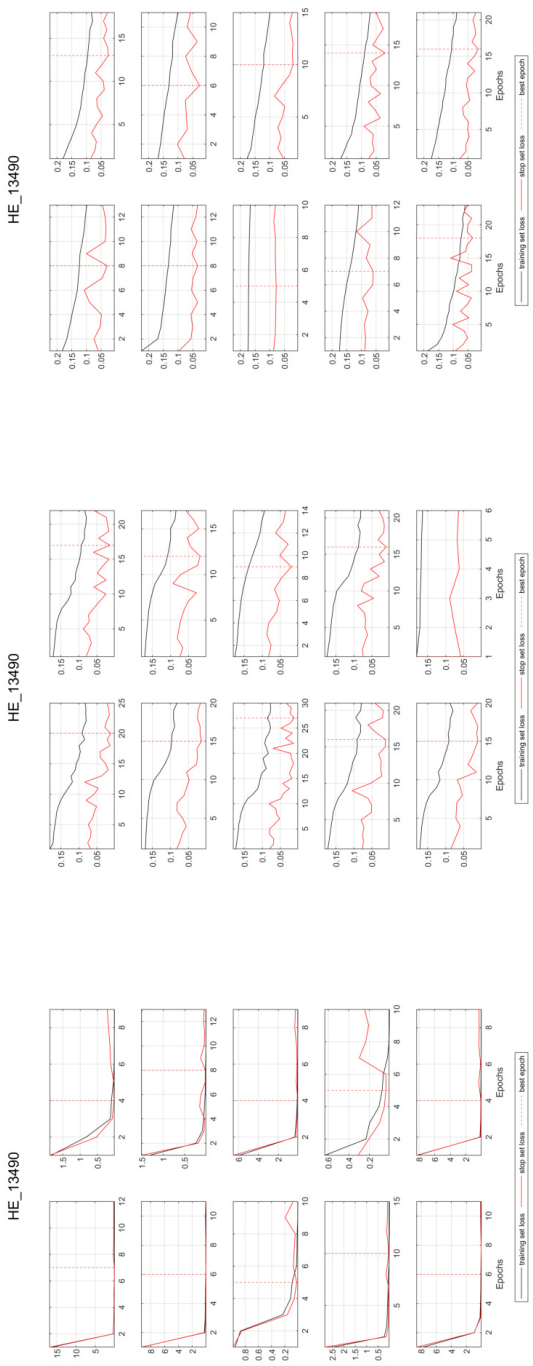

Figure S87: Seq2Val training and early stopping loss (MSE) for all 10 model initializations for well HE_13490: NARX (top), LSTM (middle), CNN (bottom)

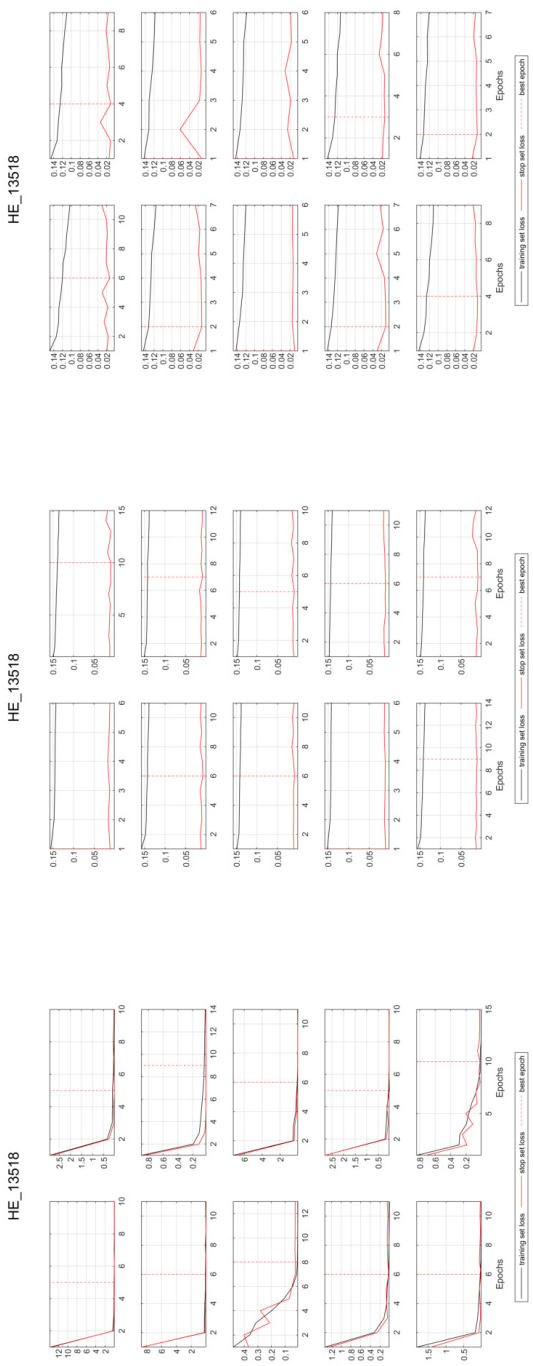

Figure S88: Seq2Val training and early stopping loss (MSE) for all 10 model initializations for well HE_13518: NARX (top), LSTM (middle), CNN (bottom)

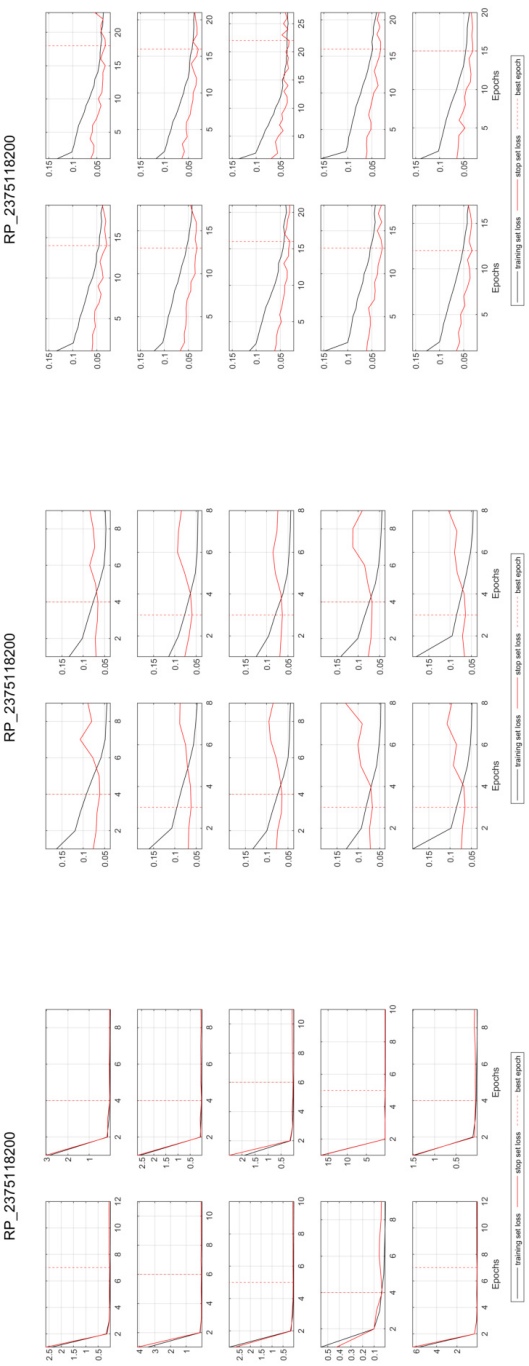

Figure S89: Seq2Val training and early stopping loss (MSE) for all 10 model initializations for well RP_2375118200: NARX (top), LSTM (middle), CNN (bottom)

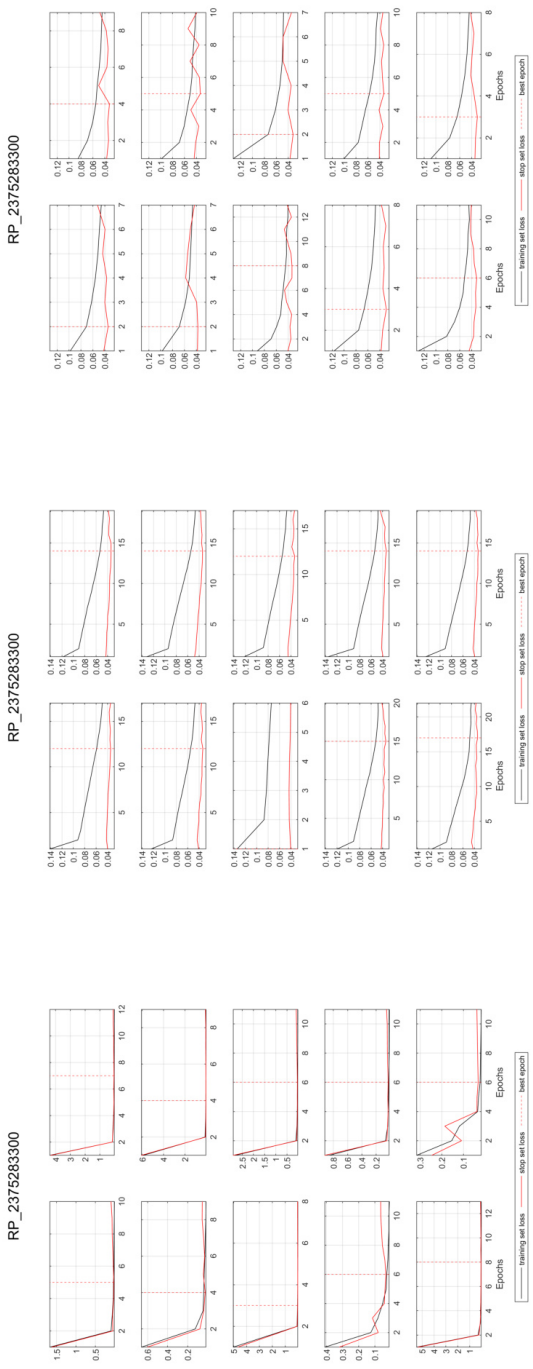

Figure S90: Seq2Val training and early stopping loss (MSE) for all 10 model initializations for well RP_2375283300: NARX (top), LSTM (middle), CNN (bottom)

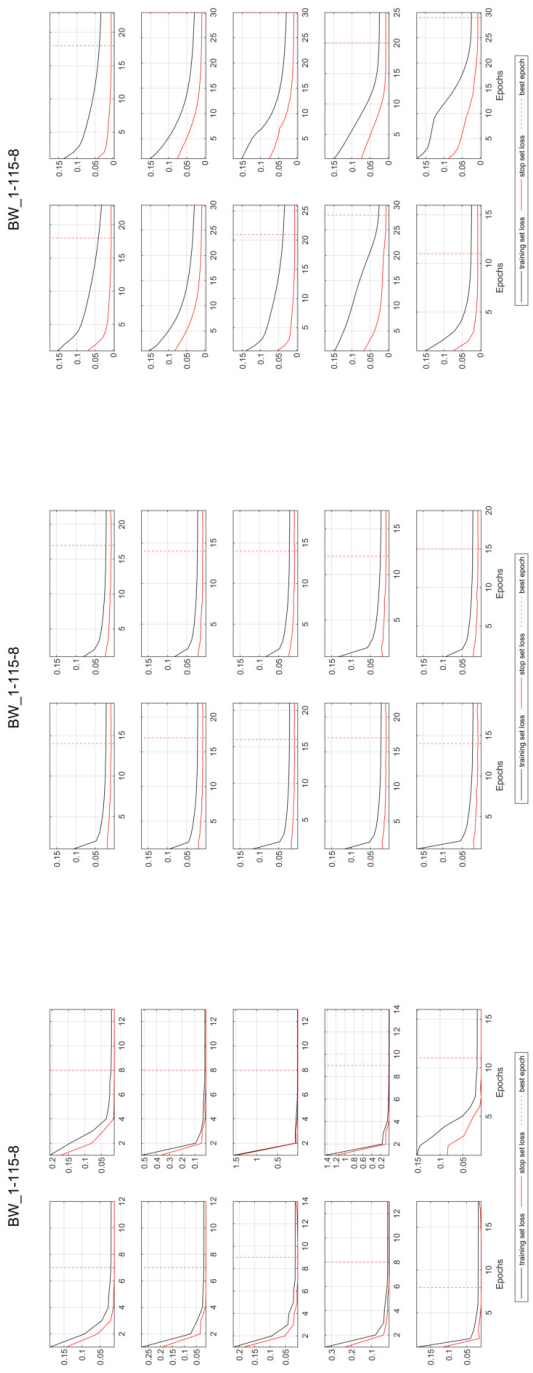

Figure S91: Seq2Val GWL_{t-1} training and early stopping loss (MSE) for all 10 model initializations for well BW_1-115-8: NARX (top), LSTM (middle), CNN (bottom)

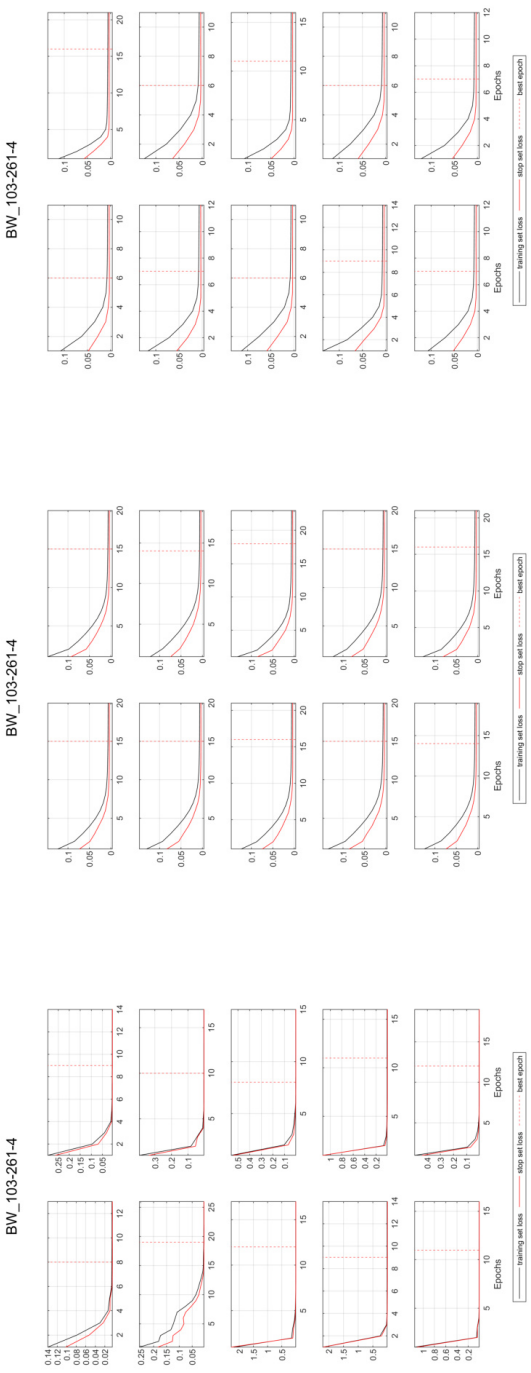

Figure S92: Seq2Val GWL_{t-1} training and early stopping loss (MSE) for all 10 model initializations for well BW_103-261-4: NARX (top), LSTM (middle), CNN (bottom)

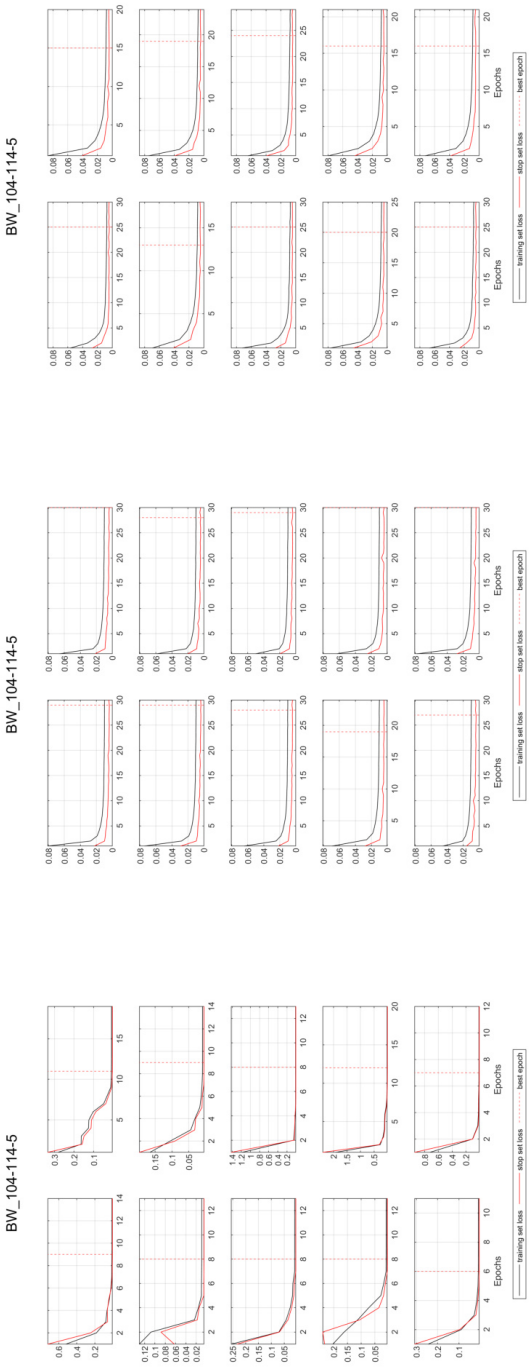

Figure S93: Seq2Val GWL_{t-1} training and early stopping loss (MSE) for all 10 model initializations for well BW_104-114-5: NARX (top), LSTM (middle), CNN (bottom)

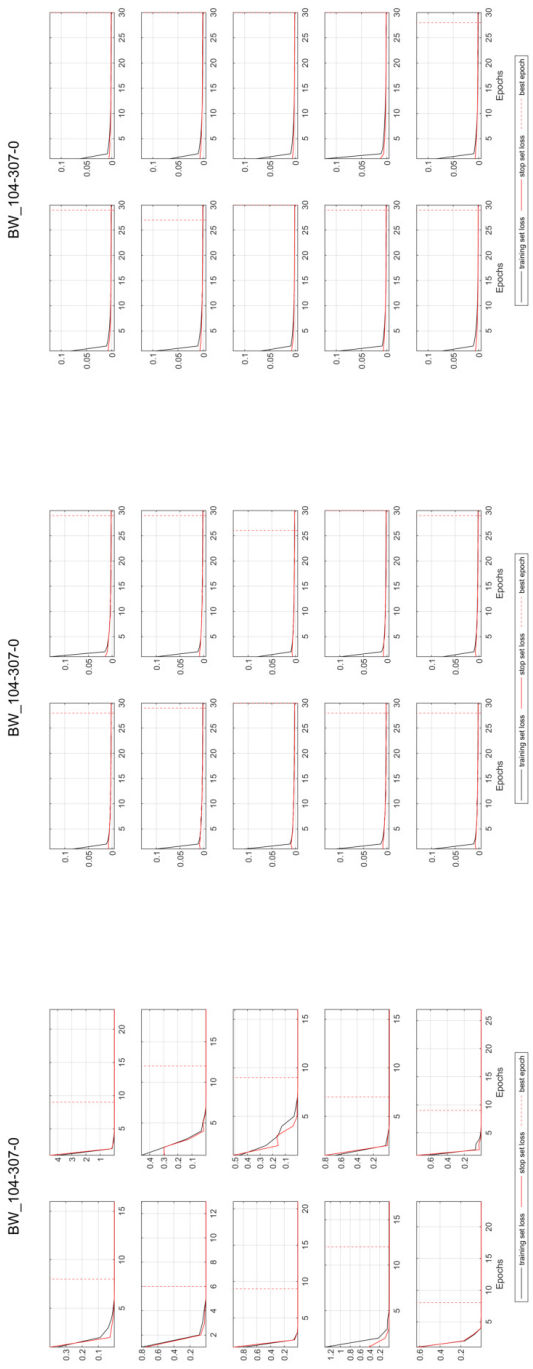

Figure S94: Seq2Val GWL_{t-1} training and early stopping loss (MSE) for all 10 model initializations for well BW_104-307-0: NARX (top), LSTM (middle), CNN (bottom)

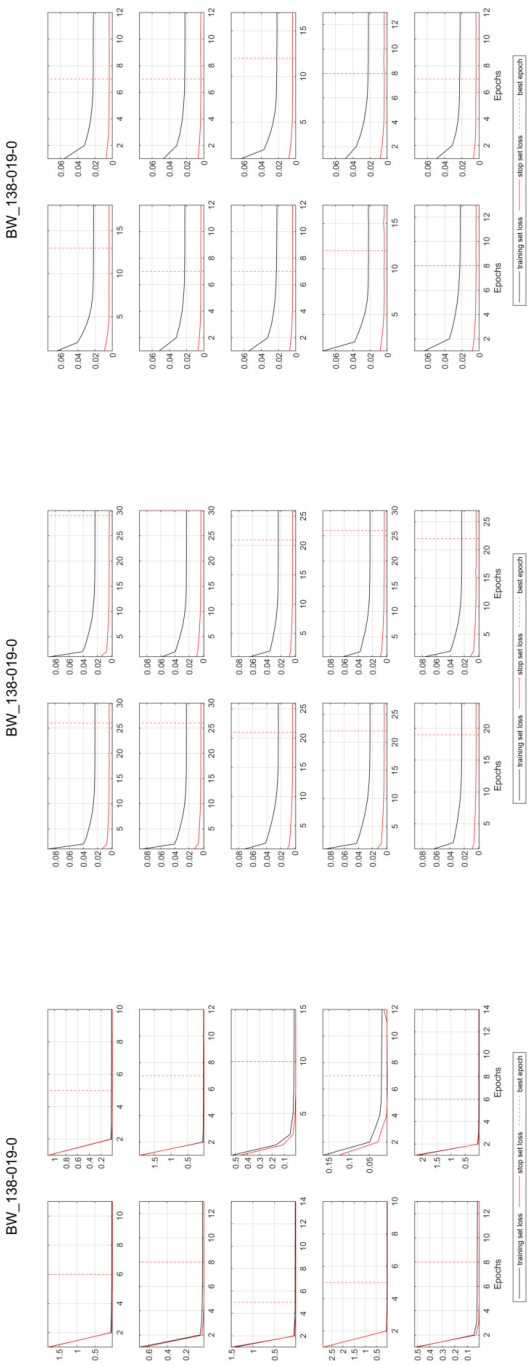

Figure S95: Seq2Val GWL_{t-1} training and early stopping loss (MSE) for all 10 model initializations for well BW_138-019-0: NARX (top), LSTM (middle), CNN (bottom)

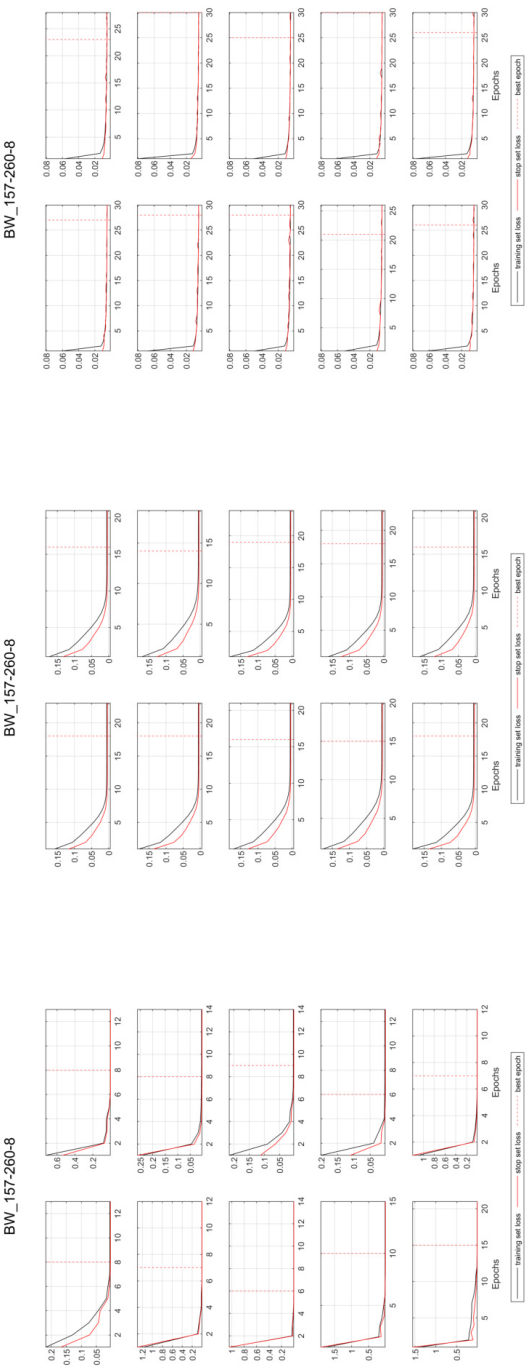

Figure S96: Seq2Val GWL_{t-1} training and early stopping loss (MSE) for all 10 model initializations for well BW_157-260-8: NARX (top), LSTM (middle), CNN (bottom)

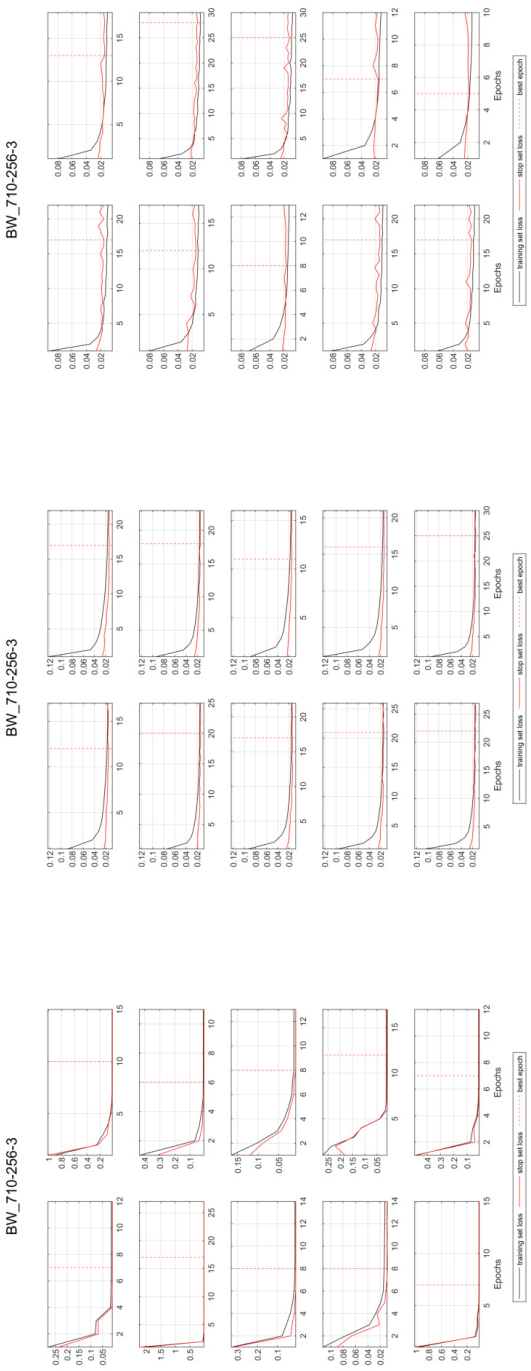

Figure S97: Seq2Val GWL_{t-1} training and early stopping loss (MSE) for all 10 model initializations for well BW_710-256-3: NARX (top), LSTM (middle), CNN (bottom)

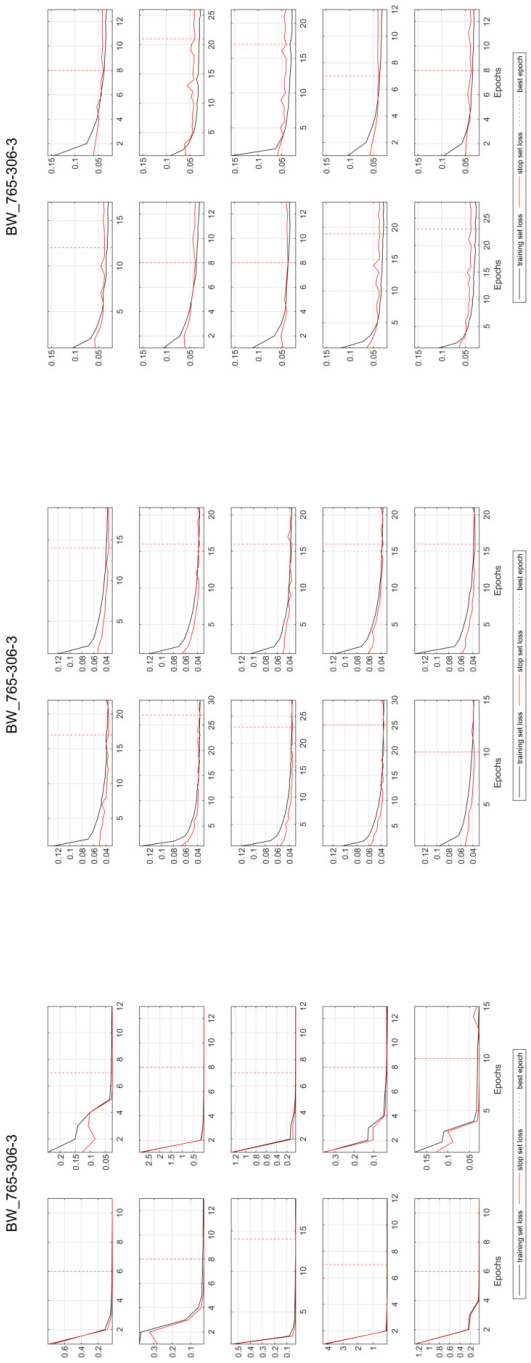

Figure S98: Seq2Val GWL_{t-1} training and early stopping loss (MSE) for all 10 model initializations for well BW_765-306-3: NARX (top), LSTM (middle), CNN (bottom)

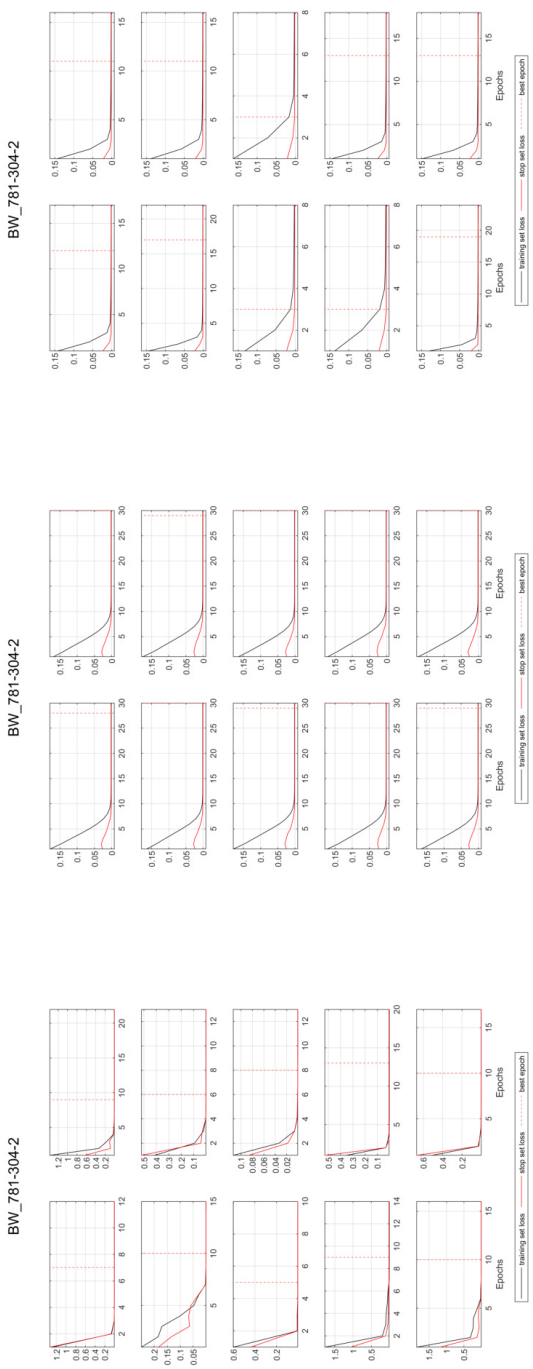

Figure S99: Seq2Val GWL_{t-1} training and early stopping loss (MSE) for all 10 model initializations for well BW_781-304-2: NARX (top), LSTM (middle), CNN (bottom)

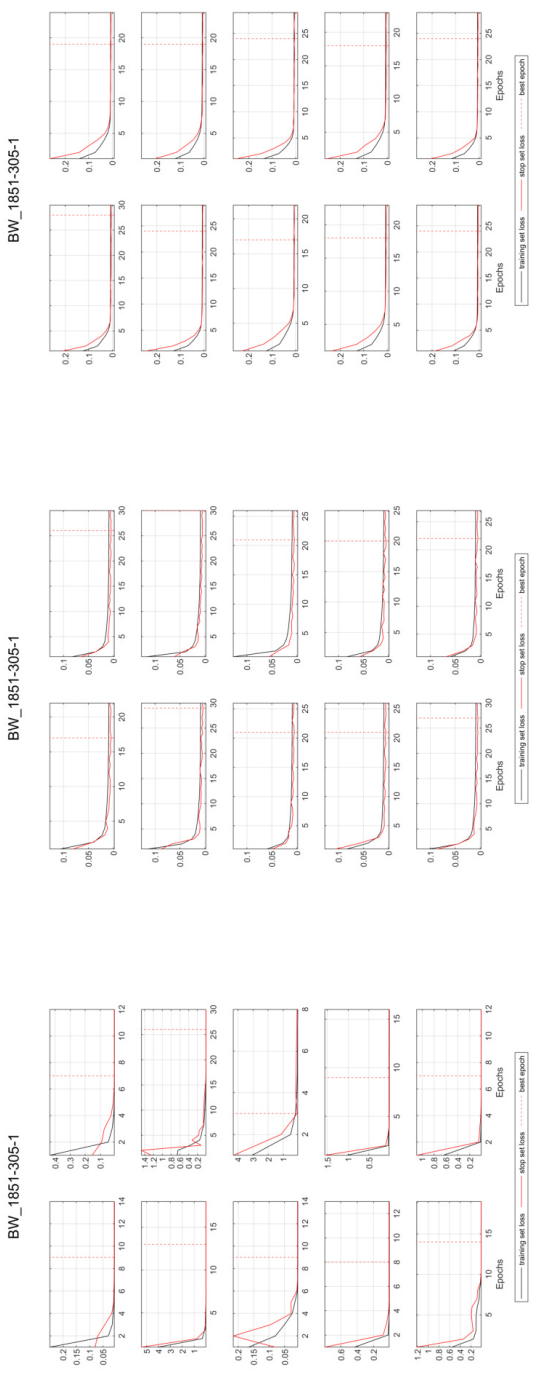

Figure S100: Seq2Val GWL_{t-1} training and early stopping loss (MSE) for all 10 model initializations for well BW_1851-305-1: NARX (top), LSTM (middle), CNN (bottom)

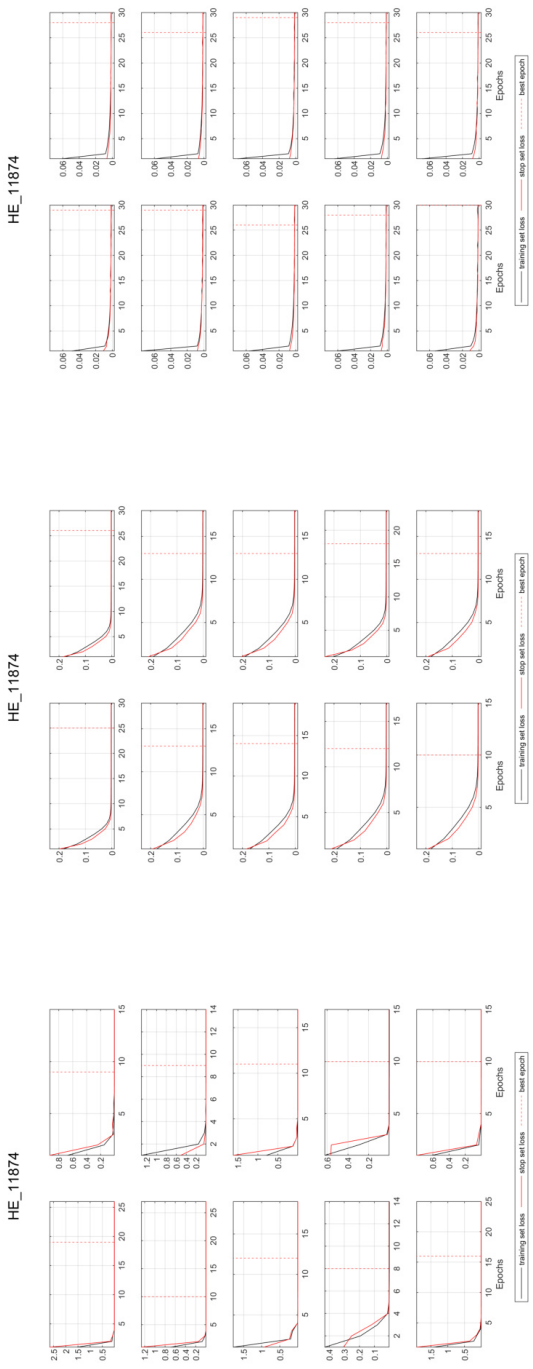

Figure S101: Seq2Val GWL_{t-1} training and early stopping loss (MSE) for all 10 model initializations for well HE_11874: NARX (top), LSTM (middle), CNN (bottom)

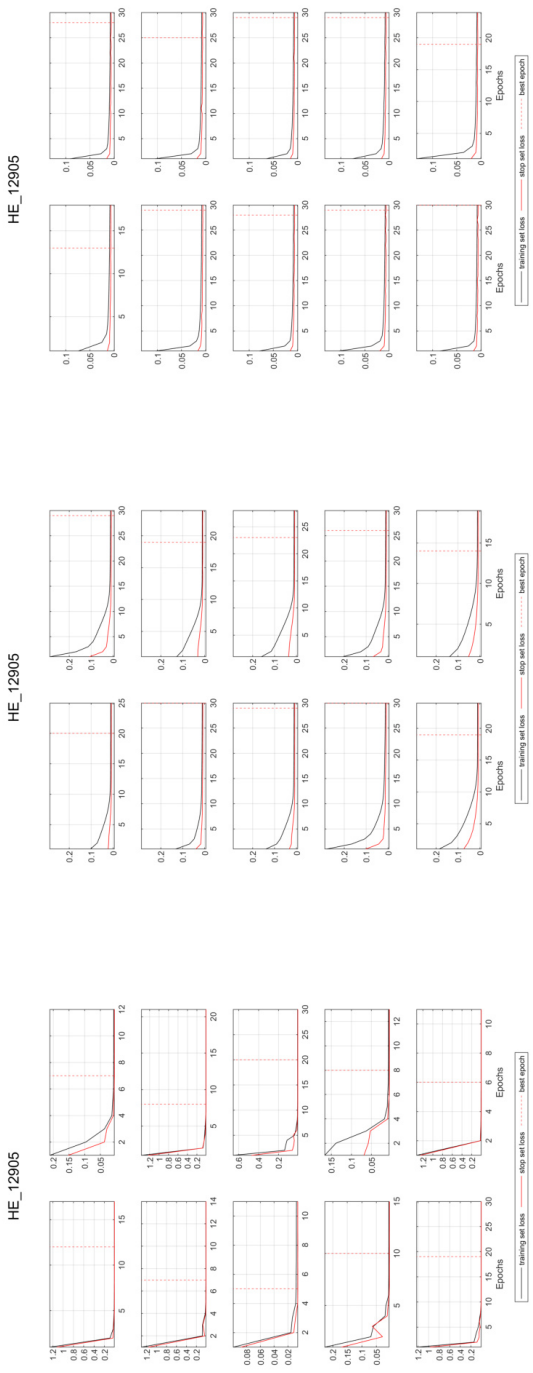

Figure S102: Seq2Val GWL_{t-1} training and early stopping loss (MSE) for all 10 model initializations for well HE_12905: NARX (top), LSTM (middle), CNN (bottom)

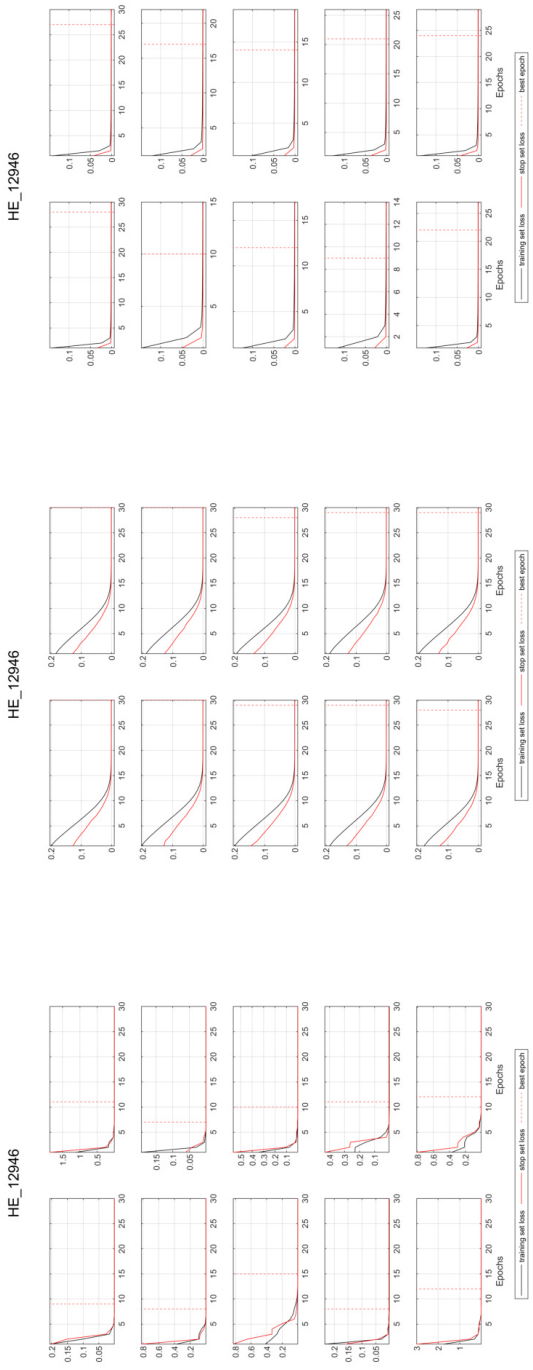

Figure S103: Seq2Val GWL_{t-1} training and early stopping loss (MSE) for all 10 model initializations for well HE_12946: NARX (top), LSTM (middle), CNN (bottom)

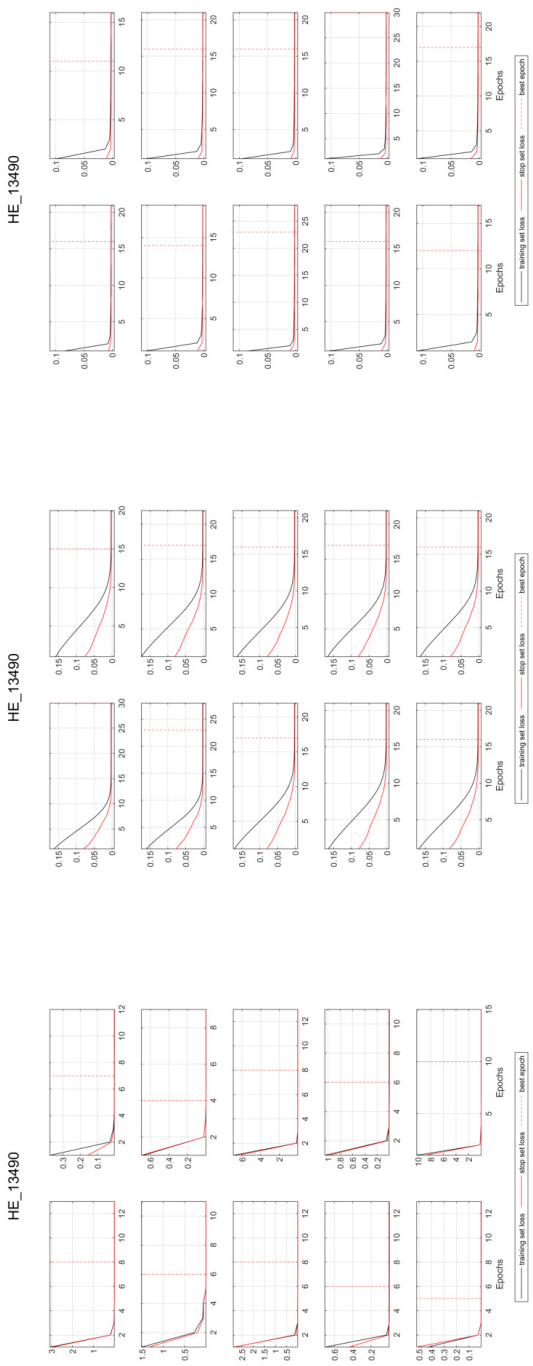

Figure S104: Seq2Val GWL_{t-1} training and early stopping loss (MSE) for all 10 model initializations for well HE_13490: NARX (top), LSTM (middle), CNN (bottom)

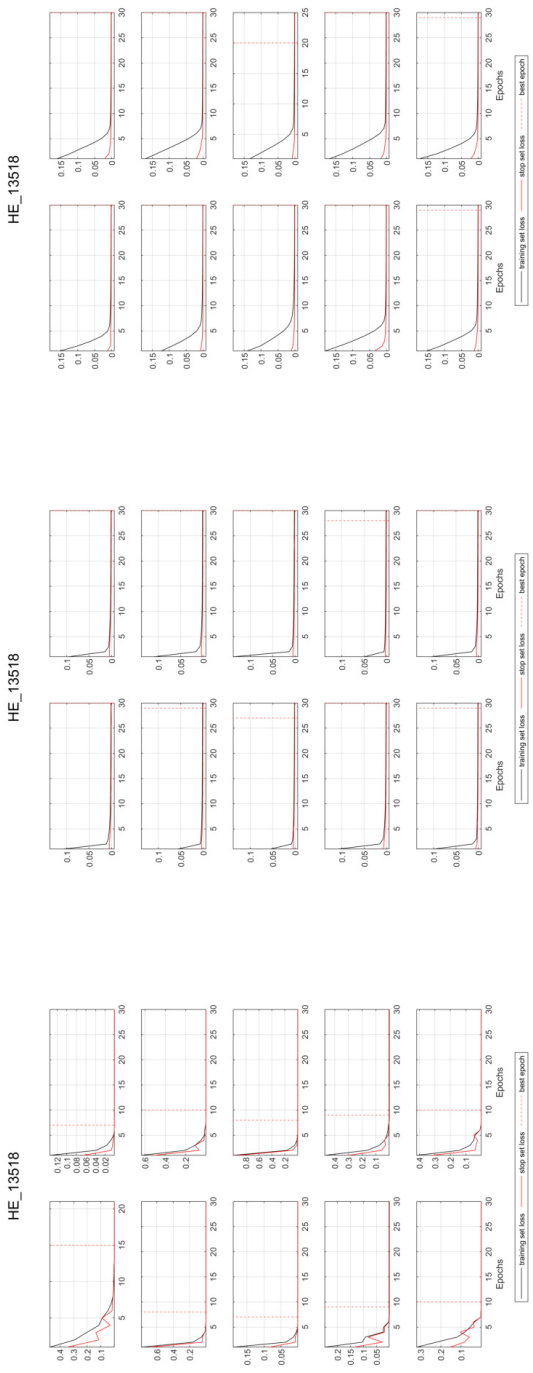

Figure S105: Seq2Val GWL_{t-1} training and early stopping loss (MSE) for all 10 model initializations for well HE_13518: NARX (top), LSTM (middle), CNN (bottom)

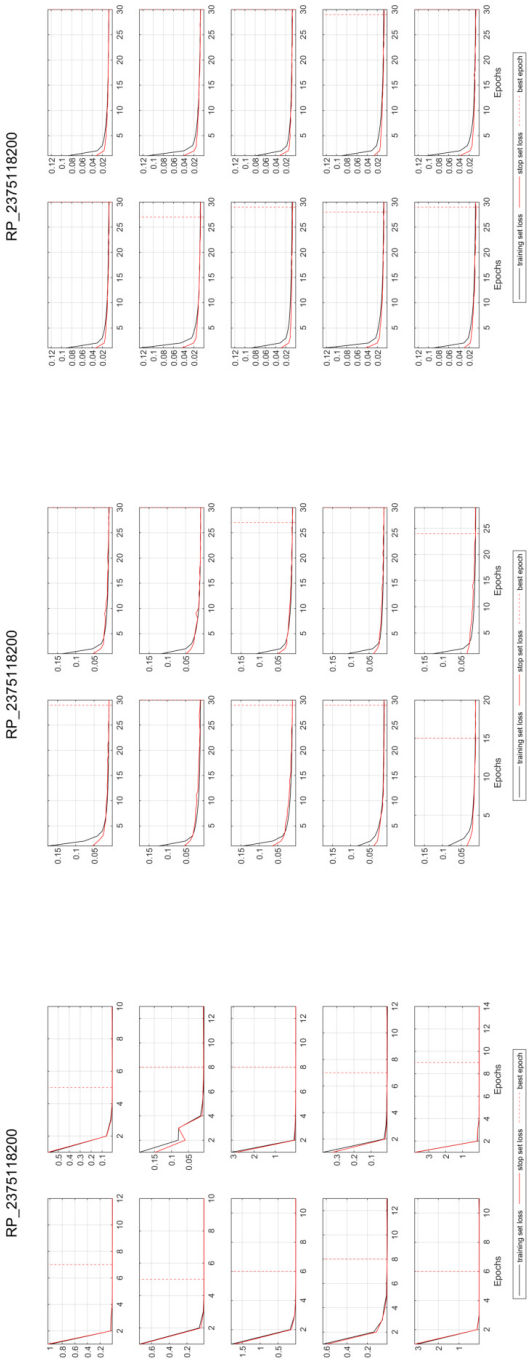

Figure S106: Seq2Val GWL_{t-1} training and early stopping loss (MSE) for all 10 model initializations for well RP_2375118200: NARX (top), LSTM (middle), CNN (bottom)

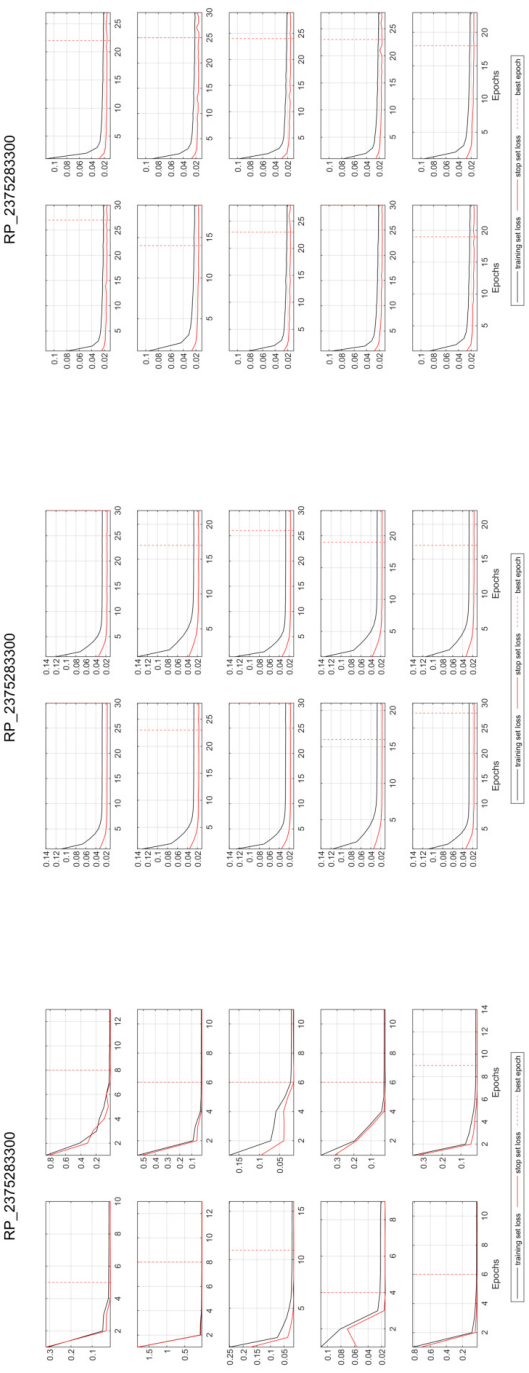

Figure S107: Seq2Val GWL_{t-1} training and early stopping loss (MSE) for all 10 model initializations for well RP_2375283300: NARX (top), LSTM (middle), CNN (bottom)

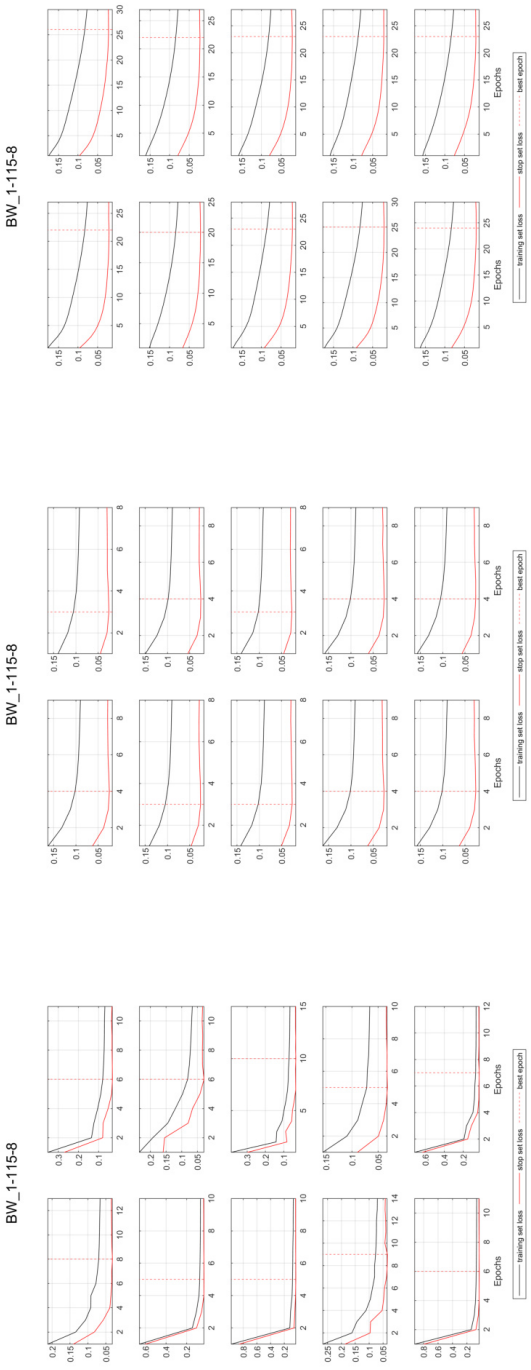

Figure S108: Seq2Seq training and early stopping loss (MSE) for all 10 model initializations for well BW_1-115-8: NARX (top), LSTM (middle), CNN (bottom)

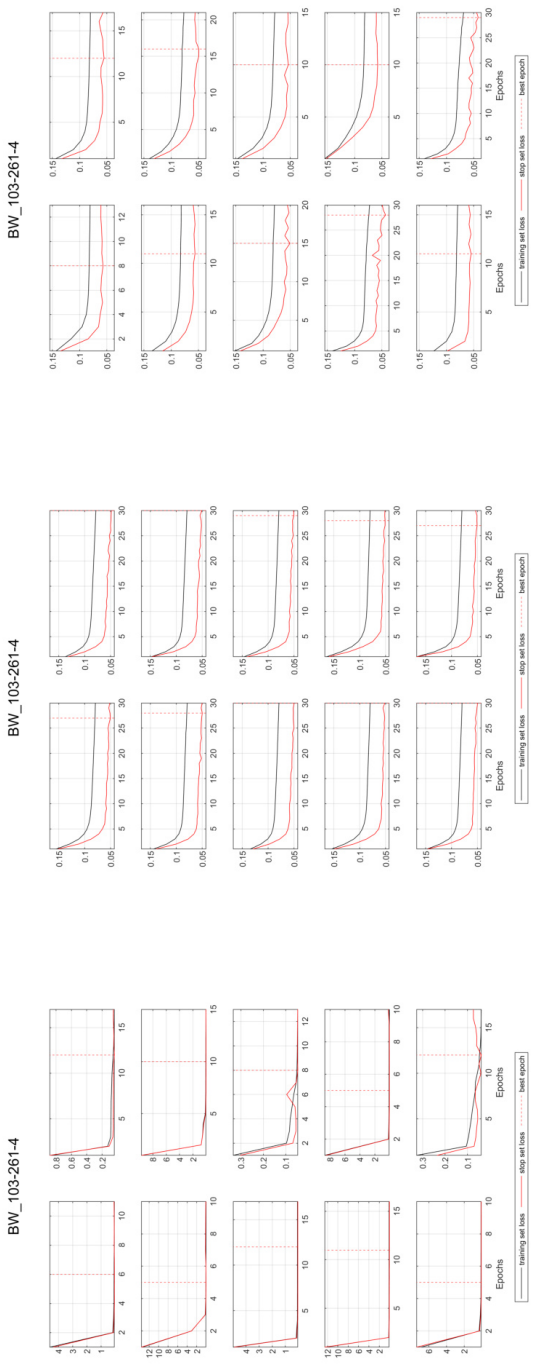

Figure S109: Seq2Seq training and early stopping loss (MSE) for all 10 model initializations for well BW_103-261-4: NARX (top), LSTM (middle), CNN (bottom)

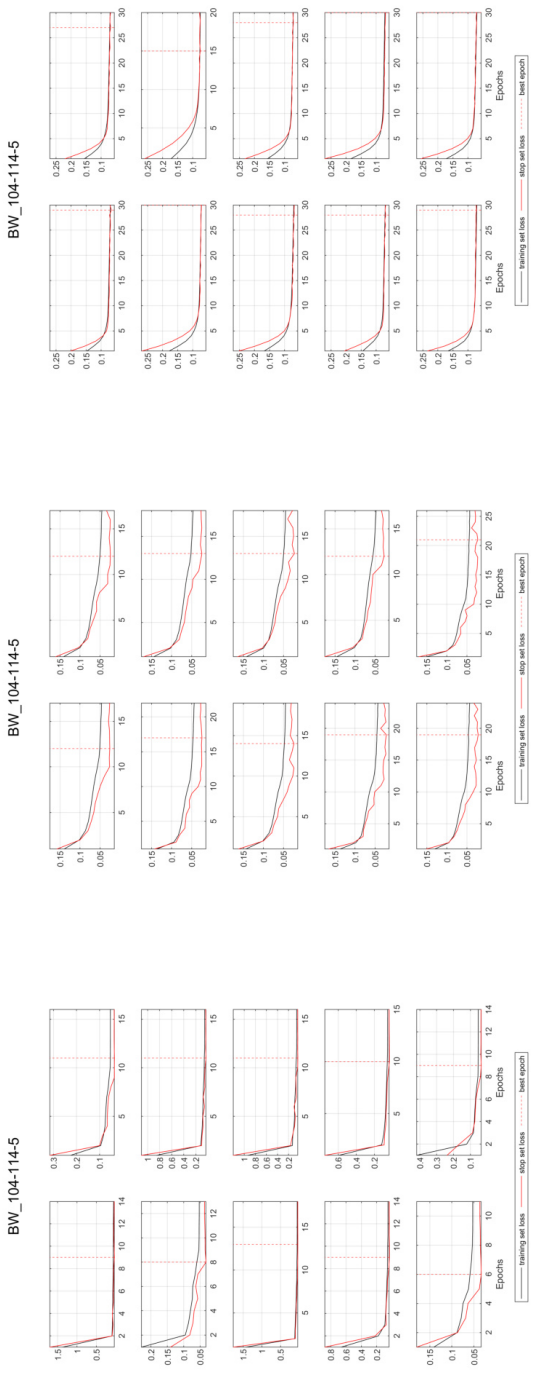

Figure S110: Seq2Seq training and early stopping loss (MSE) for all 10 model initializations for well BW_104-114-5: NARX (top), LSTM (middle), CNN (bottom)

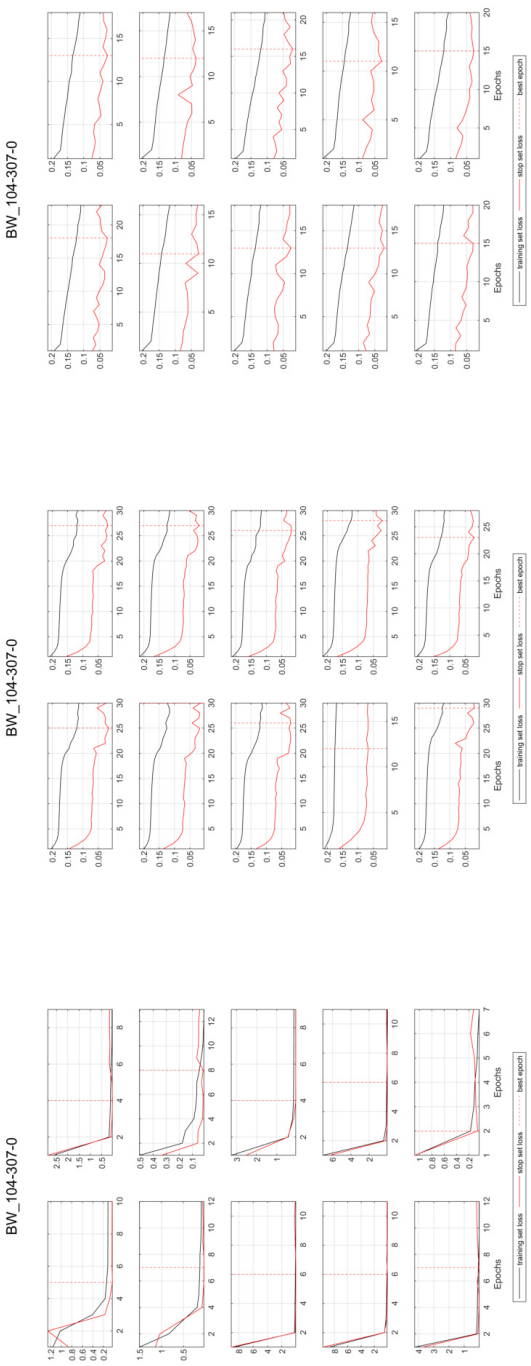

Figure S111: Seq2Seq training and early stopping loss (MSE) for all 10 model initializations for well BW_104-307-0: NARX (top), LSTM (middle), CNN (bottom)

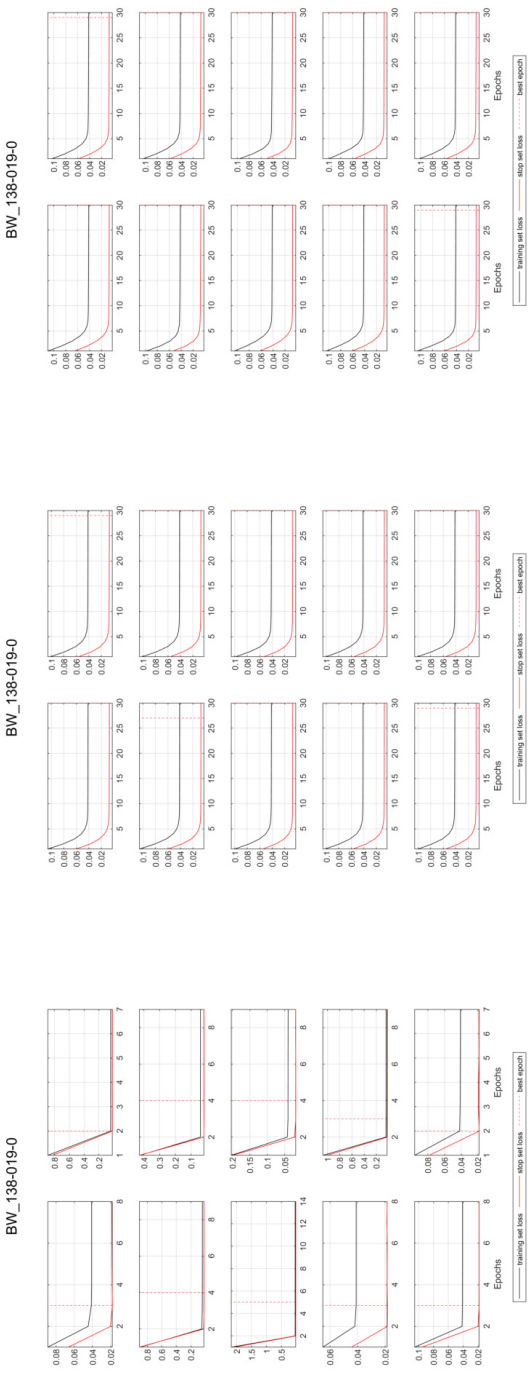

Figure S112: Seq2Seq training and early stopping loss (MSE) for all 10 model initializations for well BW_138-019-0: NARX (top), LSTM (middle), CNN (bottom)

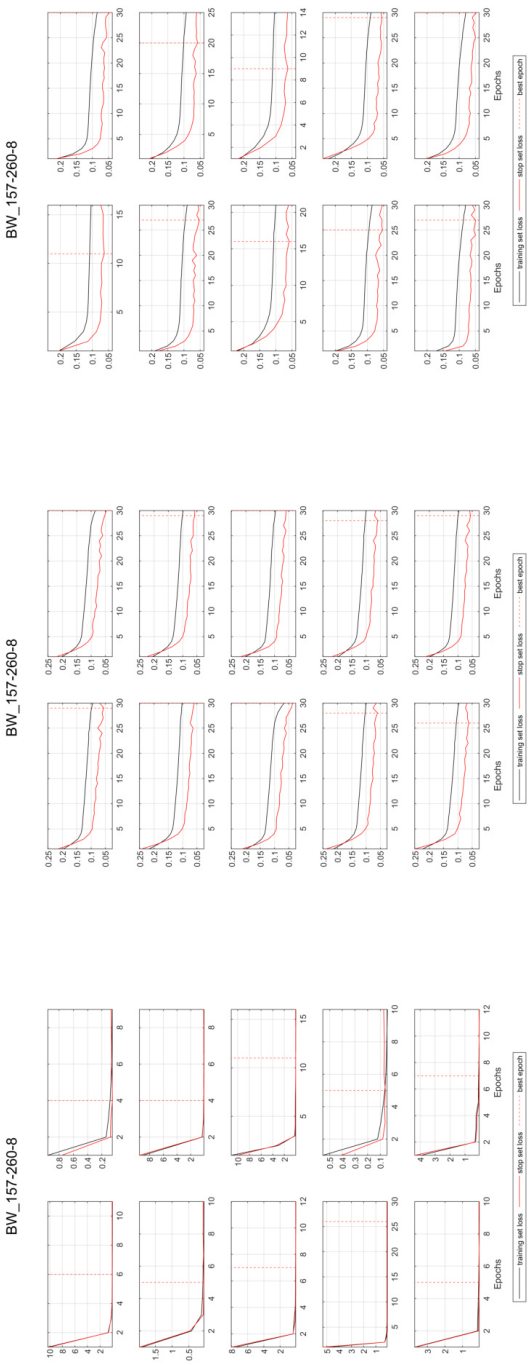

Figure S113: Seq2Seq training and early stopping loss (MSE) for all 10 model initializations for well BW_157-260-8: NARX (top), LSTM (middle), CNN (bottom)

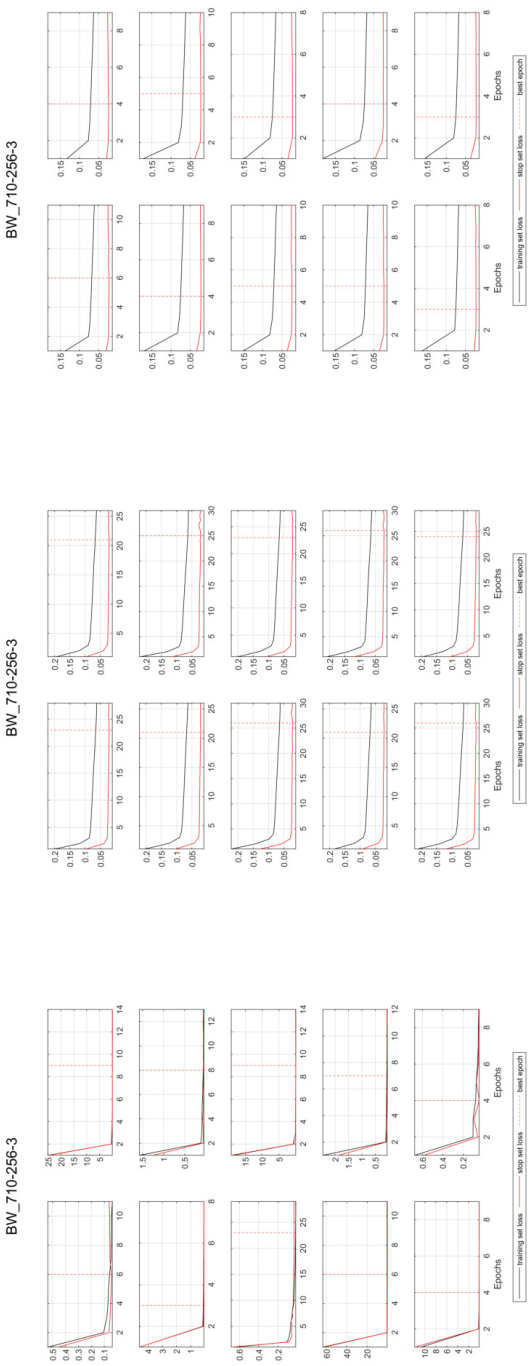

Figure S114: Seq2Seq training and early stopping loss (MSE) for all 10 model initializations for well BW_710-256-3: NARX (top), LSTM (middle), CNN (bottom)

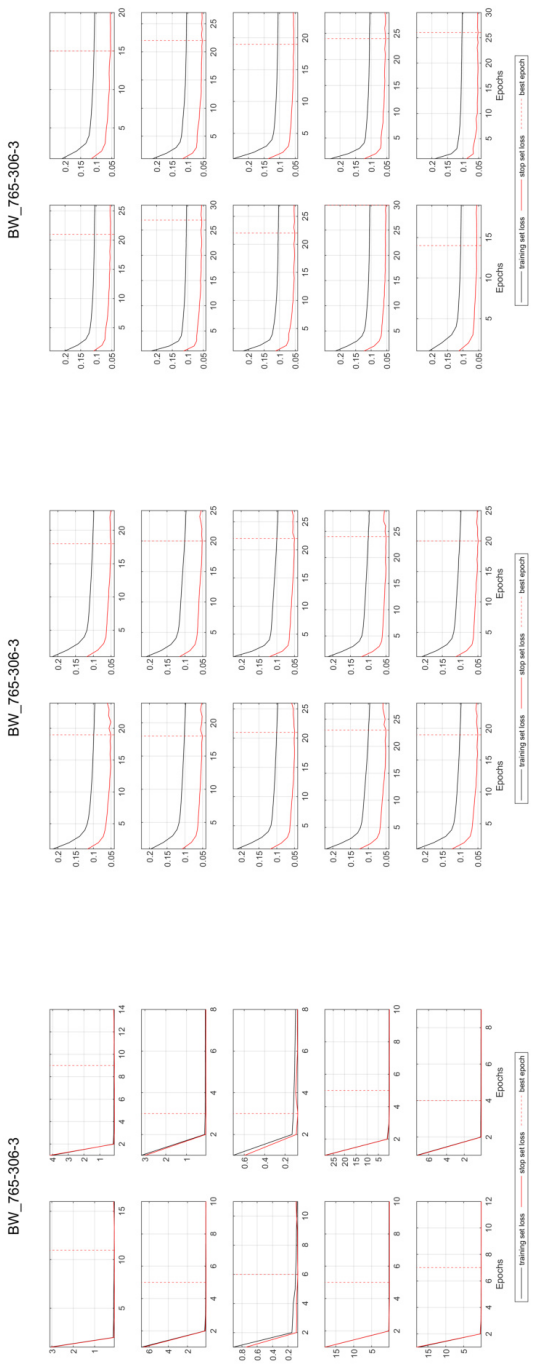

Figure S115: Seq2Seq training and early stopping loss (MSE) for all 10 model initializations for well BW_765-306-3: NARX (top), LSTM (middle), CNN (bottom)

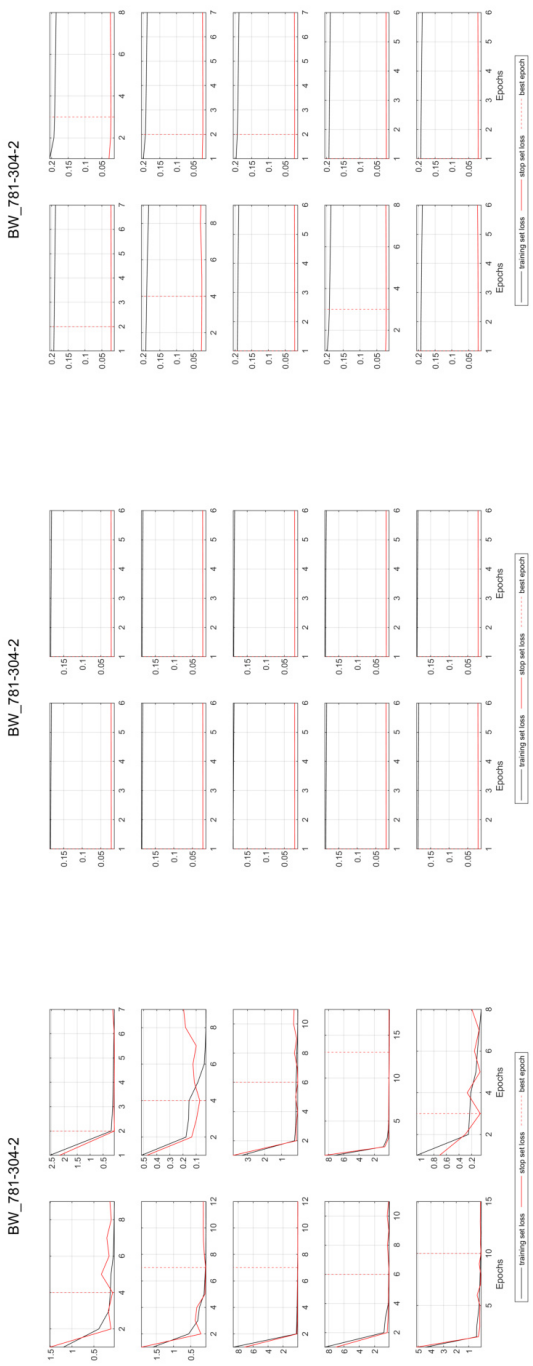

Figure S116: Seq2Seq training and early stopping loss (MSE) for all 10 model initializations for well BW_781-304-2: NARX (top), LSTM (middle), CNN (bottom)

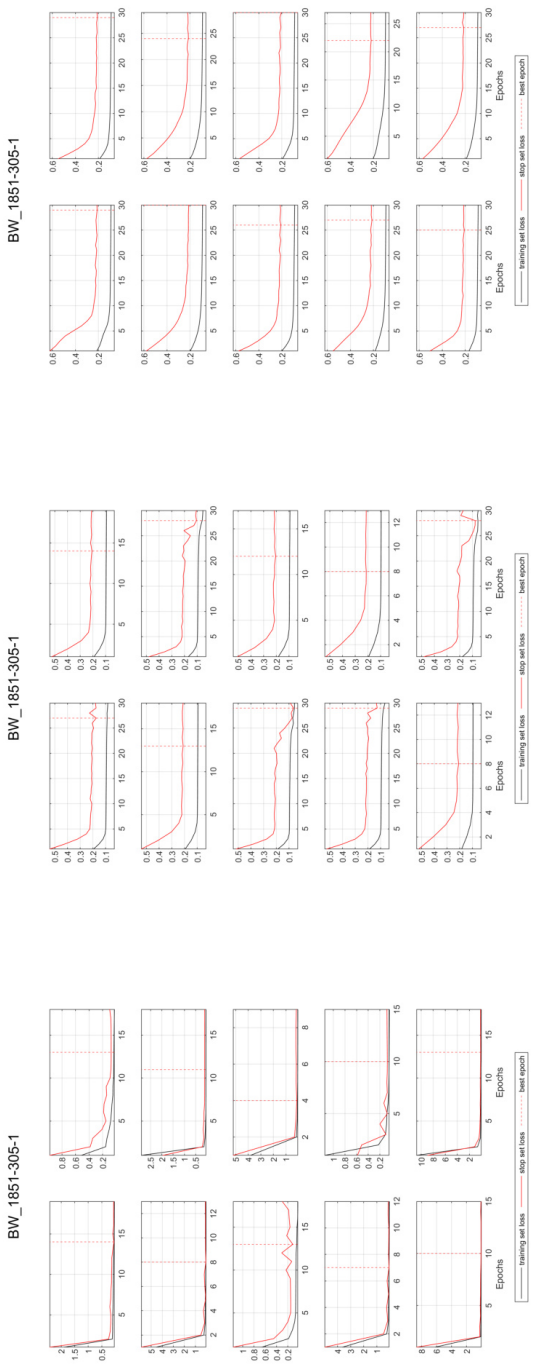

Figure S117: Seq2Seq training and early stopping loss (MSE) for all 10 model initializations for well BW_1851-305-1: NARX (top), LSTM (middle), CNN (bottom)

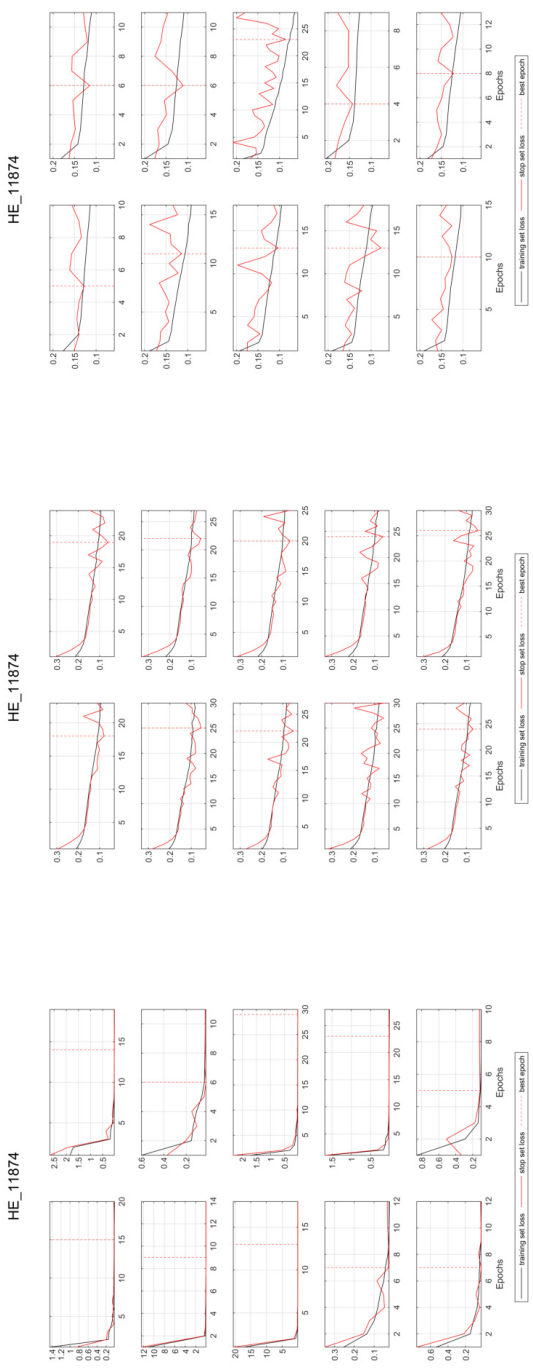

Figure S118: Seq2Seq training and early stopping loss (MSE) for all 10 model initializations for well HE_11874: NARX (top), LSTM (middle), CNN (bottom)

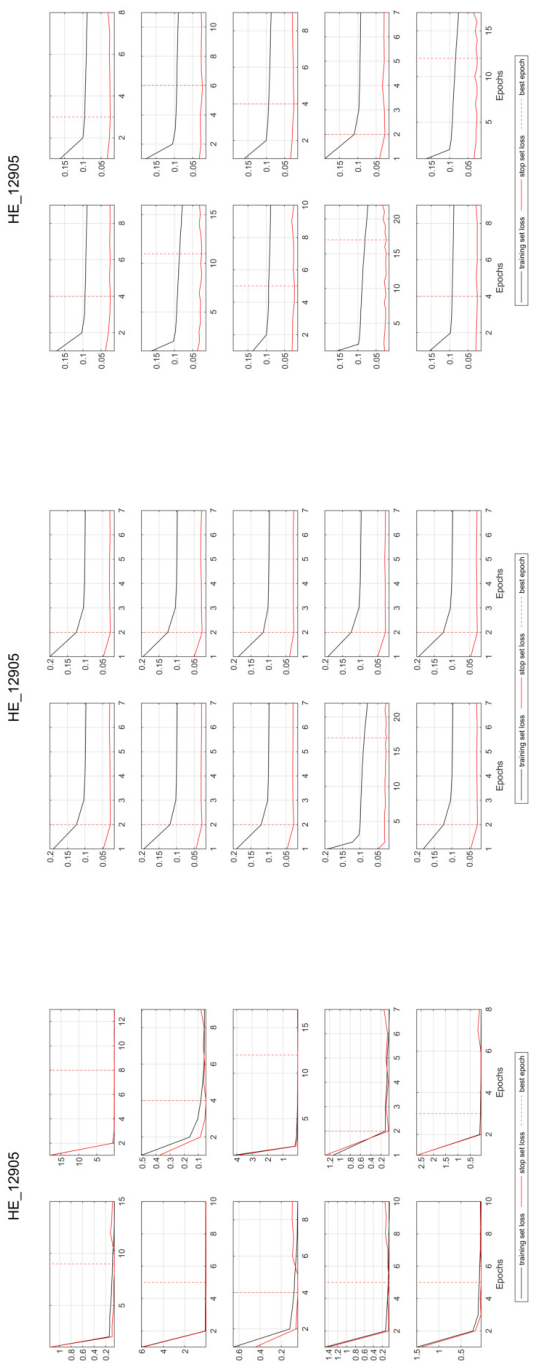

Figure S119: Seq2Seq training and early stopping loss (MSE) for all 10 model initializations for well HE_12905: NARX (top), LSTM (middle), CNN (bottom)

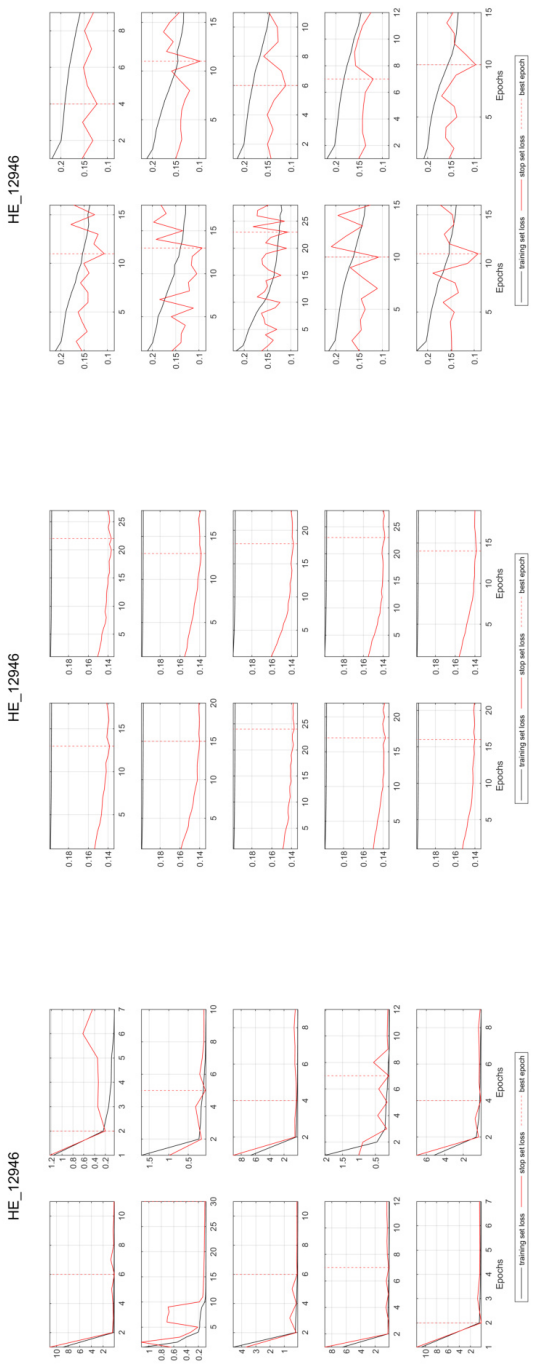

Figure S120: Seq2Seq training and early stopping loss (MSE) for all 10 model initializations for well HE_12946: NARX (top), LSTM (middle), CNN (bottom)

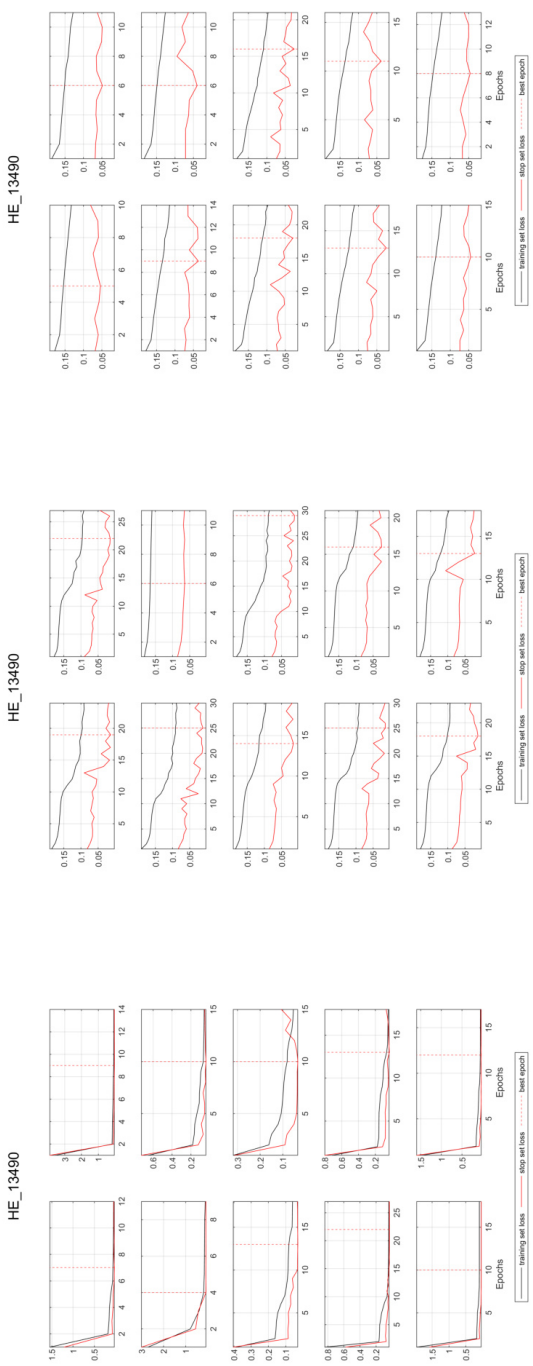

Figure S121: Seq2Seq training and early stopping loss (MSE) for all 10 model initializations for well HE_13490: NARX (top), LSTM (middle), CNN (bottom)

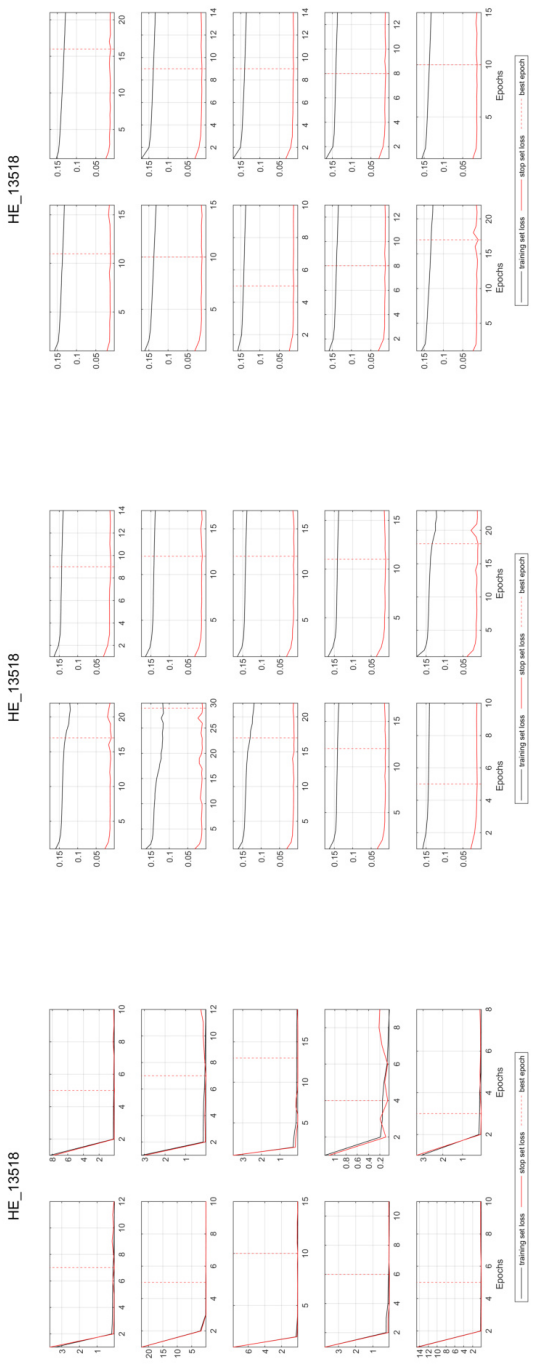

Figure S122: Seq2Seq training and early stopping loss (MSE) for all 10 model initializations for well HE_13518: NARX (top), LSTM (middle), CNN (bottom)

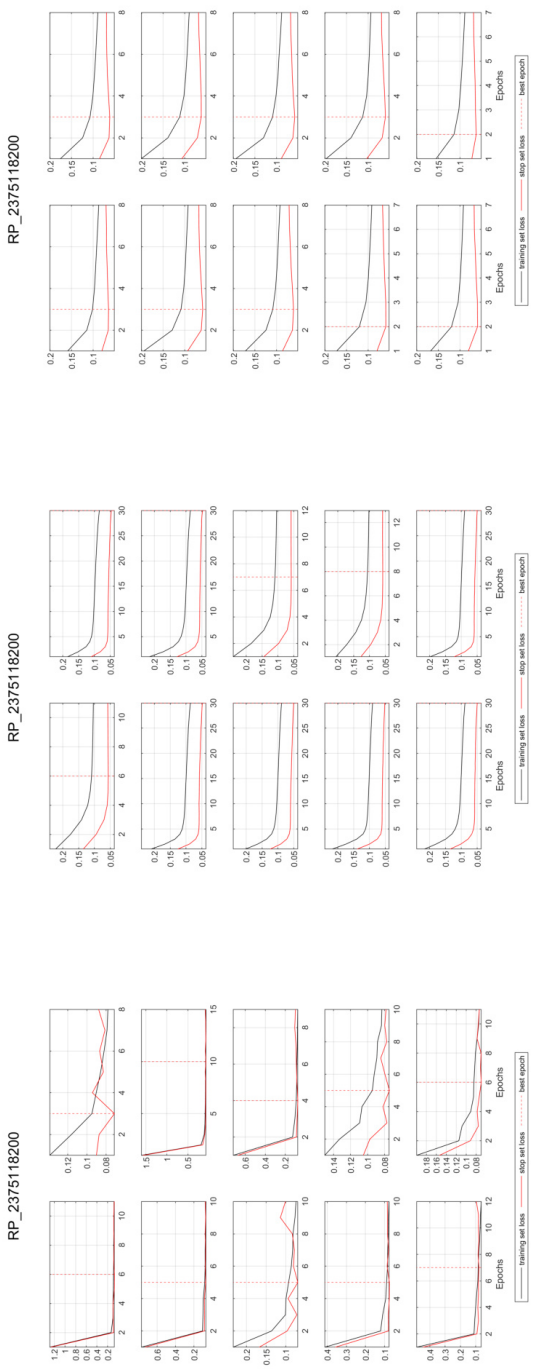

Figure S123: Seq2Seq training and early stopping loss (MSE) for all 10 model initializations for well RP_2375118200: NARX (top), LSTM (middle), CNN (bottom)

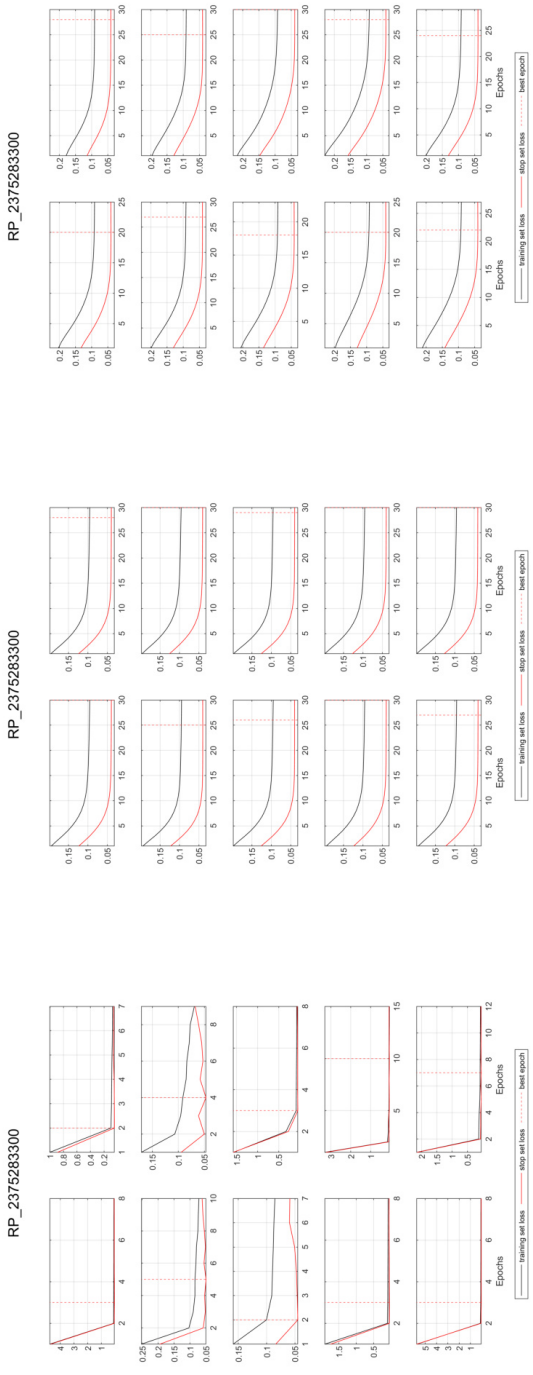

Figure S124: Seq2Seq training and early stopping loss (MSE) for all 10 model initializations for well RP_2375283300: NARX (top), LSTM (middle), CNN (bottom)

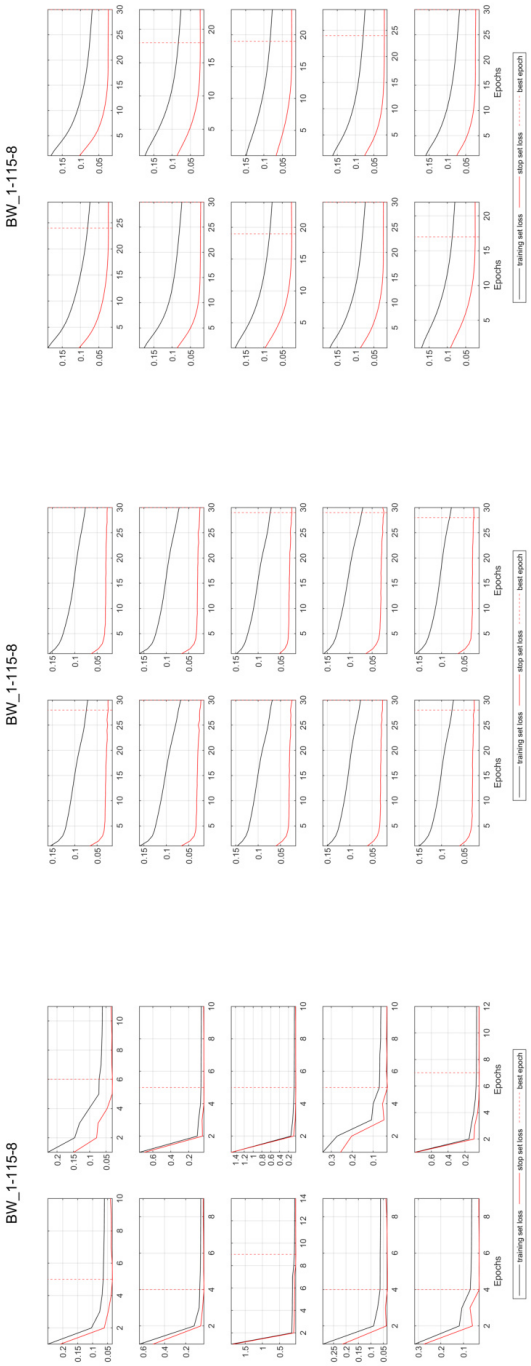

Figure S125: Seq2Seq GWL_{t-1} training and early stopping loss (MSE) for all 10 model initializations for well BW_1-115-8: NARX (top), LSTM (middle), CNN (bottom)

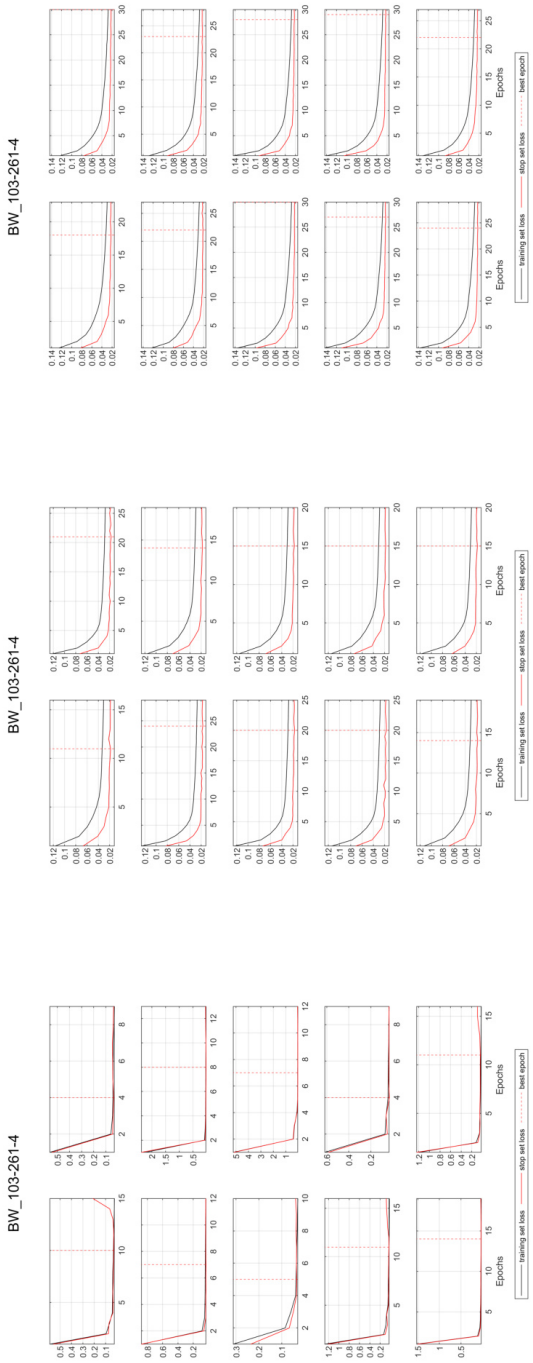

Figure S126: Seq2Seq GWL$_{t-1}$ training and early stopping loss (MSE) for all 10 model initializations for well BW_103-261-4: NARX (top), LSTM (middle), CNN (bottom)

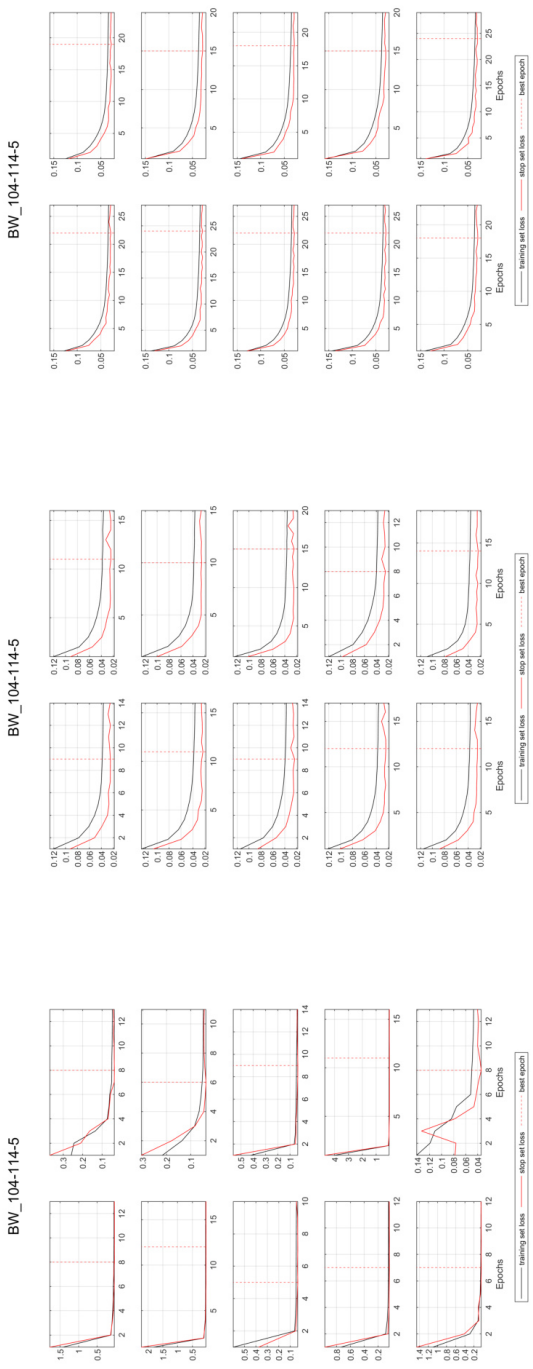

Figure S127: Seq2Seq GWL_{t-1} training and early stopping loss (MSE) for all 10 model initializations for well BW_104-114-5: NARX (top), LSTM (middle), CNN (bottom)

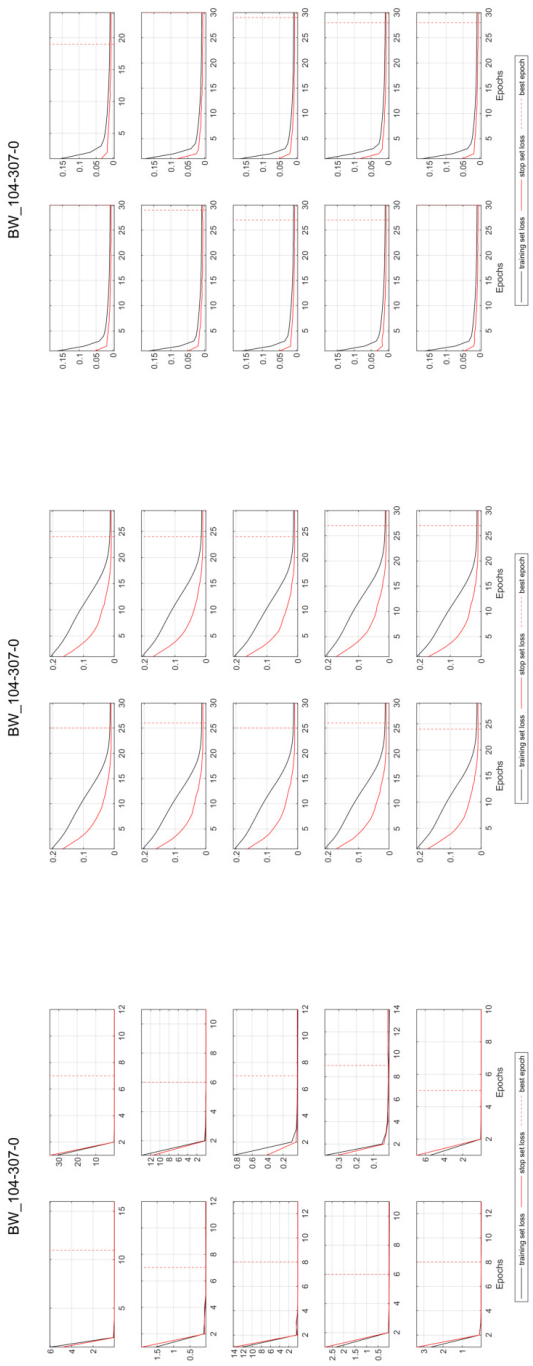

Figure S128: Seq2Seq GWL_{t-1} training and early stopping loss (MSE) for all 10 model initializations for well BW_104-307-0: NARX (top), LSTM (middle), CNN (bottom)

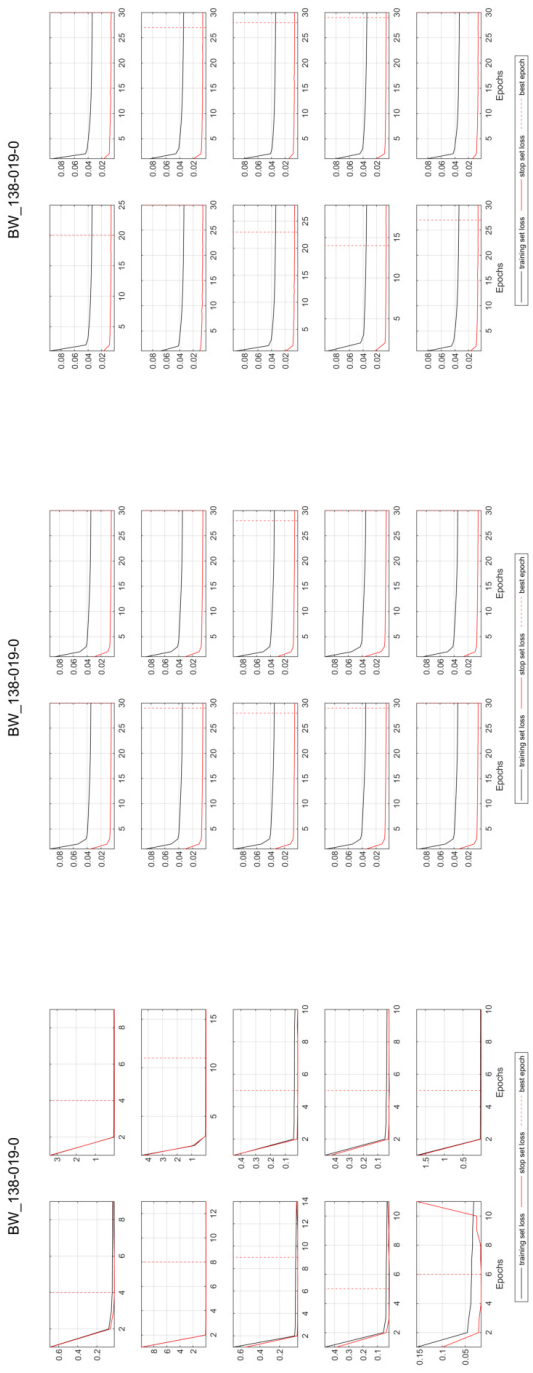

Figure S129: Seq2Seq GWL_{t-1} training and early stopping loss (MSE) for all 10 model initializations for well BW_138-019-0: NARX (top), LSTM (middle), CNN (bottom)

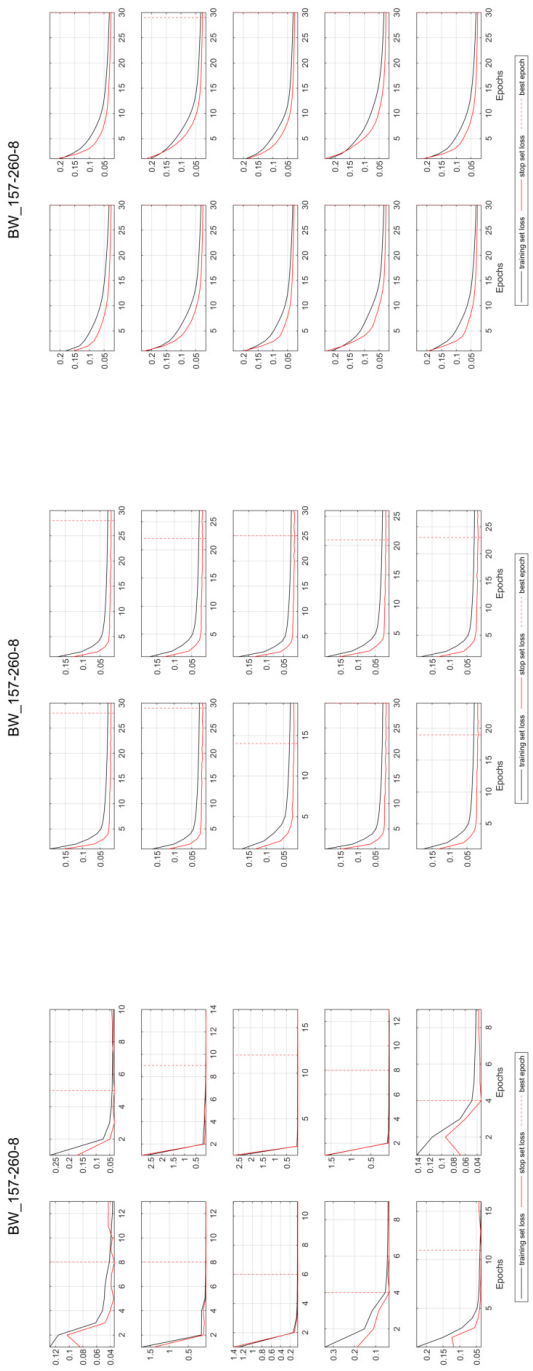

Figure S130: Seq2Seq GWL_{t-1} training and early stopping loss (MSE) for all 10 model initializations for well BW_157-260-8: NARX (top), LSTM (middle), CNN (bottom)

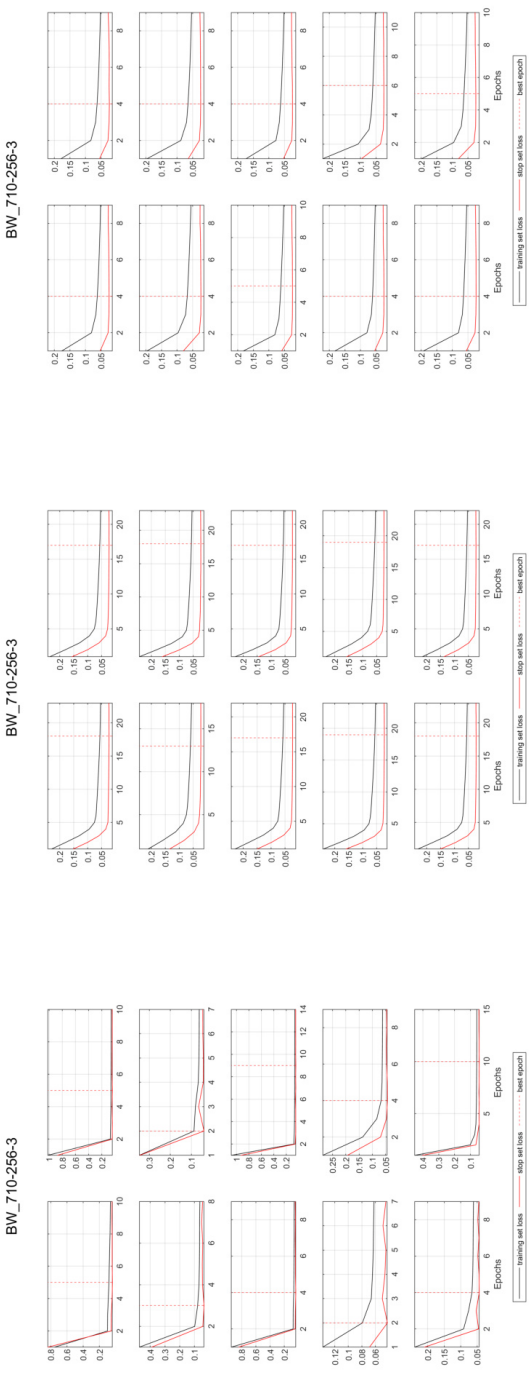

Figure S131: Seq2Seq GWL_{t-1} training and early stopping loss (MSE) for all 10 model initializations for well BW_710-256-3: NARX (top), LSTM (middle), CNN (bottom)

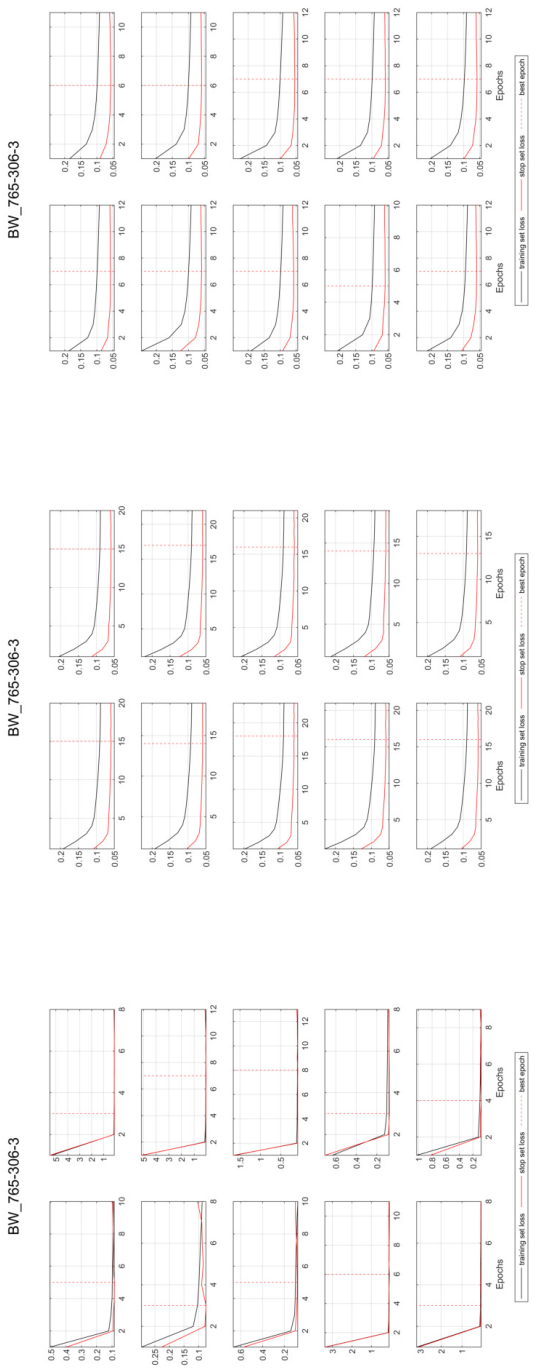

Figure S132: Seq2Seq GWL_{t-1} training and early stopping loss (MSE) for all 10 model initializations for well BW_765-306-3: NARX (top), LSTM (middle), CNN (bottom)

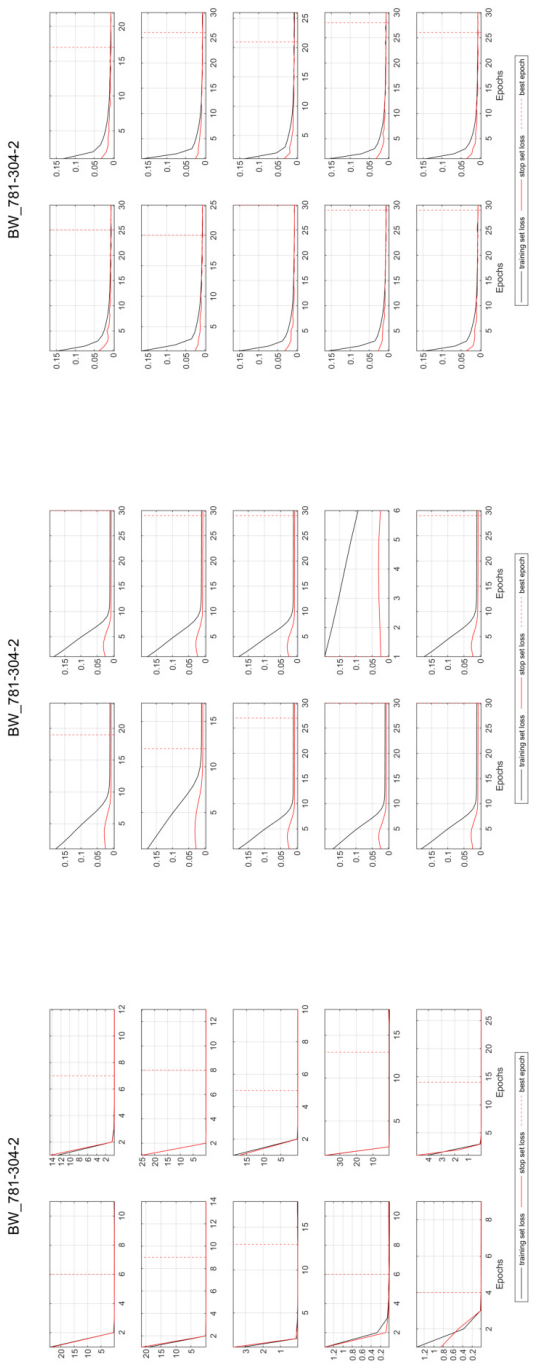

Figure S133: Seq2Seq GWL_{t-1} training and early stopping loss (MSE) for all 10 model initializations for well BW_781-304-2: NARX (top), LSTM (middle), CNN (bottom)

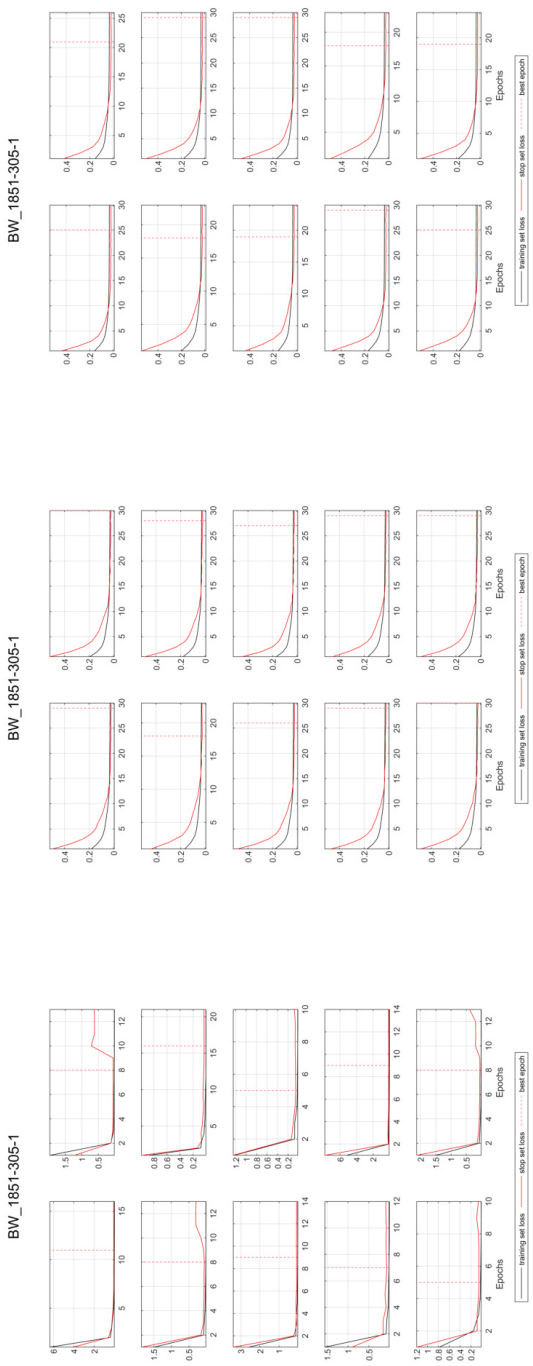

Figure S134: Seq2Seq GWL_{t-1} training and early stopping loss (MSE) for all 10 model initializations for well BW_1851-305-1: NARX (top), LSTM (middle), CNN (bottom)

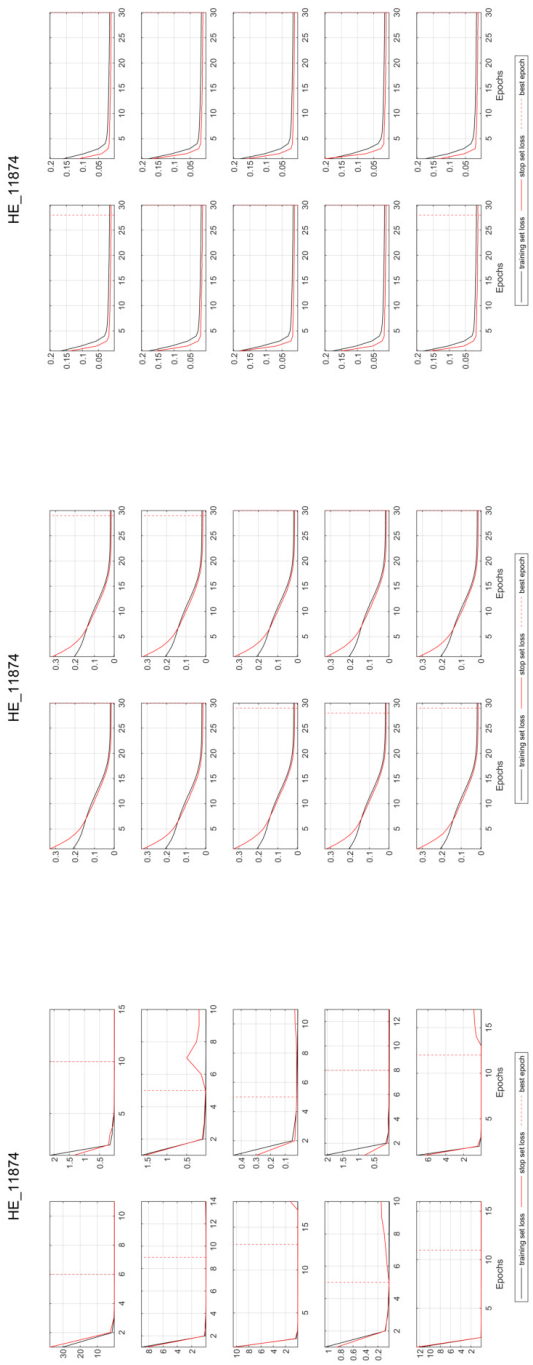

Figure S135: Seq2Seq GWL_{t-1} training and early stopping loss (MSE) for all 10 model initializations for well HE_11874: NARX (top), LSTM (middle), CNN (bottom)

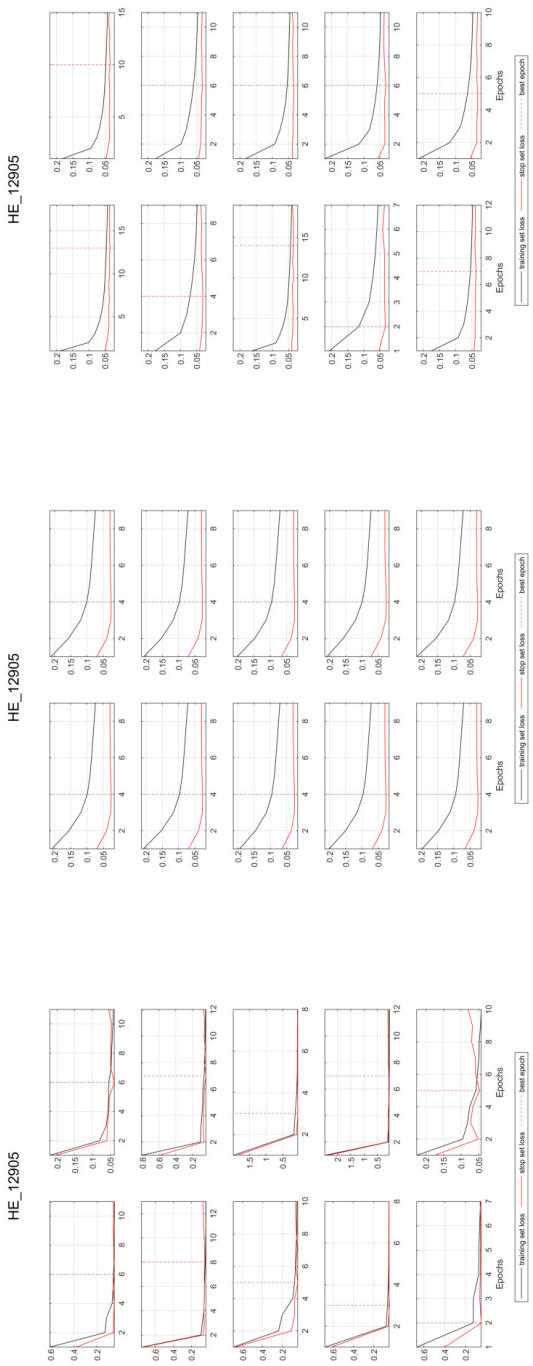

Figure S136: Seq2Seq GWL_{t-1} training and early stopping loss (MSE) for all 10 model initializations for well HE_12905: NARX (top), LSTM (middle), CNN (bottom)

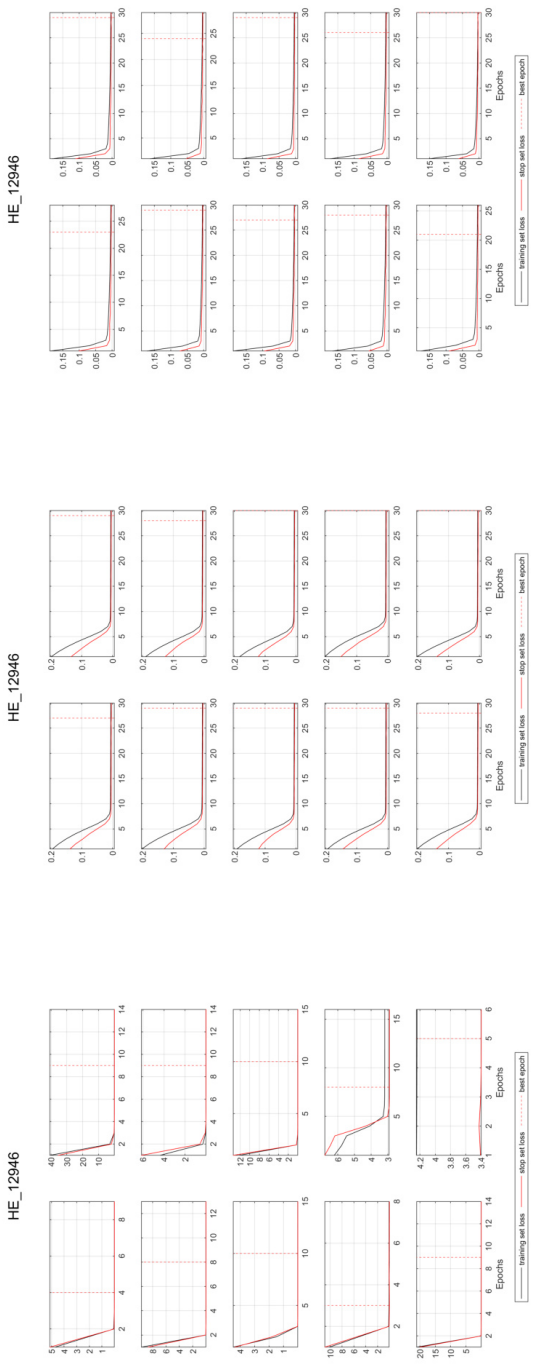

Figure S137: Seq2Seq GWL_{t-1} training and early stopping loss (MSE) for all 10 model initializations for well HE_12946: NARX (top), LSTM (middle), CNN (bottom)

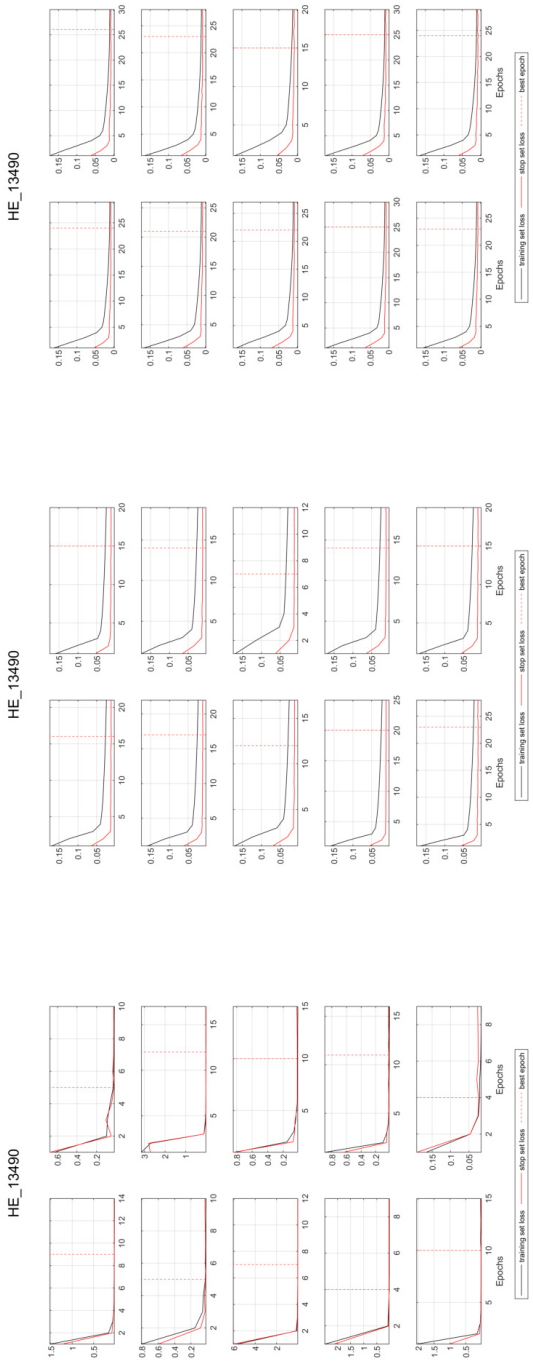

Figure S138: Seq2Seq GWL_{t-1} training and early stopping loss (MSE) for all 10 model initializations for well HE_13490: NARX (top), LSTM (middle), CNN (bottom)

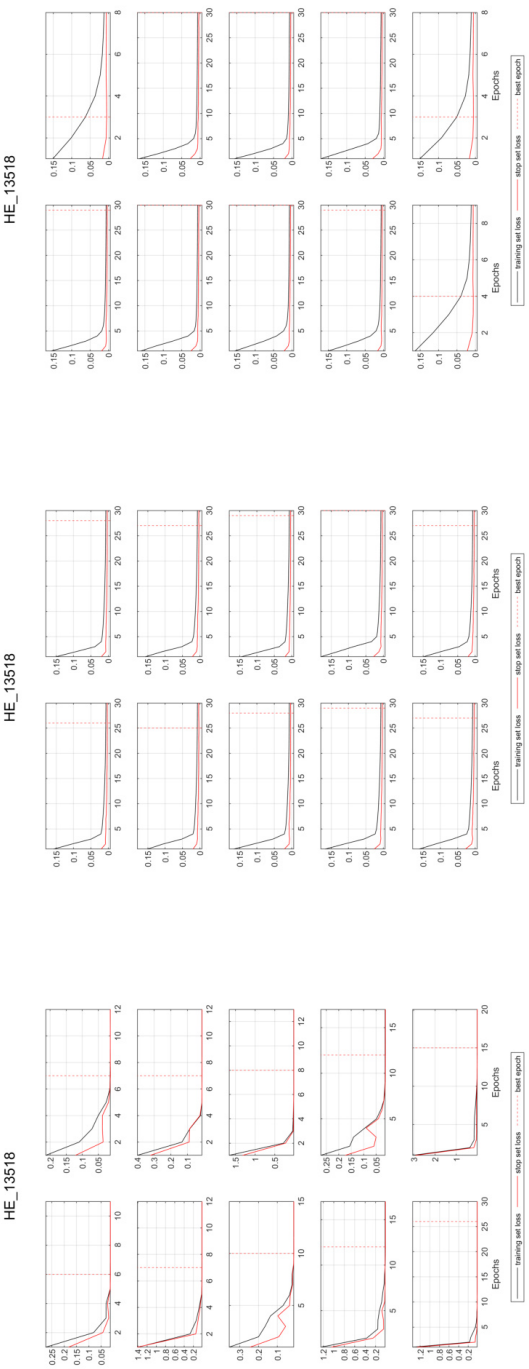

Figure S139: Seq2Seq GWL_{t-1} training and early stopping loss (MSE) for all 10 model initializations for well HE_13518: NARX (top), LSTM (middle), CNN (bottom)

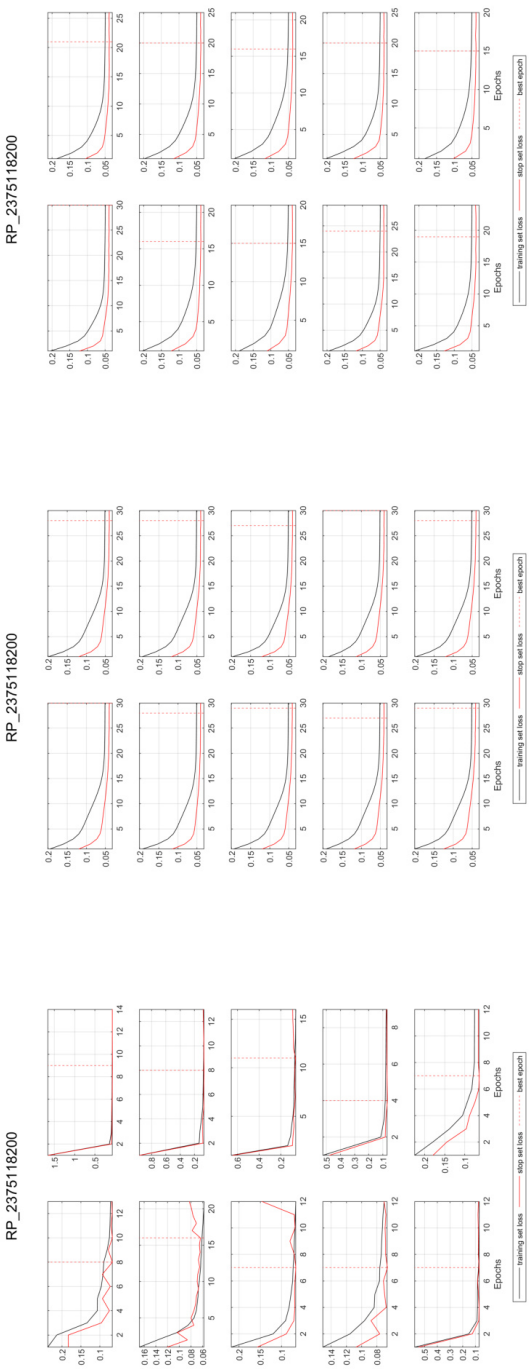

Figure S140: Seq2Seq GWL_{t-1} training and early stopping loss (MSE) for all 10 model initializations for well RP_2375118200: NARX (top), LSTM (middle), CNN (bottom)

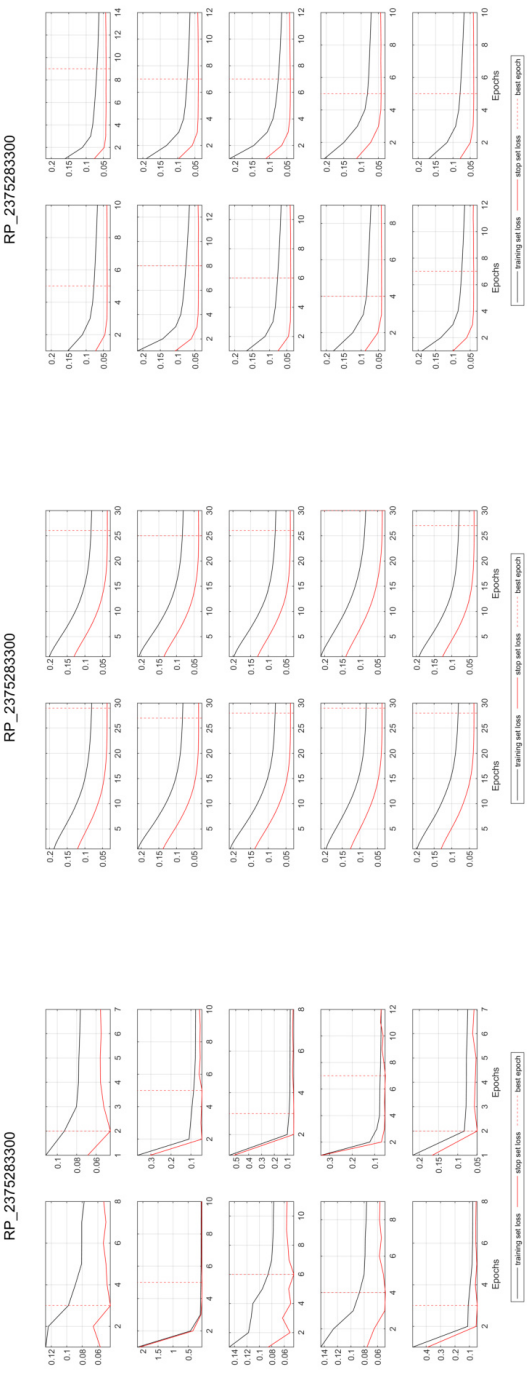

Figure S141: Seq2Seq GWL_{t-1} training and early stopping loss (MSE) for all 10 model initializations for well RP_2375283300: NARX (top), LSTM (middle), CNN (bottom)